1994-03

A computational investigation of wake-induced airfoil flutter in incompressible flow and active flutter control

Turner, Mark A.

Monterey, California. Naval Postgraduate School

NAVAL POSTGRADUATE SCHOOL
Monterey, California

THESIS

A COMPUTATIONAL INVESTIGATION OF WAKE-INDUCED AIRFOIL FLUTTER IN INCOMPRESSIBLE FLOW AND ACTIVE FLUTTER CONTROL

by

Mark A. Turner

March 1994

Thesis Advisor: Max F. Platzer

Approved for public release; distribution is unlimited

Unclassified

SECURITY CLASSIFICATION OF THIS PAGE

REPORT DOCUMENTATION PAGE

Form Approved
OMB No. 0704-0188

1a. REPORT SECURITY CLASSIFICATION Unclassified	1b. RESTRICTIVE MARKINGS
2a. SECURITY CLASSIFICATION AUTHORITY	3. DISTRIBUTION/AVAILABILITY OF REFORT Approved for public release; distribution is unlimited.
2b. DECLASSIFICATION/DOWNGRADING SCHEDULE	
4. PERFORMING ORGANIZATION REPORT NUMBER(S)	5. MONITORING ORGANIZATION REPORT NUMBER(S)
6a. NAME OF PERFORMING ORGANIZATION Naval Postgraduate School 6b. OFFICE SYMBOL (If applicable) AA/PL	7a. NAME OF MONITORING ORGANIZATION Naval Postgraduate School
6c. ADDRESS (City, State, and ZIP Code) Monterey, CA 93943-5000	7b. ADDRESS (City, State, and ZIP Code) Monterey, CA 93943-5000
8a. NAME OF FUNDING/SPONSORING ORGANIZATION 8b. OFFICE SYMBOL (If applicable)	9. PROCUREMENT INSTRUMENT IDENTIFICATION NUMBER
8c. ADDRESS (City, State, and ZIP Code)	10. SOURCE OF FUNDING NUMBERS PROGRAM ELEMENT NO. / PROJECT NO. / TASK NO. / WORK UNIT ACCESSION NO.

11. TITLE (Include Security Classification)
A COMPUTATIONAL INVESTIGATION OF WAKE-INDUCED AIRFOIL FLUTTER IN INCOMPRESSIBLE FLOW AND ACTIVE FLUTTER CONTROL

12. PERSONAL AUTHOR(S)
Mark A. Turner

13a. TYPE OF REPORT	13b. TIME COVERED	14. DATE OF REPORT (Year,Month,Day)	15. PAGE COUNT
Master's Thesis	FROM _____ TO _____	March 1994	110

16. SUPPLEMENTARY NOTATION
The views expressed in this thesis are those of the author and do not reflect the official policy or position of the Department of Defense or the U.S. Government.

17. COSATI CODES			18. SUBJECT TERMS (Continue on reverse if necessary and identify by block number)
FIELD	GROUP	SUB-GROUP	Flutter, Wake-Induced Flutter, Active Flutter Control, Theodorsen Comaprison, Unsteady Panel Methods.

19. ABSTRACT (Continue on reverse if necessary and identify by block number)

In this thesis several incompressible oscillatory flow and flutter problems were investigated. A previously developed unsteady panel code for single airfoil bending torsion flutter analysis was compared to Theodorsen's classical theory. The panel code agrees with Theodorsen's bending-torsion flutter analysis for natural frequency ratios (ω_h/ω_α) less than 1.2. Also, a two airfoil unsteady panel code was modified for one degree of freedom flutter analysis. Code verification was completed by first comparing flat plate theory to the unsteady aerodynamic force and moment coefficients and then using the equation of motion to determine regions of instability. The possibility of active flutter control was investigated by positioning a small control airfoil in front of a neutrally stable reference airfoil. Results show that the flutter boundary may be changed through the placement, oscillation or scaling of a second airfoil upstream. A comparison with pitch damping curves published by Loewy confirms that the code is capable of predicting wake-induced airfoil flutter.

20. DISTRIBUTION/AVAILABILITY OF ABSTRACT	21. ABSTRACT SECURITY CLASSIFICATION	
[X] UNCLASSIFIED/UNLIMITED [ ] SAME AS RPT. [ ] DTIC USERS	Unclassified	
22a. NAME OF RESPONSIBLE INDIVIDUAL Max F. Platzer	22b. TELEPHONE (Include Area Code) (408) 656 - 2058	22c. OFFICE SYMBOL AA/PL

DD Form 1473, JUN 86 Previous editions are obsolete. SECURITY CLASSIFICATION OF THIS PAGE

S/N 0102-LF-014-6603 Unclassified

Approved for public release; distribution is unlimited.

A COMPUTATIONAL INVESTIGATION OF WAKE-INDUCED AIRFOIL FLUTTER IN INCOMPRESSIBLE FLOW AND ACTIVE FLUTTER CONTROL

by

Mark A. Turner
Lieutenant, United States Navy
B.S., Miami University, 1986

Submitted in partial fulfillment of the
requirements for the degree of

MASTER OF SCIENCE IN AERONAUTICAL ENGINEERING

from the

NAVAL POSTGRADUATE SCHOOL
March 1994

Author: [redacted]
Mark A. Turner

Approved by: [redacted]
Max F. Platzer, Thesis Advisor

[redacted]
I. Tuncer, Second Reader

[redacted]
Daniel J. Collins, Chairman
Department of Aeronautics and Astronautics

ABSTRACT

In this thesis several incompressible oscillatory flow and flutter problems were investigated. A previously developed unsteady panel code for single airfoil bending torsion flutter analysis was compared to Theodorsen's classical theory. The panel code agrees with Theodorsen's bending-torsion flutter analysis for natural frequency ratios (ω_h/ω_α) less than 1.2. In addition, a two airfoil unsteady panel code was modified for one degree of freedom flutter analysis. Code verification was accomplished by first comparing flat plate theory to the unsteady aerodynamic force and moment coefficients and then using the equation of motion to determine regions of instability. The possibility of active flutter control was investigated by positioning a small control airfoil in front of a neutrally stable reference airfoil. Results show that the flutter boundary may be changed through the scaling, placement, or oscillation of a second airfoil upstream. A comparison with pitch damping curves published by Loewy confirms that the code is capable of predicting wake-induced airfoil flutter.

TABLE OF CONTENTS

Table of Symbols

a	elastic axis position from mid chord
b	half chord length
C_α	torsional stiffness
C_h	stiffness in flexure or plunge
$C_{L\alpha}$	coefficient of lift due to pitch
C_{Lh}	coefficient of lift due to plunge
$C_{M\alpha}$	coefficient of moment due to pitch
C_{Mh}	coefficient of moment due to plunge
g	structural damping
h	plunge deflection
h_0	plunge amplitude
I_α	moment of inertia about elastic axis
K_p	reduced frequency based on full chord (panel)
K_t	reduced frequency based on half chord (Theodorsen)
M	mass of wing per unit span
m	frequency ratio ω/Ω
r	blade section radius
r_α	radius of gyration
S_α	static moment of inertia
U	free stream velocity
X	flutter frequency ratio
x_α	center of gravity from elastic axis
α	pitch angle

α_0 pitch amplitude

μ wing density parameter

ω frequency of oscillation

ω_α natural frequency in pitch

ω_h natural frequency in plunge

Ω rotational speed of rotor system

ACKNOWLEDGMENTS

The research for this thesis was conducted using the facilities of the Department of Aeronautics and Astronautics at the Naval Postgraduate School. I would like to give my sincere appreciation to professor Max F. Platzer for his guidance, many hours of council and patience that led to the completion of this thesis. In addition, I would like to thank Dr. I. Tuncer for his timely advice and recommendations to overcome difficulties.

I. INTRODUCTION

A. GENERAL

In this thesis, two unsteady panel codes UPOTFLUT described by Riester [Ref. 1] and USPOTF2C developed by Pang [Ref. 2] are modified and verified.

The UPOTFLUT (Unsteady Potential Flow and Flutter) was developed by Teng [Ref. 3] for unsteady inviscid and incompressible flow over a single airfoil. The code is based upon the panel method by Hess and Smith [Ref. 4] that includes simple harmonic motion of the airfoil which is continuously shedding vortices into the wake. Riester [Ref. 1] extended the single airfoil code for bending-torsion flutter analysis.

The USPOTF2F (Unsteady Potential Flow) code [Ref. 2] is a two airfoil code that permits steady and unsteady analysis of airfoil-wake interaction between two airfoils. A phase subroutine is added to convert the time dependent lift and moment histories into the frequency domain.

Building upon the work of Riester [Ref. 1] which focused mainly on aerodynamic verification of UPOTFLUT code, the two dimensional bending-torsion flutter problem is examined. Theodorsen [Ref. 5, page 11] presents flat plate flutter speeds for comparison to UPOTFLUT computations. Specific cases are selected to compare the aerodynamic forces and solutions of the flutter determinant.

The two airfoil USPOTF2 code's unsteady aerodynamics are verified for pitch and plunge. Then the instability of one degree of freedom pitching oscillations is chosen to explore active flutter control. Pitch damping dependence upon

upstream airfoil size and position is fully explored. Emphasis is placed upon the wake effect and the code's ability to predict wake-induced flutter.

Whenever possible, the theoretical work of Theodorsen [Ref. 5], Smilg [Ref. 6], Loewy [Ref. 7] and other numerical examples are used for comparison to verify accuracy and trends. However, for many of the computations performed no other analytical theories and applicable experimental data exist.

B. SCOPE

Chapter II contains bending-torsion flutter verification using the single airfoil UPOTFLUT code and Theodorsen theory. Aerodynamic verification of force and moment coefficients using the two airfoil USPOTF2F code is accomplished in Chapter III. Chapter IV develops the equations of motion for steady-state oscillations in one degree of freedom. An in-ground effect numerical simulation is completed by oscillating airfoils out of phase. The positioning and size of the control airfoil for active flutter control are investigated in Chapter V. Application to rotary wings along with a comparison to wake-induced flutter theory is also discussed.

II. SINGLE AIRFOIL ANALYSIS

The results discussed and presented in this chapter were produced from the UPOTFLUT code. This single airfoil analysis builds on work by Riester [Ref. 1].

A. INTRODUCTION TO UNSTEADY PANEL CODE THEORY

Given a two-dimensional airfoil, the governing equation to solve the inviscid, incompressible flow over the airfoil is Laplace's equation. Since the two-dimensional Laplace equation is linear, the principle of superposition may be applied. The four elementary flows: uniform flow, source flow, doublet flow and vortex flow are used to determine the flow around arbitrary bodies. For non-lifting bodies a uniform flow and source flow are required. For lifting bodies the vortex flow, must also be included to provide circulation. The boundary conditions which must be satisfied are flow tangency at the surface and the Kutta condition at the trailing edge.

Steady-state panel methods as described by Hess and Smith [Ref. 4] may be extended to airfoils in simple harmonic motion. The continuous change in the lift implies a continually changing circulation about the airfoil. The Helmholtz vortex theorem requires that any change in the circulation around an airfoil must be matched by the appearance of an equal counter-vortex or starting vortex to achieve constant total circulation in the flow field. The starting vortices are assumed to be shed from the trailing edge after each time step and move with the local flow velocity.

Riester [Ref. 1], page 23, showed that for single airfoil analysis 3 cycles is a sufficient wake length for amplitude and phase analysis when Kp = 1.0. The benchmark chosen for computations is 3 cycles, 65 time steps per cycle. A

NACA0007 airfoil geometry was chosen for comparison to flat plate theory. A thinner airfoil does not provide accurate results due to insufficient number of panels to adequately resolve the leading edge and vortex interaction between top and bottom surfaces.

B. TWO DEGREE OF FREEDOM EQUATIONS OF MOTION AND FLUTTER DETERMINANT

If a positive concentrated load, on a cantilever wing of uniform cross section is applied at the leading edge of the wing tip, the tip cross section will be displaced upwards and twist, thus increasing the angle of attack. If a similar concentrated load is applied at the trailing edge, the tip cross section will flex upwards and the angle of attack will decrease. A point exists between the leading edge and trailing edge where a concentrated load may be applied without twisting or causing the airfoil to rotate. This point is called the shear center or the flexural center of the airfoil. The elastic axis is defined as the locus of shear centers of the cross section, thus it is a natural reference line.

Forces acting upon the airfoil are the elastic restoring forces, inertial forces and aerodynamic forces. Displacement variables for two degree of freedom, simple harmonic motion are pitch (α) and plunge (h):

$C_\alpha \equiv$ torsional stiffness of wing

$C_h \equiv$ stiffness of wing in flexure

$M \equiv$ mass of wing per unit span

$S_\alpha \equiv$ static moment referred to elastic axis

$I_\alpha \equiv$ moment of inertia about elastic axis

The elastic restoring forces are hC_h and αC_α. The inertial forces respectively in pitch and plunge are:

$$\ddot{\alpha} I_\alpha + \ddot{h} S_\alpha$$

$$\ddot{h}\,M + \ddot{\alpha}\,S_\alpha$$

Applying equilibrium by equating the inertial forces to the external aerodynamic and structural elastic forces and assuming zero structural damping yields:

$$\ddot{\alpha}\,I_\alpha + \ddot{h}\,S_\alpha = \text{Moment} - \alpha C_\alpha$$

$$\ddot{h}\,M + \ddot{\alpha}\,S_\alpha = \text{Lift} - hC_h$$

The natural frequencies in pitch and plunge are:

$$\omega_h = \sqrt{\frac{C_h}{M}}$$

$$\omega_\alpha = \sqrt{\frac{C_\alpha}{I_\alpha}}$$

Substituting into the equations of motion:

$$\ddot{h}M + \ddot{\alpha}\,S_\alpha + hM\omega_h^2 = \text{Lift}$$

$$\ddot{\alpha}I_\alpha + \ddot{h}\,S_\alpha + \alpha I_\alpha \omega_\alpha^2 = \text{Moment}$$

For simple harmonic motion:

$$h = h_o e^{i\omega t} \qquad \alpha = \alpha_o e^{i\omega t}$$

$$h = -\omega^2 h_o e^{i\omega t} \qquad \alpha = -\omega^2 \alpha_o e^{i\omega t}$$

$$e^{i\omega t}\left(-\omega^2 h_o M - \omega^2 \alpha_o S_\alpha + h_o M\omega_h^2\right) = \text{Lift}$$

$$e^{i\omega t}\left(-\omega^2 \alpha_o I_\alpha - \omega^2 h_o S_\alpha + \alpha_o I_\alpha \omega_\alpha^2\right) = \text{Moment}$$

The panel code nondimensionalizes lift and moment using the characteristic length of chord (2b) vice semichord.

$$\text{Lift} = \left(C_{L\alpha} + C_{Lh}\right)\frac{1}{2}\rho U^2\, 2b$$

$$\text{Moment} = \left(C_{M\alpha} + C_{Mh}\right)\frac{1}{2}\rho U^2\, 4b^2$$

Introducing dimensionless flutter parameters:

$$\text{Wing density parameter } \mu = \frac{M}{\pi\rho b^2}$$

Center of gravity from elastic axis: $x_\alpha = \frac{S_\alpha}{Mb}$

Radius of gyration: $r_\alpha^2 = \frac{I_\alpha}{Mb^2}$

Flutter frequency ratio: $X = \left(\frac{\omega_\alpha}{\omega}\right)^2$

The equations of motion become:

$$\frac{1}{Mb}\left[\left(-\omega^2 h_o M - \omega^2 \alpha_o S_\alpha + h_o M \omega_h^2\right) = \left(C_{L\alpha} + C_{Lh}\right)\frac{1}{2}\rho U^2 2b\right]$$

$$\frac{1}{Mb^2}\left[\left(-\omega^2 \alpha_o I_\alpha - \omega^2 h_o S_\alpha + \alpha_o I_\alpha \omega_\alpha^2\right) = \left(C_{M\alpha} + C_{Mh}\right)\frac{1}{2}\rho U^2 4b^2\right]$$

$$-\frac{h_o}{b} - \alpha_o x_\alpha + \frac{h_o}{b}\left(\frac{\omega_h}{\omega}\right)^2 = \left(C_{L\alpha} + C_{Lh}\right)\frac{\pi\rho U^2 4b^2}{\pi M\omega^2 4b^2}$$

$$-\alpha_o r_\alpha^2 - \frac{h_o}{b}x_\alpha + \alpha_o r_\alpha^2\left(\frac{\omega_\alpha}{\omega}\right) = \left(C_{M\alpha} + C_{Mh}\right)\frac{\pi\rho U^2 8b^2}{\pi M\omega^2 4b^2}$$

$$-\alpha_o x_\alpha + \frac{h_o}{b}\left(\left(\frac{\omega_h}{\omega}\right)^2 - 1\right) = \left(C_{L\alpha} + C_{Lh}\right)\frac{4}{\pi\mu K_p^2}$$

$$\alpha_o r_\alpha^2\left(\left(\frac{\omega_\alpha}{\omega}\right) - 1\right) - \frac{h_o}{b}(x_\alpha) = \left(C_{M\alpha} + C_{Mh}\right)\frac{8}{\pi\mu K_p^2}$$

Rearrange the two equations into the form:

$$A\left(\frac{h}{b}\right) + B(\alpha) = 0$$

$$D\left(\frac{h}{b}\right) + E(\alpha) = 0$$

where

$$A = \mu\left(1 - \left(\frac{\omega_\alpha}{\omega}\right)^2\left(\frac{\omega_h}{\omega_\alpha}\right)^2\right) + \frac{2C_{Lh}}{\left(\frac{h}{2b}\right)K_p^2}$$

$$B = \mu x_\alpha + \frac{4C_{L\alpha}}{\pi\alpha K_p^2}$$

$$D = \mu x_\alpha + \frac{4C_{Mh}}{\pi\left(\frac{h}{2b}\right)K_p^2}$$

$$E = \mu r_\alpha^2\left(1 - \left(\frac{\omega_\alpha}{\omega}\right)^2\right) + \frac{8C_{M\alpha}}{\pi\alpha K_p^2}$$

$$\Delta = \begin{vmatrix} A & B \\ D & E \end{vmatrix} = \Delta_{Real} + \Delta_{Imaginary}$$

To find the critical flutter speed and frequency the characteristic equation is solved for U and ω. Since Δ is complex both the real and imaginary parts must equal zero yielding two real quadratic equations for two unknowns. The real equation typically assumes a parabolic shape and the imaginary equation intersects on the lower branch as shown in Figure 2.1.

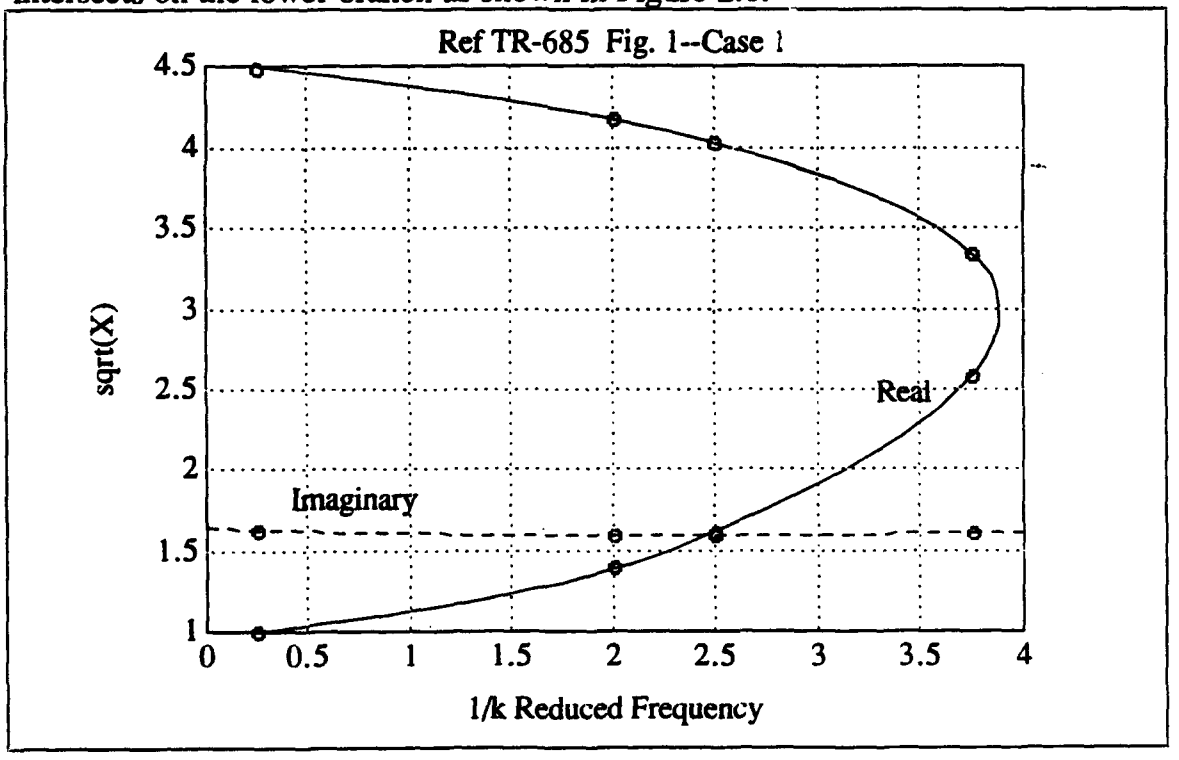

Figure 2.1 Real and Imaginary Roots of Flutter Determinant

C. MODIFICATION OF UPOTFLUT

Significant modifications to the UPOTFLUT code involved nondimensionalizing flutter determinant parameters.

The phase subroutine converts the time history of lift and moment into the form:

$$F(t) = Amp * \cos(\omega t + \phi)$$

Where Amp is the amplitude, ω is frequency of oscillation and ϕ is ıgle of phase lag of the aerodynamic forces to the motion of the airfoil. An ıterative numerical scheme to find the phase shift involves summing the differences between actual time history and the fitted curve over a half cycle, then shifting ϕ to minimize error. When iterations start with a phase error of π the total error ıs a maximum, hence the error curve's derivative equals zero. If initial phase shift step size is too small, the numerical scheme will remain at a maximum instead of converging to minimize error. Initial step size of four degrees is sufficient to ensure convergence.

D. VERIFICATION OF UPOTFLUT

NACA TR-685 page 11 [Ref. 5] provides the closed form solution of a flat plate for comparison with the UPOTFLUT code. The results of Case (a) are identical to code validation performed by Riester [Ref. 1] page 101. Case (a) and Case (b) results are tabulated in Table 2.1. In general, the panel code results agree with Theodorsen's theory. Next, the xalpha = 0.2 Case (h) was calculated using UPOTFLUT panel code. Case (h) physically represents a heavy wing with the center of mass aft of the elastic axis. The pivot axis is located at 35 percent of chord. These parameters make the cross section inherently susceptible to flutter.

As illustrated in Figure 2.3, the panel code results and Theodorsen theory diverge at natural frequency ratios greater than 0.8.

The Theodorsen theoretical curve was verified using two dimensional flutter analysis described by Fung, page 235 [Ref. 8]. The analysis was completed by programming the fundamentals of flutter theory in MATLAB [Appendix A] using unsteady aerodynamic coefficients found on page 412 of Scanlan and Rosenbaum [Ref. 9]. The non-linear complex quadratic equations are solved by using a bisection root solving numerical scheme. Calculated non-dimensional flutter speeds coincided with published coefficients for ω_h/ω_α less than 1.2. For ω_h/ω_α greater than 1.2, the critical reduced frequencies encountered are greater than 4.0 based upon semichord ($K_t = 4.0$). At high reduced frequencies, the flutter determinant becomes ill conditioned and very sensitive to small changes in any of the flutter variables. Theodorsen did not have the computational power of computers in 1940 when TR-685 was published. Therefore, his results were recomputed. Although Theodorsen's curve for Case (h) in TR-685, page 11 was found to be inaccurate for frequency ratios greater than 1.25 (as shown in Figure 2.3), the new theoretical curve using numerical methods did not correct the large discrepancy between his theory and the panel code. The source for this discrepancy may come from the computation of the unsteady aerodynamics or from the flutter calculations. Figures 2.4 through 2.11 and Table 2.3 indicate close agreement between the aerodynamic coefficients for lower reduced frequencies with errors increasing slightly at higher frequencies. The panel code unsteady aerodynamic coefficients are derived and discussed by Riester [Ref. 1] and reproduced here specifically for TR-685 page 11 Case (h).

The agreement between Theodorsen's and the panel code unsteady aerodynamics suggests that the discrepancy in flutter coefficient is mainly due to the solution of the flutter determinant. The flutter coefficient is defined as:

$$\frac{U}{b\omega_\alpha} = \frac{1}{\sqrt{X}} \frac{1}{K_t}$$

Figure's 2.12 through 2.14 and Table 2.4 compare the real and imaginary roots of the flutter determinant from theory and the panel code. The intersection point of the real and imaginary roots represents the flutter frequency. It is shown in Figure 2.13 that the critical reduced frequency may differ by up to a factor of three from Theodorsen's result for high critical frequencies and high frequency ratios.

```
 4
*************************************************************************
      AIRFOIL TYPE : NACA 0007 AIRFOIL
      NLOWER = 100 , NUPPER = 100
*************************************************************************
IFLAG  NLOWER  NUPPER
 0       100     100
AIRFOIL TYPE
 3
IRAMP  IOSCIL   ALPI      ALPMAX       PIVOT
  0      1     -1.0      1.0          0.0
FREQ   RFQSTP  RFQFNL
 0.04     0.02  0.2
IGUST  UGUST   VGUST
  0     0.      0.
ITRANS  DELHX  DELHY  DELI   PHASE
  0    0.00   .01     -.01   0.00
CYCLE  NTCYCLE     TOL
  3      65      0.001
naot &  naot X aoa values multiplied by 10 (integer)
 2      05 10  20 25 39 50
wh/walpha ratio    mass ratio    xalpha    (ralpha)**2
  0.4                 3            0.2          0.25
Comments...

IRAMP  0: n/a             RFREQ is based on full chord
       1: Straight ramp
       2: Modified ramp

IOSCIL 0: n/a             RFREQ is based on full chord
       1: Sinusoidal pitch, motion starts at min Aoa

PIVOT  : Position of elastic axis if leading edge=0 and trailing edge=1

ITRANS 0: n/a
       1: Translational harmonic oscillation

CYCLE  : # of cycles for oscillatory motions
        -In case of ramp, cycle=1.5 denotes airfoil is held
         at max aoa for the duration of .5 cycle
        -For steady state solution set it to 0

NTCYCLE: # of time steps for each cycle
          CYCLE*NTCYCLE is limited to 200 currently.

NAOT: # of input aoa for cp output
      - angles should be in increasing order,
      - for oscilatory motions angles should increase
        first, then decrease. Decreasing angles are for
        the return cycle..
```

Figure 2.2 Typical UPOTFLUT.IN input file

TABLE 2.1 TR-685 CASE(A) and CASE(B) COMPARISON

Mechanism of Flutter			
Panel Code 1 deg pitch, 0.01 h/2b plunge; 200 panels			
NACA0007; 3 cycles 65 time steps per cycle;			
TR-685 pg. 11 case a.			
Xalpha = 0.2	Flutter Speed	Flutter Speed	
wh/walpha	panel	theory	
0.01	1.66	1.70	
0.20	1.71	1.72	
0.40	1.77	1.80	
0.60	1.90	2.05	
0.80	2.29	2.47	
Xalpha = 0.4			
wh/walpha	panel	theory	
0.01	1.18	1.20	
0.20	1.18	1.19	
0.25	1.19	1.19	
0.40	1.19	1.18	
0.60	1.22	1.22	
0.80	1.30	1.32	
1.00	1.40	1.45	
TR-685 pg. 11 case b			
Xalpha = 0.1			
wh/walpha	panel	theory	
0.01	1.85	1.65	
0.10	1.87	1.70	
0.20	2.02	1.86	
0.30	2.30	2.06	
Xalpha = 0.2			
wh/walpha	panel	theory	
0.20	1.30	1.22	
0.40	1.34	1.28	
0.60	1.43	1.41	
0.80	1.67	1.60	
1.00	2.44	1.90	

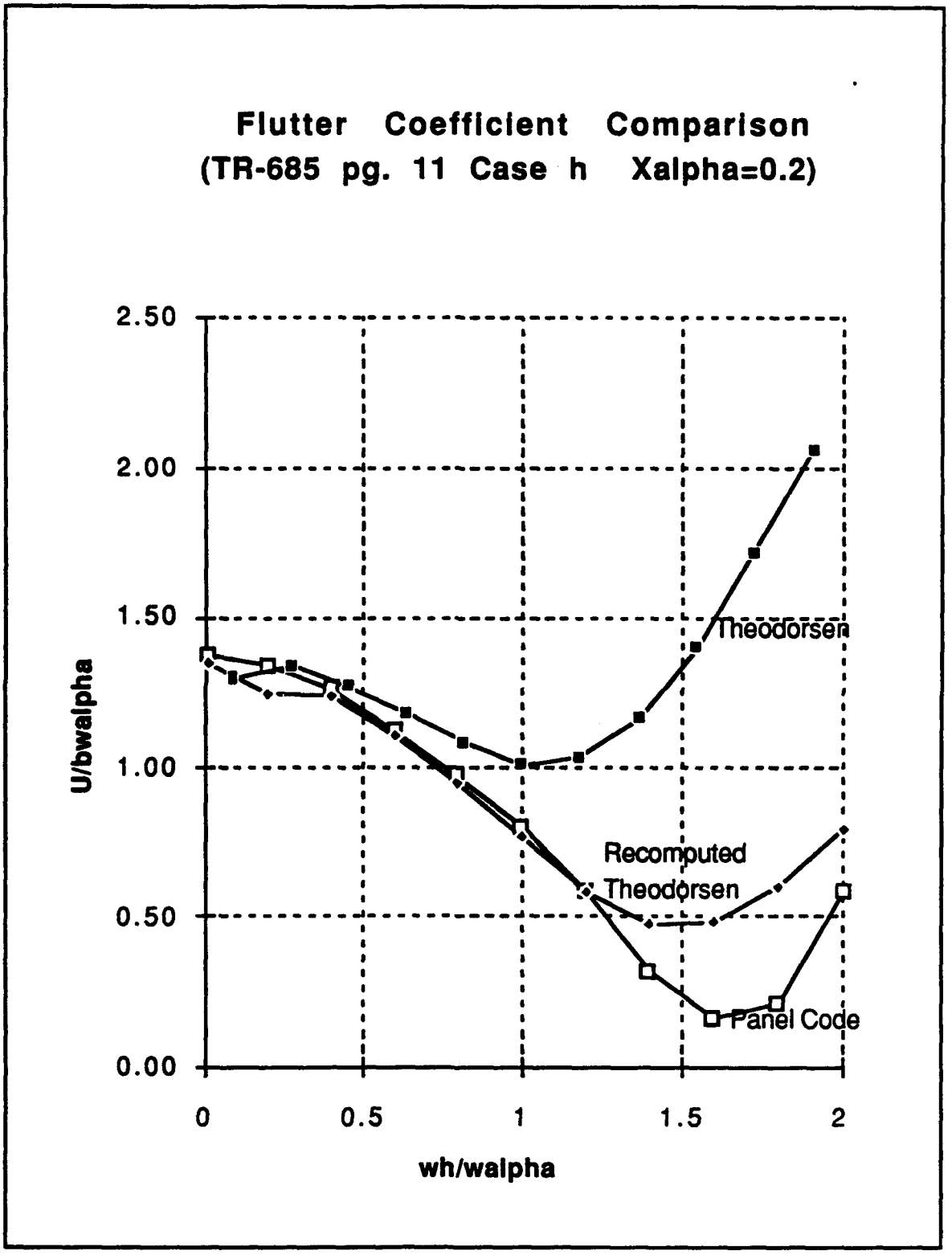

Figure 2.3 Flutter Coefficient Comparison

TABLE 2.2 TR-685 CASE (H) COMPARISON

TR - 685 pg. 11 Case h; mass ratio=4; a =-0.3; Xalpha=0.2			
Panel Code 1 deg pitch; 0.01 h/2b plunge; 200 panels;			
NACA0007; 3 cycles 65 time steps per cycle			
wh/walpha	Published	Numerical	Panel Code
0.01	1.37	1.3474	1.296
0.2	1.34	1.2456	1.341
0.4	1.26	1.2385	1.274
0.6	1.12	1.1088	1.182
0.8	0.97	0.9467	1.078
1.0	0.80	0.7628	1.009
1.2	0.58	0.5854	1.029
1.4	0.32	0.4758	1.162
1.6	0.16	0.4883	1.398
1.8	0.21	0.6015	1.708
2.0	0.58	0.7951	2.058

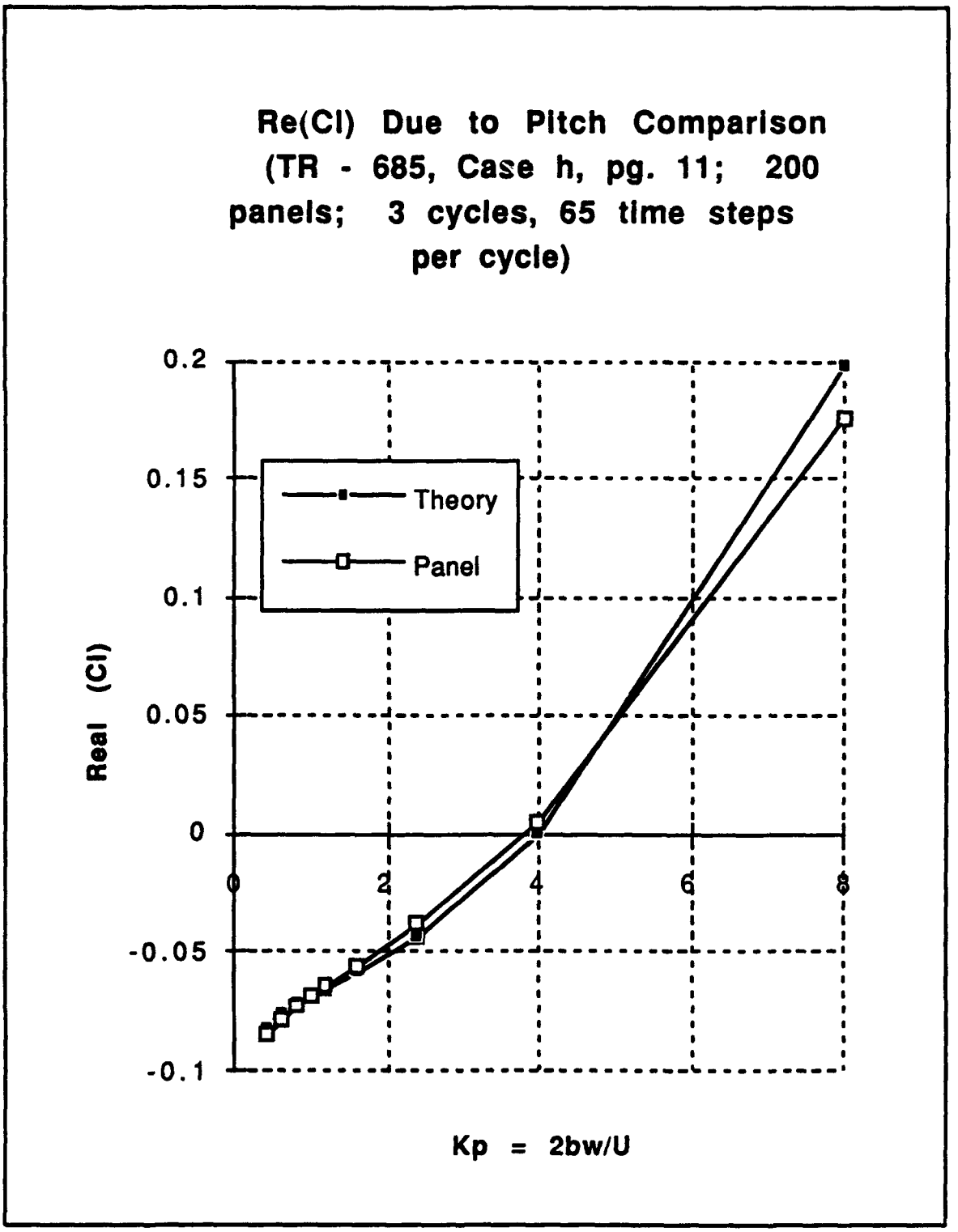

Figure 2.4 Real(Cl) Due to Pitch

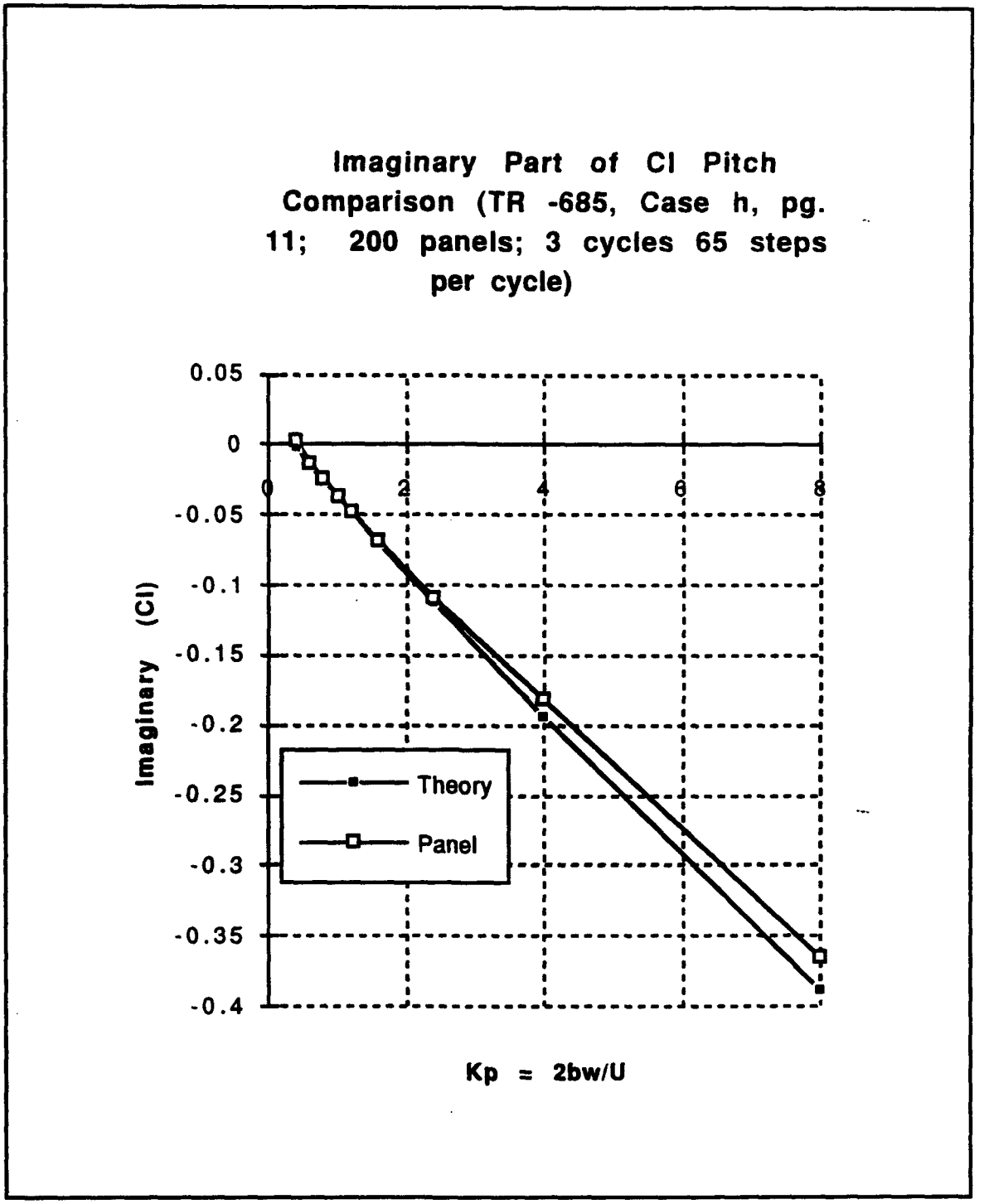

Figure 2.5 Imaginary(Cl) Due to Pitch

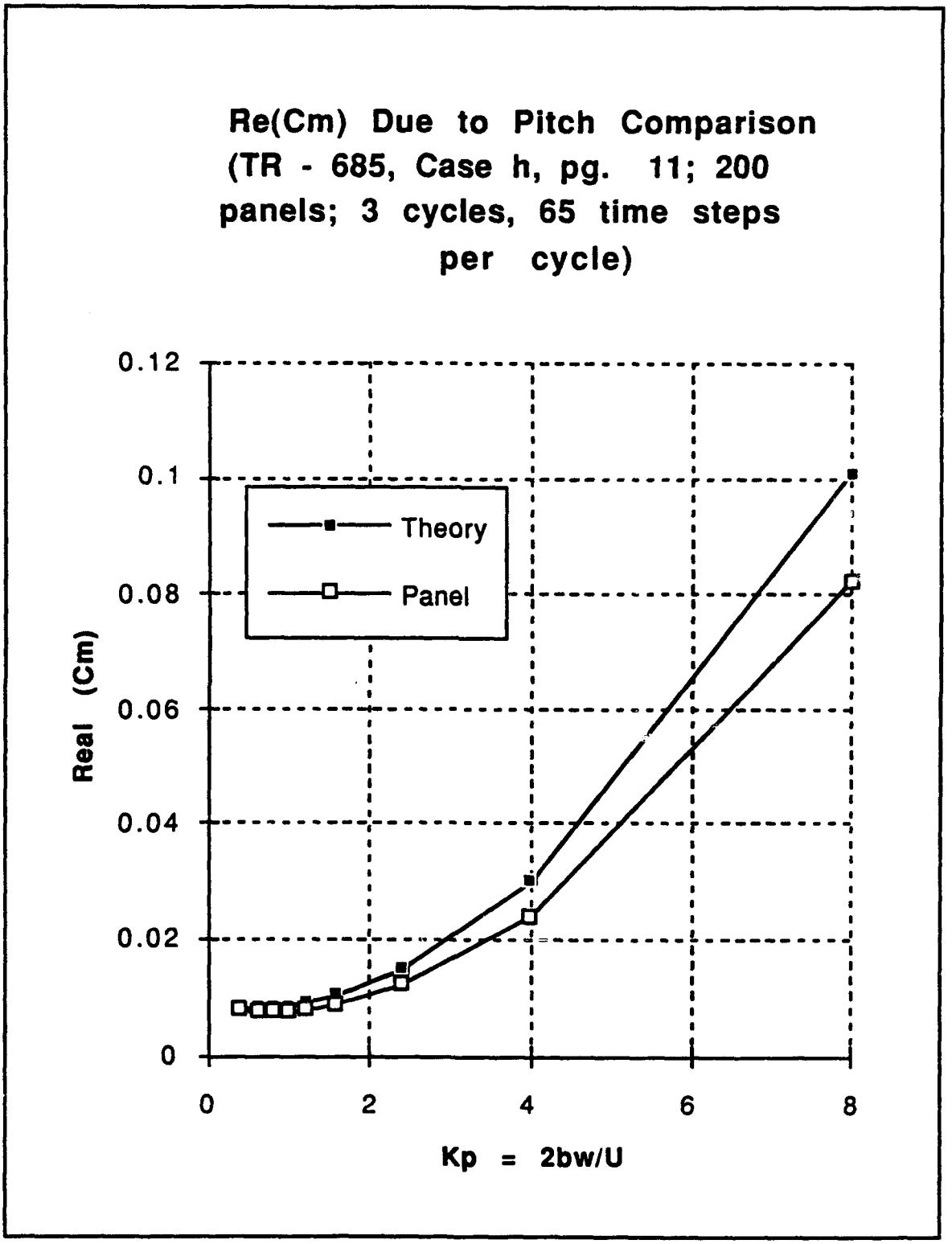

Figure 2.6 Real(Cm) Due to Pitch

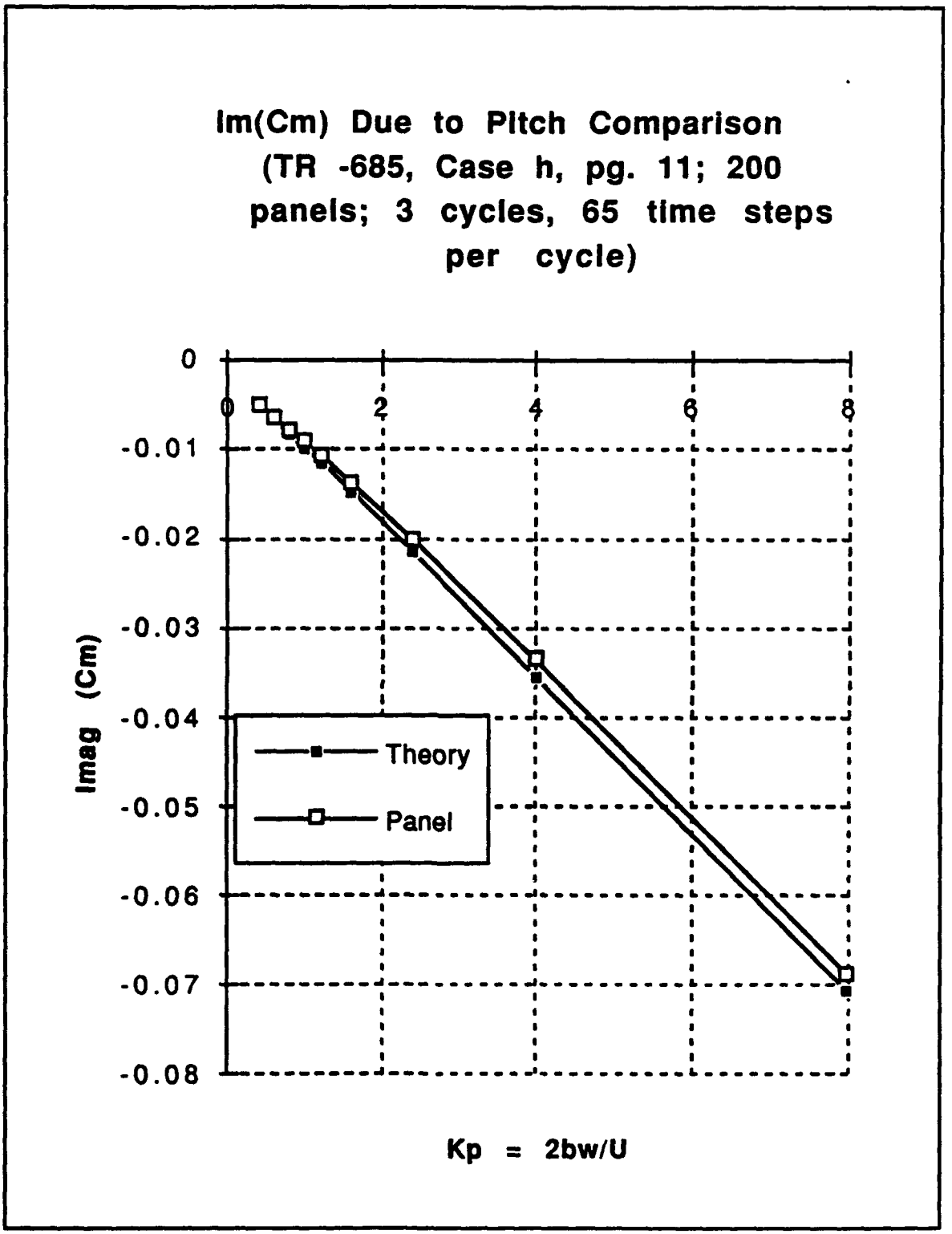

Figure 2.7 Imaginary(Cm) Due to Pitch

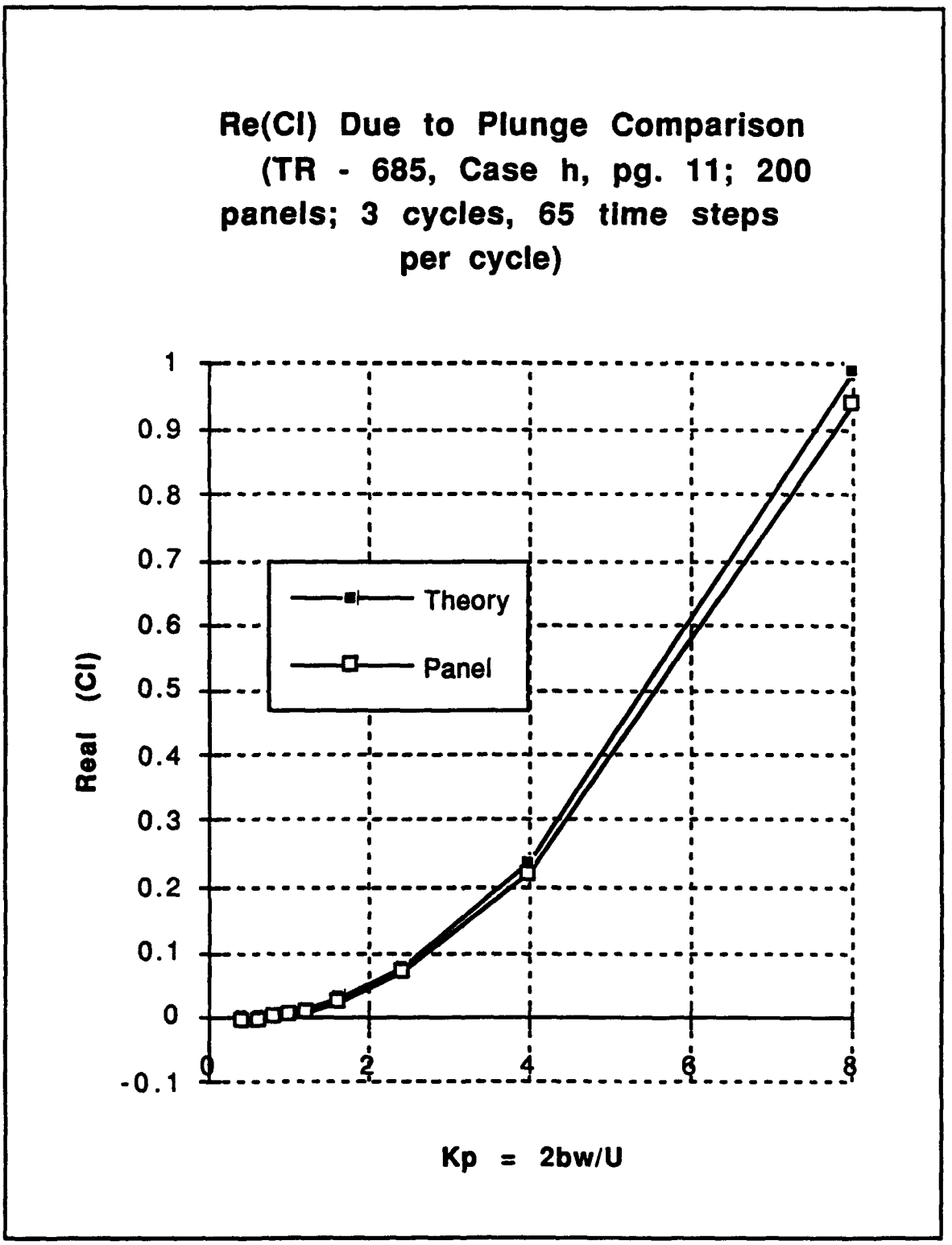

Figure 2.8 Real(Cl) Due to Plunge

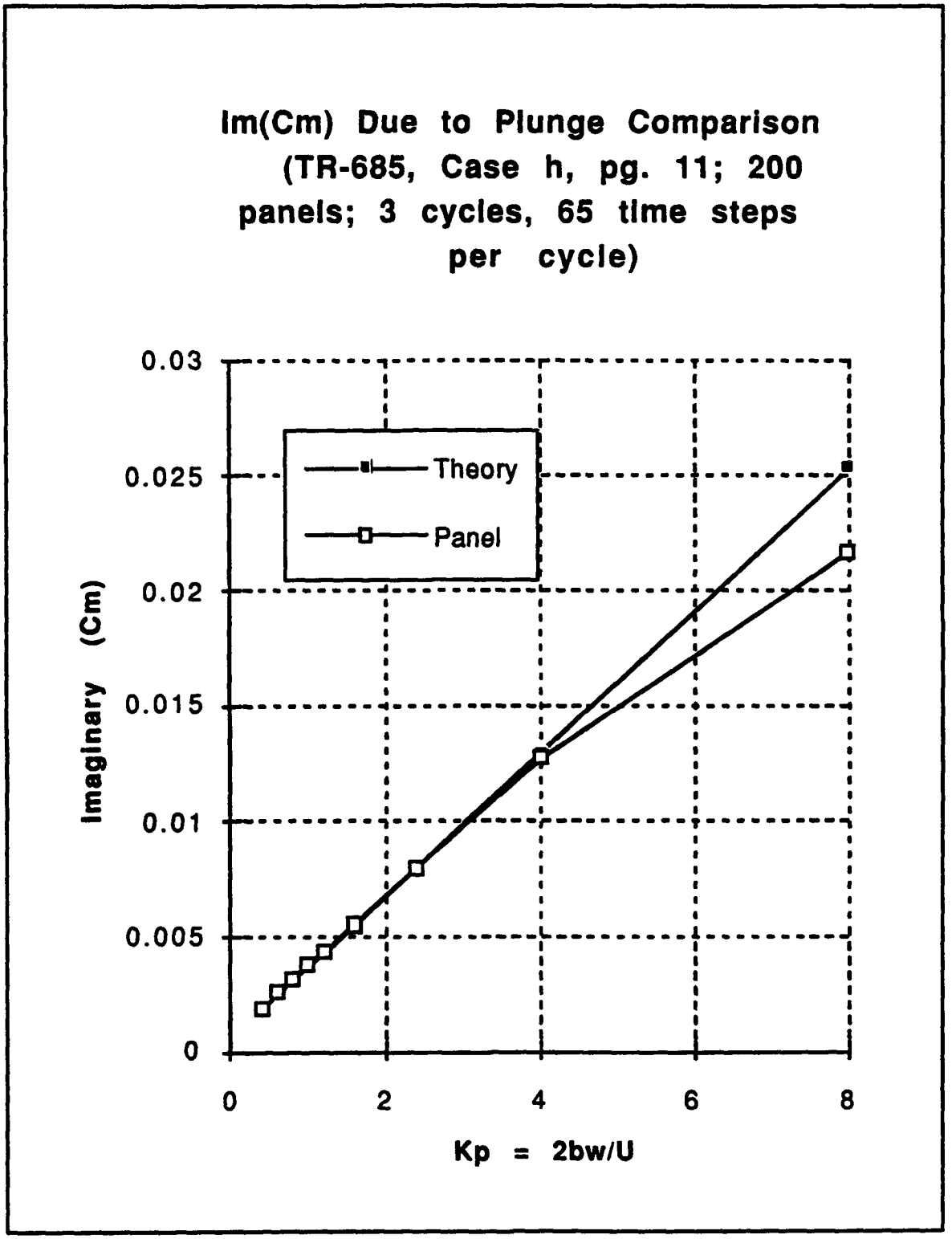

Figure 2.9 Imaginary(Cm) Due to Plunge

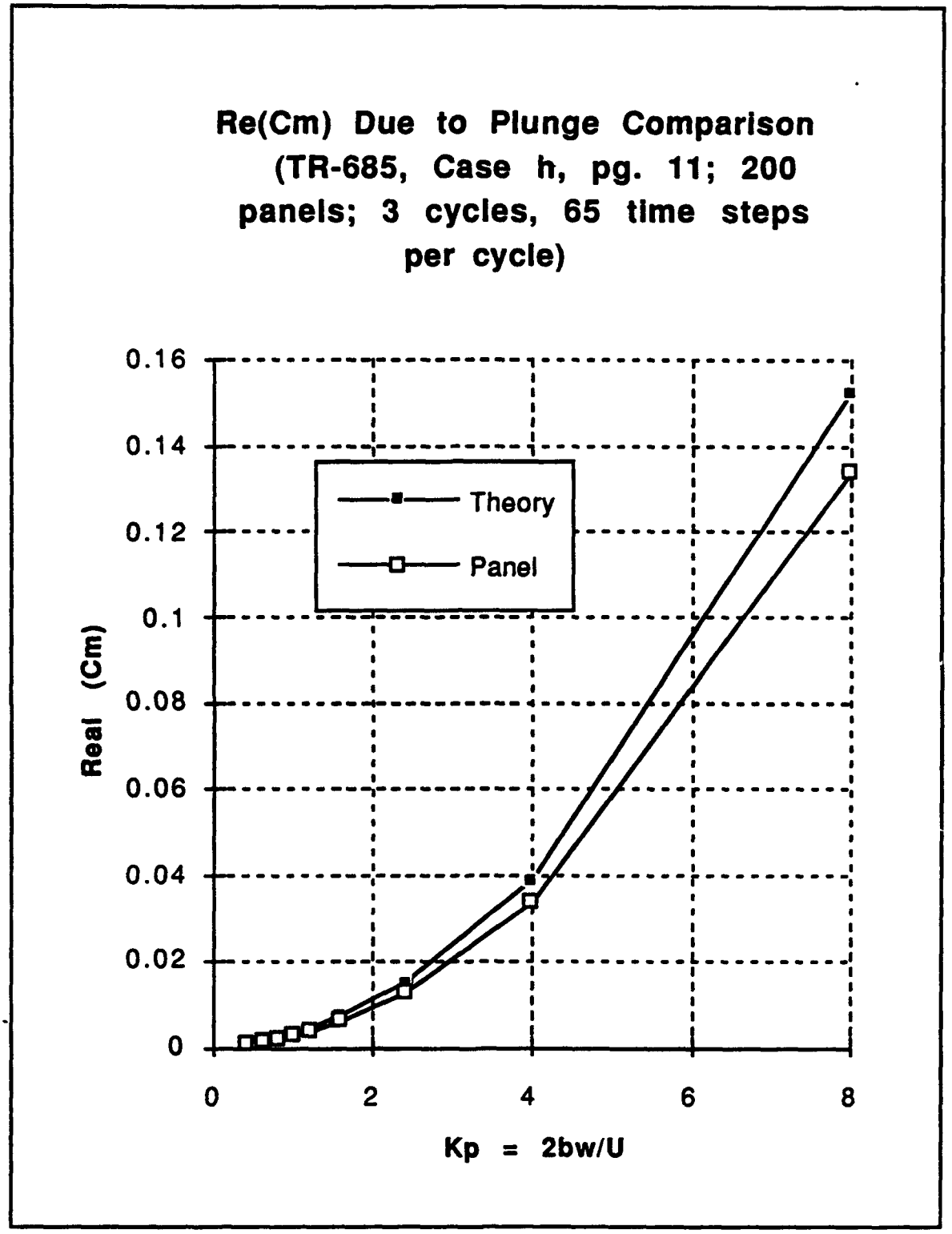

Figure 2.10 Real(Cm) Due to Plunge

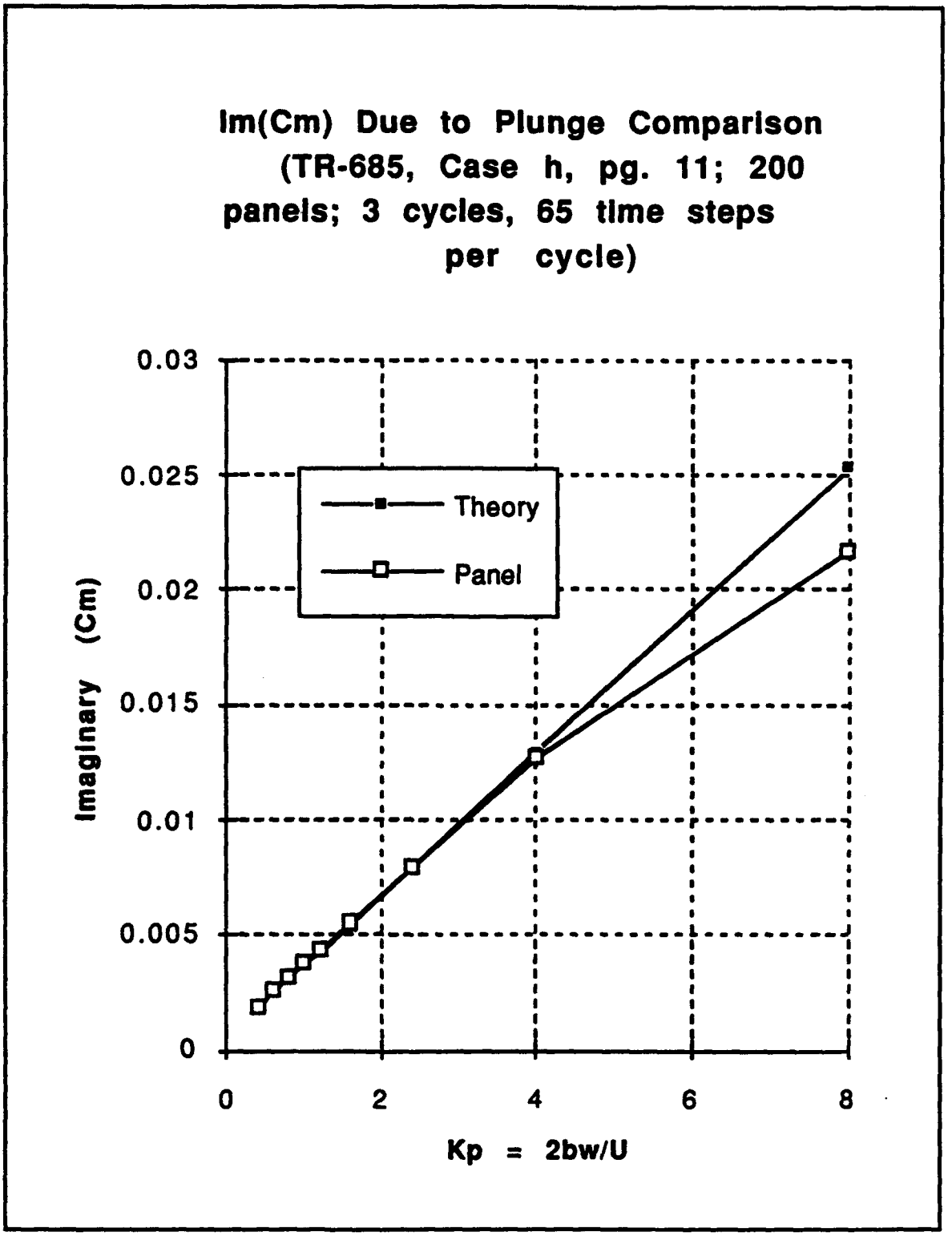

Figure 2.11 Imaginary(Cm) Due to Plunge

TR-685 pg. 11 Case h; mass ratio = 4, a = -0.3, Xalpha = 0.2

Theodorsen Theory for 1 deg pitch and 0.01 h/2b plunge

Kpanel	Cl pitch Real	Cl pitch Imag	Cm pitch Real	Cm pitch Imag	Cl plunge Real	Cl plunge Imag	Cm plunge Real	Cm plunge Imag
0.4	-0.0824	-0.0031	0.0085	-0.0052	-0.0022	-0.0183	0.0009	0.0018
0.6	-0.0762	-0.0143	0.0083	-0.0068	-0.0011	-0.0251	0.0015	0.0025
0.8	-0.0717	-0.0258	0.0084	-0.0084	0.0018	-0.0314	0.0023	0.0031
1.0	-0.0681	-0.0371	0.0087	-0.0100	0.0062	-0.0376	0.0033	0.0038
1.2	-0.0648	-0.0483	0.0092	-0.0116	0.0122	-0.0436	0.0044	0.0044
1.6	-0.0584	-0.0700	0.0107	-0.0149	0.0285	-0.0557	0.0072	0.0056
2.4	-0.0437	-0.1120	0.0152	-0.0217	0.0773	-0.0799	0.0149	0.0080
4.0	-0.0006	-0.1933	0.0302	-0.0355	0.2368	-0.1289	0.0391	0.0129
8.0	0.1972	-0.3894	0.1009	-0.0707	0.9900	-0.2532	0.1523	0.0253

Panel code - 1 deg pitch, .01 (h/2b) plunge, 100 panels top and bottom, 3 cycles 65 calculations, .005 tolerance

Kpanel	Cl pitch Real	Cl pitch Imag	Cm pitch Real	Cm pitch Imag	Cl plunge Real	Cl plunge Imag	Cm plunge Real	Cm plunge Imag
0.4	-0.0854	0.0024	0.0082	-0.0049	-0.0031	-0.0188	0.0008	0.0018
0.6	-0.0785	-0.0129	0.0078	-0.0064	-0.0025	-0.0255	0.0013	0.0025
0.8	-0.0727	-0.0247	0.0077	-0.0078	-0.0002	-0.0319	0.0020	0.0031
1.0	-0.0682	-0.0364	0.0078	-0.0093	0.0028	-0.0380	0.0028	0.0037
1.2	-0.0641	-0.0476	0.0081	-0.0108	0.0089	-0.0442	0.0037	0.0043
1.6	-0.0559	-0.0689	0.0090	-0.0139	0.0236	-0.0566	0.0060	0.0055
2.4	-0.0384	-0.1085	0.0123	-0.0203	0.0688	-0.0821	0.0126	0.0080
4.0	0.0048	-0.1821	0.0241	-0.0337	0.2195	-0.1363	0.0337	0.0127
8.0	0.1759	-0.3648	0.0822	-0.0688	0.9379	-0.2900	0.1340	0.0217

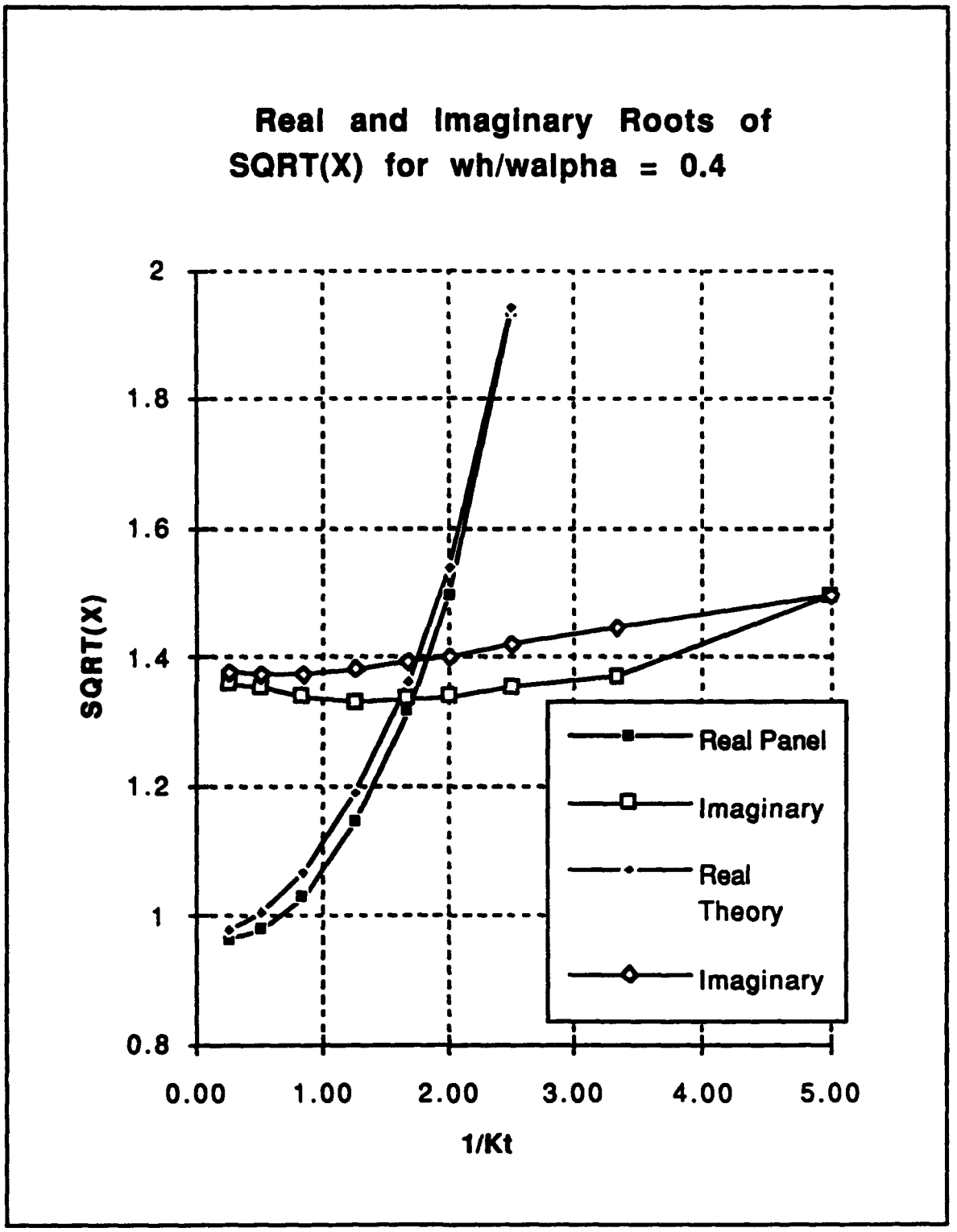

Figure 2.12 Roots for Frequency Ratio of 0.4

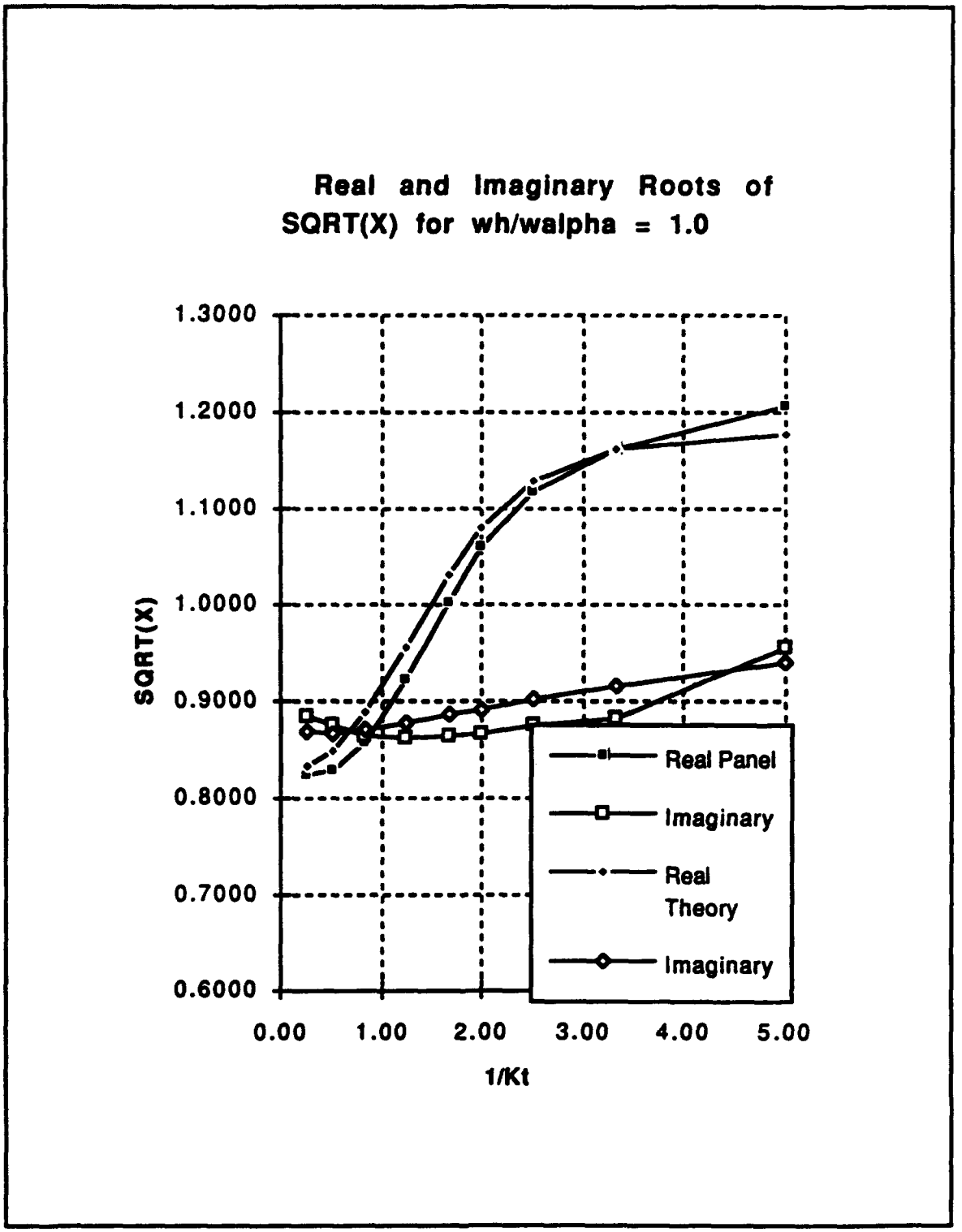

Figure 2.13 Roots for Frequency Ratio of 1.0

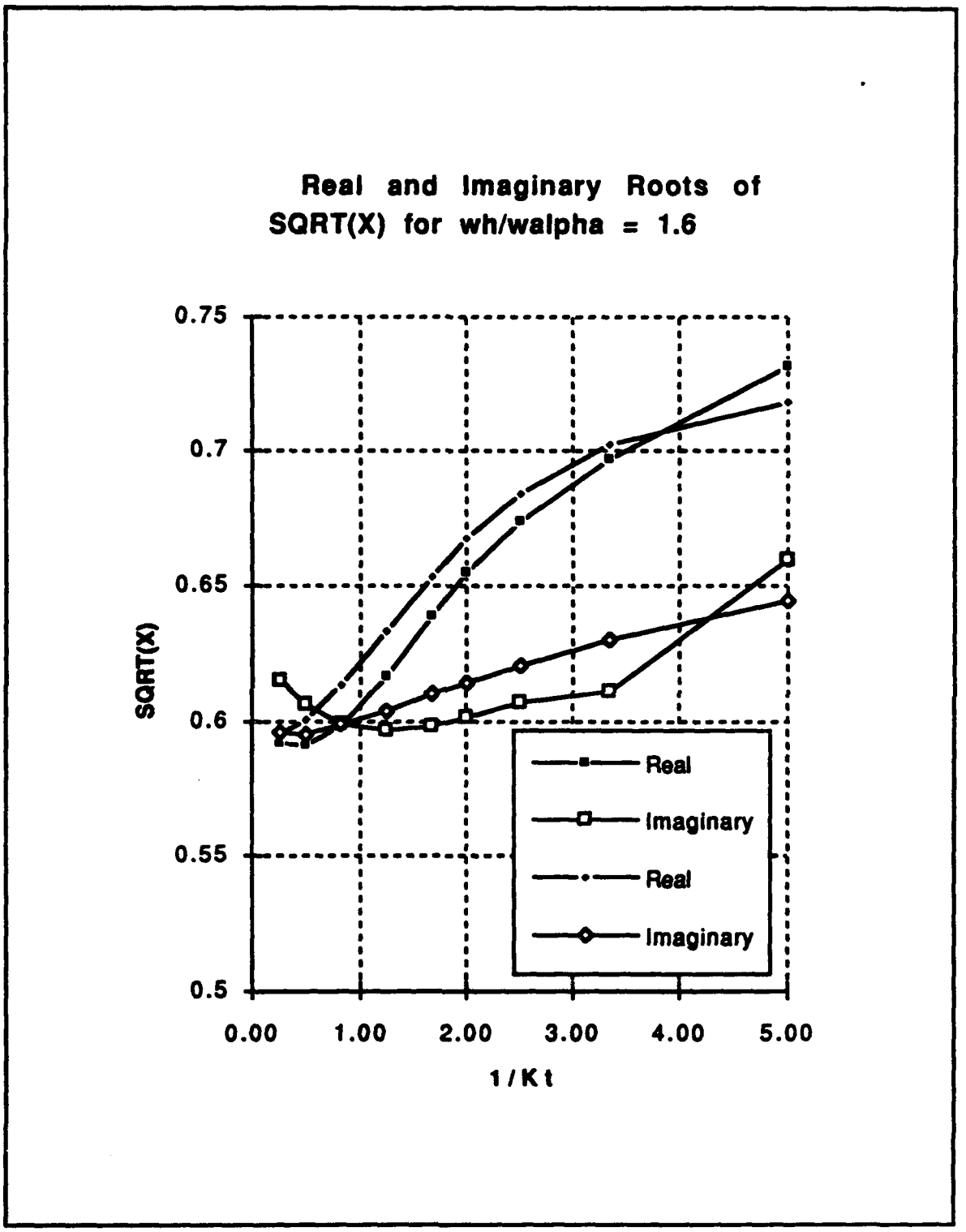

Figure 2.14 Roots for Frequency Ratio of 1.6

TABLE 2.4 SOLUTIONS OF FLUTTER DETERMINANT

The roots SQRT(X) of the real and imaginary equations against 1/Kt.					
TR - 685 pg. 11 Case h; mass ratio = 4; a = -0.3; Xalpha = 0.2;NACA0007					
1 deg pitch; 0.01 h/2b plunge; 200 panels; 3 cycles 65 time steps per cycle;					
		wratio 0.4			
Reduced Frequency		panel		theory	
Kpanel	1/Ktheodorsen	Real Panel	Imaginary	Real Theory	Imaginary
8.0	0.25	0.9628	1.3573	0.9783	1.3793
4.0	0.50	0.9771	1.3533	1.0047	1.3723
2.4	0.83	1.0273	1.3386	1.0675	1.3747
1.6	1.25	1.1422	1.3315	1.1899	1.3820
1.2	1.67	1.3145	1.3338	1.3621	1.3925
1.0	2.00	1.4963	1.3400	1.5403	1.4025
0.8	2.50	1.9345	1.3536	1.9409	1.4187
0.6	3.33		1.3689		1.4465
0.4	5.00		1.4982		1.4974
		wratio 1.0			
Reduced Frequency		panel		theory	
Kpanel	1/Ktheodorsen	Real Panel	Imaginary	Real Theory	Imaginary
8.0	0.25	0.8235	0.8843	0.8317	0.8679
4.0	0.50	0.8293	0.8743	0.8489	0.8661
2.4	0.83	0.8577	0.8642	0.8880	0.8702
1.6	1.25	0.9223	0.8607	0.9561	0.8772
1.2	1.67	1.0026	0.8631	1.0303	0.8852
1.0	2.00	1.0602	0.8672	1.0806	0.8917
0.8	2.50	1.1184	0.8752	1.1293	0.9013
0.6	3.33	1.1628	0.8820	1.1624	0.9160
0.4	5.00	1.2075	0.9556	1.1767	0.9394
		wratio 1.6			
Reduced Frequency		panel		theory	
Kpanel	1/Ktheodorsen	Real	Imaginary	Real	Imaginary
8.0	0.25	0.5915	0.6148	0.5947	0.5958
4.0	0.50	0.5910	0.6059	0.6005	0.5951
2.4	0.83	0.5981	0.5988	0.6130	0.5987
1.6	1.25	0.6167	0.5966	0.6330	0.6041
1.2	1.67	0.6388	0.5985	0.6533	0.6098
1.0	2.00	0.6546	0.6014	0.6675	0.6143
0.8	2.50	0.6737	0.6068	0.6843	0.6208
0.6	3.33	0.6968	0.6107	0.7022	0.6302
0.4	5.00	0.7313	0.6592	0.7184	0.6442

III. AERODYNAMIC COEFFICIENT VERIFICATION OF TWO AIRFOIL CODE

The two airfoil USPOTF2F code was modified for one degree of freedom flutter analysis. This chapter verifies the aerodynamic force and moment coefficients by comparison to flat plate theory.

A. INTRODUCTION TO TWO AIRFOIL PANEL CODE

The USPOTF2F unsteady panel code is essentially the single airfoil UPOT code extended to two airfoils. Airfoil number one is treated as the master airfoil and remains at the origin of a cartesian coordinate system. Airfoil number two may be arbitrarily placed in reference to the master airfoil, as long as the leading airfoil's wake does not impinge upon the trailing airfoil or its wake. All aerodynamic and flutter calculations pertain to the master airfoil.

The phase subroutine computes the complex unsteady aerodynamic coefficients (refer to page 8), then the subroutine writes the coefficients to pitch.in and plunge.in files. Pitch.in contains K_p, Real($C_{L\alpha}$), Imaginary($C_{L\alpha}$), Real($C_{M\alpha}$) and Imaginary($C_{M\alpha}$) tabulated in columns from left to right respectively for single degree of freedom pitch. Plunge.in contains the same information except the coefficients are due to single degree of freedom plunge in simple harmonic motion. The phase subroutine searches the last cycle of the time history of lift and moment for a maximum and minimum value. Average lift and moment coefficients are calculated from $(C_{Lmax} - C_{Lmin})/2$. Each average is then subtracted from the time history respectively before curve fitting to a sine function:

$$F(t) = Amp * \sin(\omega t + \phi)$$

A function of this form assumes a zero average, or equal maximum and minimum magnitudes. Because, the pitch and plunge values start from zero at time equal to zero, thus this initial condition requires a sine function. The phase portion uses the first π radians of the last cycle for curve fitting. Selecting the positive area of the sine curve for integration avoids errors near $\pi/2$ and $3\pi/2$ by not including positive and negative values in the integration interval.

The product of cycles and time steps may not exceed 200 due to array sizing. As a warning to the user, note that the period of the last cycle is based upon the reduced frequency of the master airfoil. If the airfoils are oscillating at different reduced frequencies, the force and moment data for airfoil two in pitch.in and plunge.in files are invalid.

To plot the wake vortices position and airfoil geometry, use the original USPOTF2C code. Fort.10 and fort.11 contain wake vortices position for each time step. Cutting data from the last time step in fort.10 and fort.11, and then pasting the data into separate files will allow for plotting applications.

B. THEORETICAL COEFFICIENT ORIGIN

The theoretical unsteady aerodynamic coefficient values for a flat plate were calculated using the Tables of Subsonic Incompressible Aerodynamic Coefficients from Scanlan and Rosenbaum [Ref. 9] pg. 412. Riester [Ref. 1 pg. 18] derives the complex coefficient of lift and moment values. The constants and equations were programmed in MATLAB [Appendix A] for comparison to USPOTF2F.

C. GEOMETRY FOR SINGLE AIRFOIL COMPARISON

Airfoils are separated by 50 chord lengths with no shift in the horizontal direction. The interaction between the two airfoils is assumed to be negligible at this distance. Inputs of 200 panels for each airfoil, pitch and plunge amplitudes of

one degree and 0.01 chord are used. Riester [Ref. 1] showed that small amplitudes yield more accurate results, especially in plunge at high reduced frequencies. As with UPOTFLUT aerodynamic verification, 3 cycles, 65 time steps per cycle was chosen as a benchmark wake length.

D. AERODYNAMIC VERIFICATION

The comparison between theory and USPOTF2F code is presented in Figures 3.3 through 3.18 and Tables 2.1 through 2.4. For clarity, the computed aerodynamic coefficients are presented in phasor form as a magnitude and phase angle vice complex form. Phasor form allows for easier identification of errors.

It is seen that the panel code results are in agreement with theory. Magnitude errors are less than five percent and phase error typically ranged from one to three degrees. A portion of the error may be attributed to comparison of an airfoil of finite thickness to a theoretical flat plate.

```
NUMBER OF LINES FOR TITLE
          1
TWO NACA0007  OCSILLATING AIRFOILS

IFLAG    NLOWER  NUPPER
  0        75      75
NAIRFO, XSHIFT , YSHIFT, SCALE
  2        0       -100    1.0
NACA AIRFOIL TYPE,
         7
         7
ALP1    ALP2     DALP1  DALP2  TCON1  TCON2
 0.0     0.0      0.0    0.0    0.0    0.0
FREQ1    FREQ2    PIVOT1   PIVOT2
 3.0      3.0      0.0      0.0
UGUST VGUST DELHX1 DELHX2 DELHY1 DELHY2 PHASE1 PHASE2
 0.0   0.0   0.0    0.0    0.1     0.1   0.0     0.0
 TF   DTS1  DTS2   TOL    TADJ  SCL  SCM  SGAM  NGIES
  6   65   0.0    .001    0.0  0.0  0.0  0.0    1
STEADY    OUTPUT
 false      false

STEADY--TRUE IF ONLY STEADY SOLUTION. FALSE OTHERWISE.
OUTPUT--TRUE IF YOU WANT COMPLETE OUTPUT TO SCREEN.
IFLAG  :  0 IF AIRFOIL IS NACA XXXX OR 230XX
          1 OTHERWISE.
NLOWER :  NO. OF PANELS USED ON BOTH AIRFOIL LOWER SURFACES.
NUPPER :  NO. OF PANELS USED ON BOTH AIRFOIL UPPER SURFACES.
NAIRFO :  NUMBER OF AIRFOILS.
XSHIFT :  RELATIVE X DIST. FROM 2 AIRFOIL PIVOT POSITION WRT
          GLOBAL COORDINATE SYSTEM.
YSHIFT :  RELATIVE Y DIST. FROM 2 AIRFOIL PIVOT POSITION WRT
          GLOBAL COORDINATED SYSTEM.
NACA AIRFOIL TYPE : ENTER NACA 4 OR 5 DIGIT CODE FOR AIRFOILS.,
                    IF NOT A NACA AIRFOIL, SUPPLY AIRFOIL
                    X(I),Y(I) COORDS. FOR BOTH AIRFOILS IN
                    FILE CODE 2.
ALP1/2  : INITIAL ANGLE OF ATTACK FOR AIRFOILS IN DEGREES.
DALP1/2 : CHANGE IN AOA IN DEGREE FOR NON OSCILL. MOTION.
          MAX AMPLITUDE OF AOA IN DEGREE FOR ROT. HARMONIC MOTION.
TCON1/2 : NON-DIMENSIONAL RISE TIME (Vinf.t/C) OF AOA FOR
          MODIFIED RAMP CHANGE IN AOA.
FREQ1/2 : NON DIMENSIONAL OSCILL. (WC/Vinf.) FOR HARMONIC MOTIONS.
PIVOT1/2: LENGTH FROM LEADING EDGE TO PIVOT POINT FOR LOCAL SYSTEM.
          (THE GLOBAL SYSTEM'S ORGIN IS THE FIRST AIRFOILS PIVOT POSITION
UGUST   : MAG. OF NON-DIM. GUST VELOCITY ALONG GLOBAL X DIRECTION.
VGUST   : MAG. OF NON-DIM. GUST VELOCITY ALONG GLOBAL Y DIRECTION.
DELHX1/2: NON-DIM. TRANSLATIONAL CHORDWISE AMPLITUDE.
DELHY1/2: NON-DIM. TRANSLATIONAL TRANSVERSE AMPLITUDE (plunging).
PHASE1/2: PHASE ANGLE IN DEGREE BETWEEN CHORDWISE AND TRANSVERSE
          TRANSLATIONAL OSCILL. WITH THE LATTER REF. TO THAT AIRFOIL.
TF      : FINAL NON-DIM. TIME TO TERMINATE UNSTEADY FLOW SOLUTION.
DTS     : STARTING TIME STEP FOR NON-OCIILL MOTIONS(TADJ=0).
          NO. OF COMPUTAIONAL STEPS PER CYCLE FOR HARMONIC MOTION
          (FOR 2 FREQ OCILL. IT USES THE LARGEST FREQ)
          BASELINE TIME STEP FOR ALL MOTIONS(TADJ NOT =0)
DTS2    : STARTING NON-DIM TIME FOR SECOND AIRFOIL MOTION TO BEGIN.
          (0 TO BEGIN MOTION AT THE SAME TIME).
TOL     : TOLERANCE CRIERION FOR CONVERGENCE FOR (Uw)k and (Vw)k.
TADJ    : FACTOR BY WHICH DTS WILL BE ADJUSTED.
SCLA    : STEADY LIFT COEFF. FOR THE SINGLE AIRFOIL AT THE SPEC. AOA.
SCM     : STEADY MOMENT COEFF. FOR THE SINGLE AIRFOIL.
SGAM    : STEADY VORTICITY STRENGTH FOR THE SINGLE AIRFOIL.
NGIES   : OPTION TO CHANGE THE UNSTEADY KUTTA CONDITION.
          0 EQUAL PRESSURE AT THE TRAILING EDGE PANELS.
```

Figure 3.1 USPOTF2C Input Namelist for Wake Analysis (Original)

```
NUMBER OF LINES FOR TITLE
          1
TWO NACA0007  OCSILLATING AIRFOILS

IFLAG   NLOWER  NUPPER
   0      100      100
NAIRFO, XSHIFT , YSHIFT, SCALE
  2      -43.98        -25       1.0
NACA AIRFOIL TYPE,
         7
         7
FREQ1   FREQ2  DALP1     DALP2
  0.1     0.1     1.0       1.0
FREQSTEP1    FREQSTEP2    PIVOT1    PIVOT2
  0.0          0.0        0.0       0.0
FINALFREQ1   FINALFREQ2   DELHY1    DELHY2
  0.05          0.05        0.01      0.01
CYCLES  DTS1  DTS2     TOL     TADJ    SCL    SCM    SGAM    NGIES
  3      65   0.0     0.001   0.0     0.0    0.0    0.0      1
STEADY      OUTPUT
 false      false

STEADY--TRUE IF ONLY STEADY SOLUTION. FALSE OTHERWISE.
OUTPUT--TRUE IF YOU WANT COMPLETE OUTPUT TO SCREEN.
IFLAG   :  0 IF AIRFOIL IS NACA XXXX OR 230XX
           1 OTHERWISE.
NLOWER  :  NO. OF PANELS USED ON BOTH AIRFOIL LOWER SURFACES.
NUPPER  :  NO. OF PANELS USED ON BOTH AIRFOIL UPPER SURFACES.
NAIRFO  :  NUMBER OF AIRFOILS.
XSHIFT  :  RELATIVE X DIST. FROM 2 AIRFOIL PIVOT POSITION WRT
           GLOBAL COORDINATE SYSTEM.
YSHIFT  :  RELATIVE Y DIST. FROM 2 AIRFOIL PIVOT POSITION WRT
           GLOBAL COORDINATED SYSTEM.
NACA AIRFOIL TYPE : ENTER NACA 4 OR 5 DIGIT CODE FOR AIRFOILS.,
                    IF NOT A NACA AIRFOIL, SUPPLY AIRFOIL
                    X(I),Y(I) COORDS. FOR BOTH AIRFOILS IN
                    FILE CODE 2.
DALP1/2 : CHANGE IN AOA IN DEGREE FOR NON OSCILL. MOTION.
          MAX AMPLITUDE OF AOA IN DEGREE FOR ROT. HARMONIC MOTION.
FREQ1/2 : NON DIMENSIONAL OSCILL. (WC/Vinf.) FOR HARMONIC MOTIONS.
PIVOT1/2: LENGTH FROM LEADING EDGE TO PIVOT POINT FOR LOCAL SYSTEM.
          (THE GLOBAL SYSTEM'S ORGIN IS THE FIRST AIRFOILS PIVOT POSITION
DELHY1/2: NON-DIM. TRANSLATIONAL TRANSVERSE AMPLITUDE (plunging).
DTS     : STARTING TIME STEP FOR NON-OCILL MOTIONS(TADJ=0).
          NO. OF COMPUTAIONAL STEPS PER CYCLE FOR HARMONIC MOTION
          (FOR 2 FREQ OCILL. IT USES THE LARGEST FREQ)
          BASELINE TIME STEP FOR ALL MOTIONS(TADJ NOT =0)
DTS2    : STARTING NON-DIM TIME FOR SECOND AIRFOIL MOTION TO BEGIN.
          (0 TO BEGIN MOTION AT THE SAME TIME).
TOL     : TOLERANCE CRIERION FOR CONVERGENCE FOR (Uw)k and (Vw)k.
TADJ    : FACTOR BY WHICH DTS WILL BE ADJUSTED.
SCLA    : STEADY LIFT COEFF. FOR THE SINGLE AIRFOIL AT THE SPEC. AOA.
SCM     : STEADY MOMENT COEFF. FOR THE SINGLE AIRFOIL.
SGAM    : STEADY VORTICITY STRENGTH FOR THE SINGLE AIRFOIL.
NGIES   : OPTION TO CHANGE THE UNSTEADY KUTTA CONDITION.
          0 EQUAL PRESSURE AT THE TRAILING EDGE PANELS.
          1 EQUAL TANGENTAL VELOCITIES AT THE TRAILING EDGE PANELS.
```

Figure 3.2 USPOTF2F Input Namelist for Flutter Analysis (Modified)

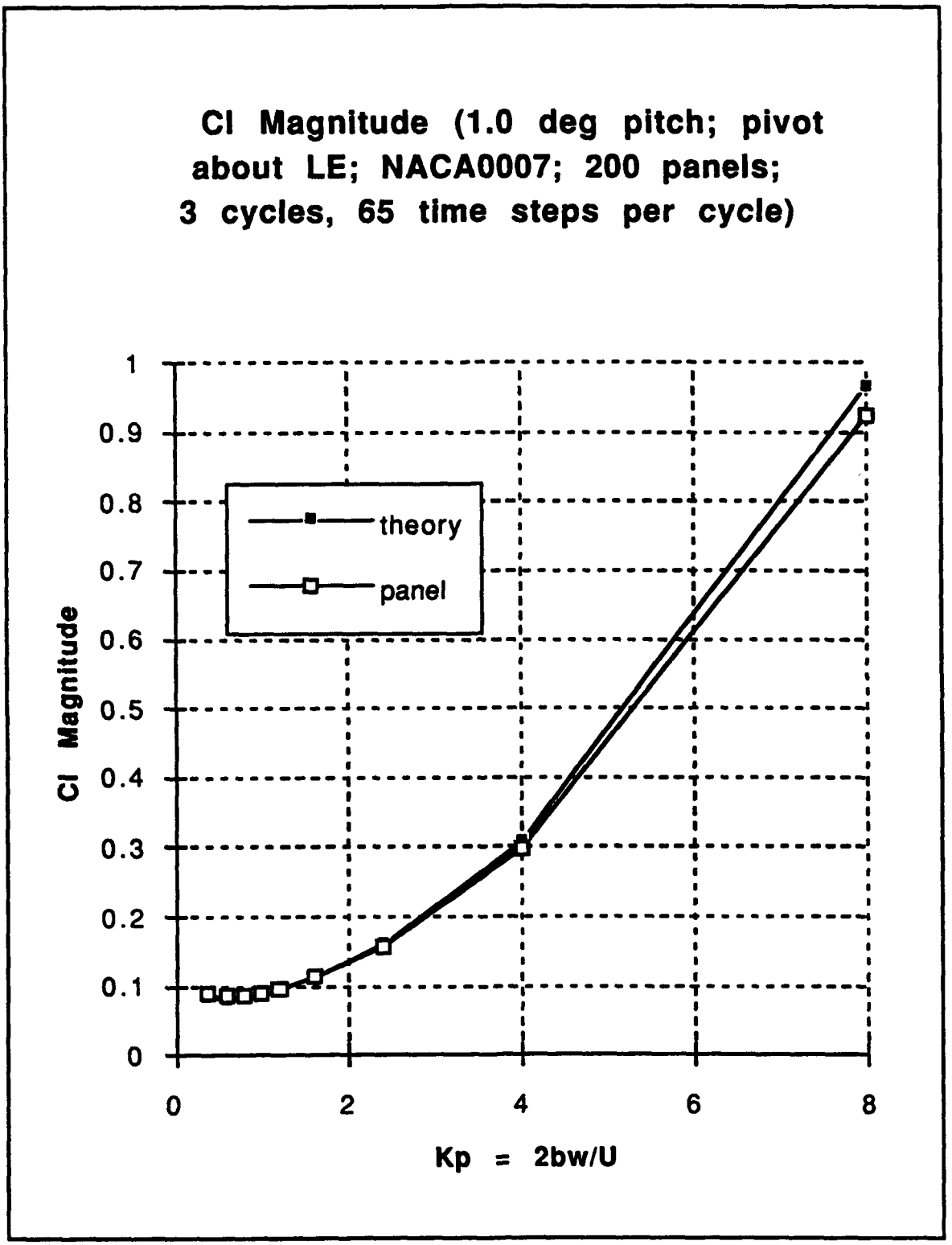

Figure 3.3 Cl Magnitude for Pitch about Leading Edge

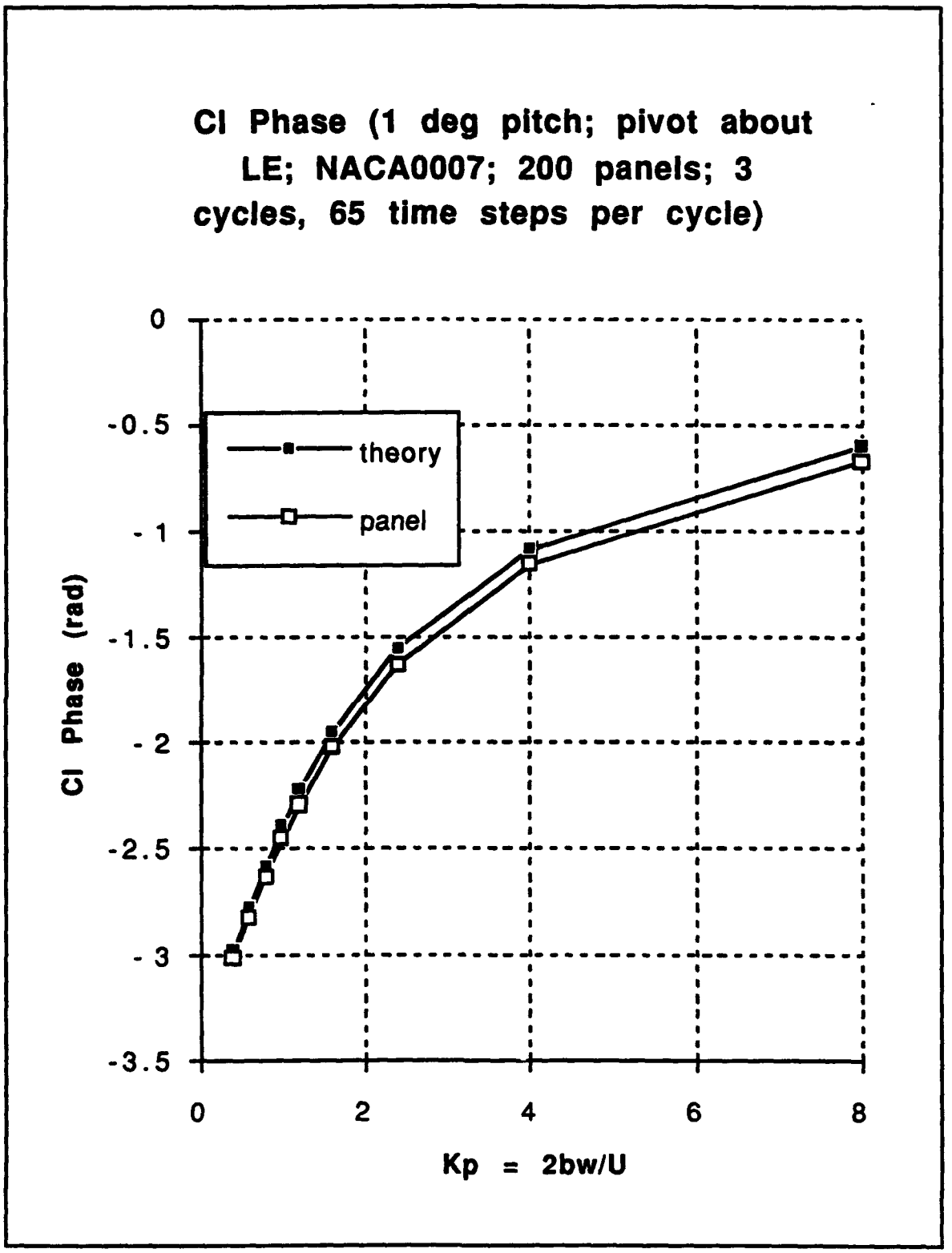

Figure 3.4 Cl Phase for Pitch about Leading Edge

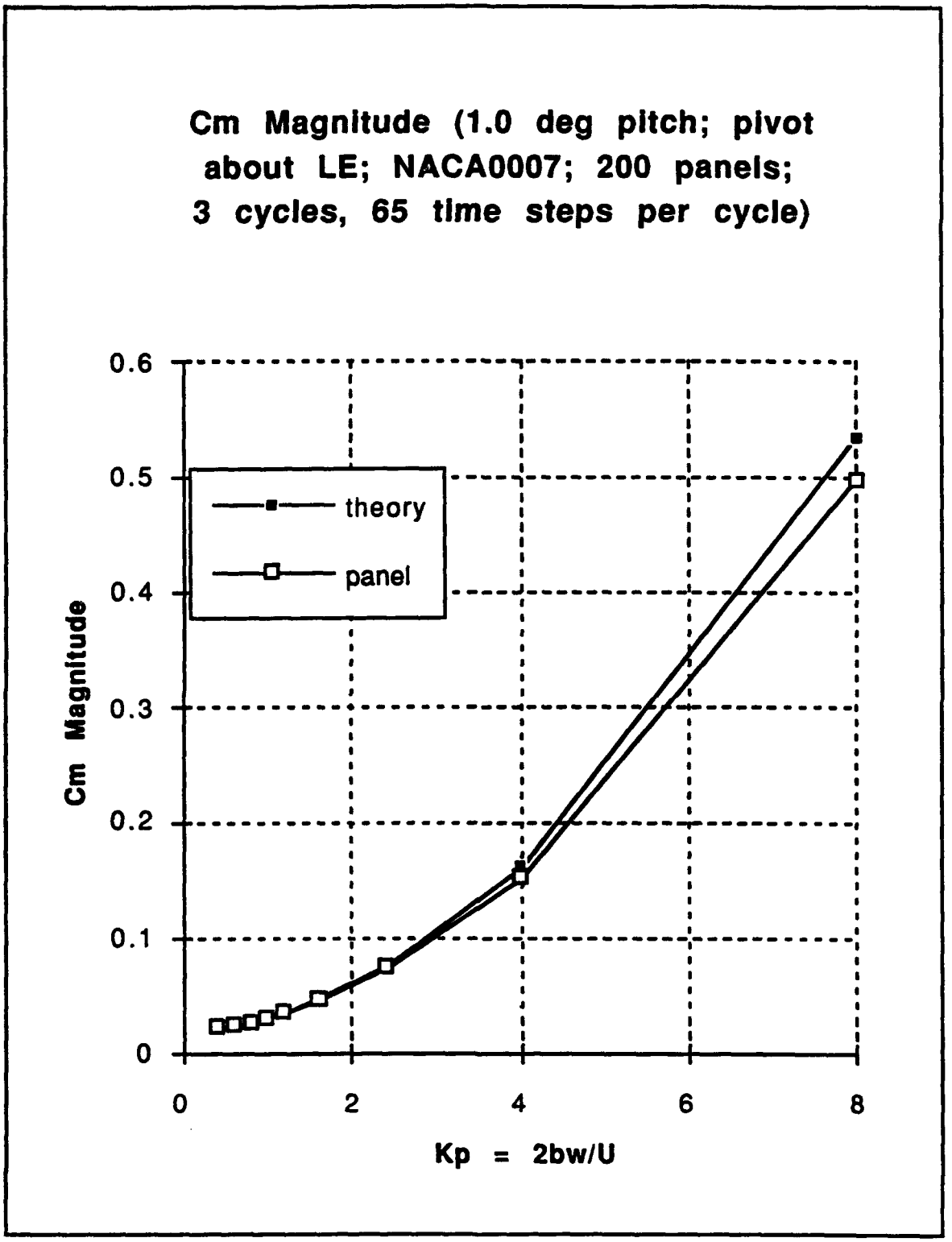

Figure 3.5 Cm Magnitude for Pitch about Leading Edge

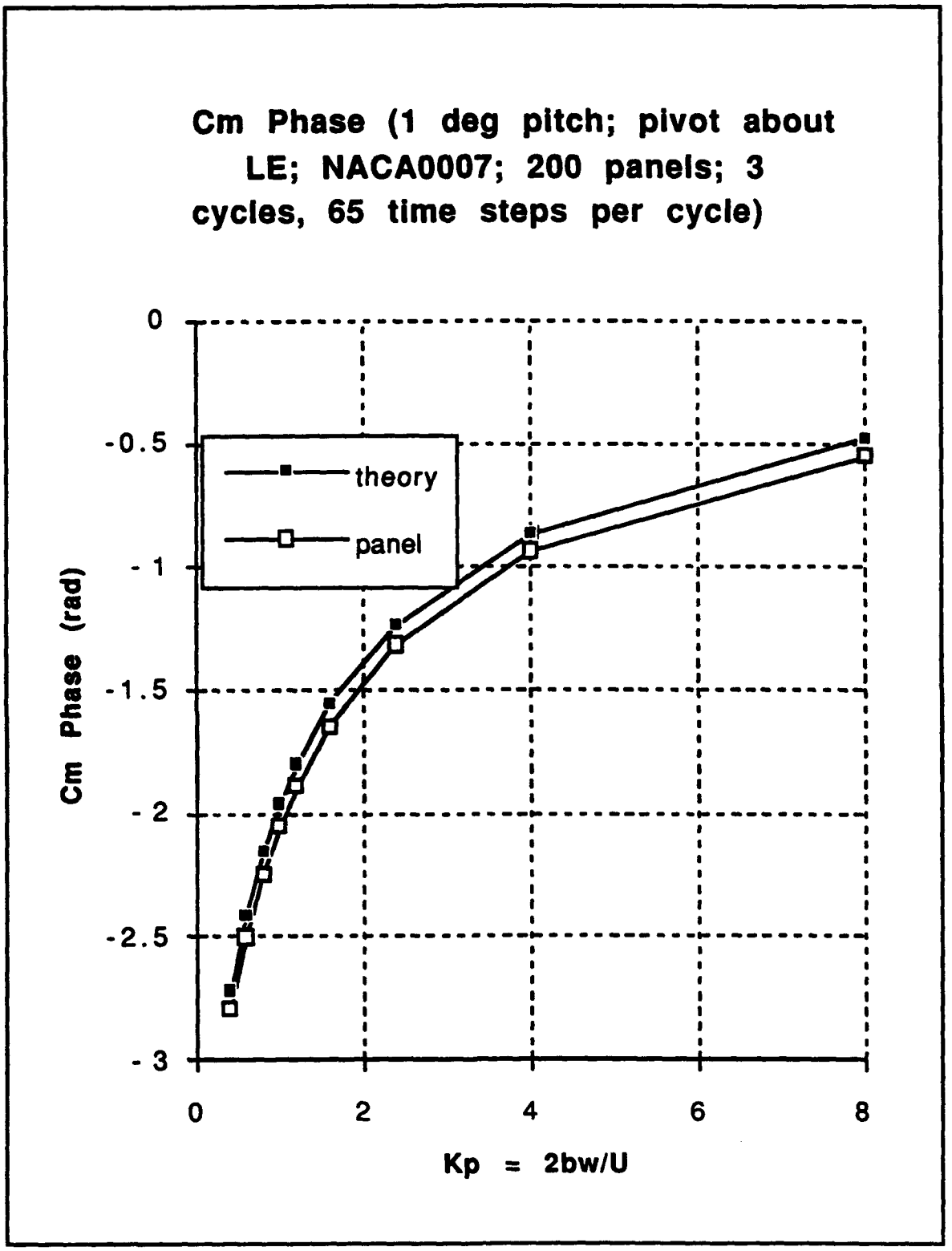

Figure 3.6 Cm Phase for Pitch about Leading Edge

TABLE 3.1 PITCH OSCILLATION PIVOT L.E.

PITCH OSCILLATION PIVOT 0.0 (Leading Edge)
1 deg; 3 cycles; 65 time steps/cycle; 100 panels top and bottom

	CL Magnitude			CL Phase			CM Magnitude			CM Phase		
Kp	theory	panel		theory	panel		theory	panel		theory	panel	
0.4	0.0850	0.0883	3.84%	-2.9735	-3.0036	0.96%	0.0222	0.0233	4.85%	-2.7221	-2.7872	2.07%
0.6	0.0823	0.0849	3.13%	-2.7738	-2.8158	1.34%	0.0236	0.0242	2.34%	-2.4174	-2.5018	2.69%
0.8	0.0837	0.0857	2.37%	-2.5747	-2.6262	1.64%	0.0267	0.0268	0.41%	-2.1622	-2.2537	2.91%
1.0	0.0880	0.0894	1.59%	-2.3899	-2.4490	1.88%	0.0310	0.0306	1.21%	-1.9600	-2.0526	2.94%
1.2	0.0943	0.0953	1.01%	-2.2240	-2.2887	2.06%	0.0361	0.0352	2.38%	-1.7989	-1.8903	2.91%
1.6	0.1118	0.1116	0.22%	-1.9463	-2.0177	2.27%	0.0479	0.0461	3.71%	-1.5559	-1.6436	2.79%
2.4	0.1608	0.1577	1.94%	-1.5489	-1.6242	2.39%	0.0774	0.0734	5.22%	-1.2345	-1.3162	2.60%
4.0	0.3079	0.2964	3.73%	-1.0838	-1.1550	2.27%	0.1613	0.1509	6.45%	-0.8656	-0.9394	2.35%
8.0	0.9692	0.9253	4.53%	-0.5961	-0.6869	2.25%	0.5345	0.4973	6.97%	-0.4776	-0.5512	2.34%

	CL Real		CL Imag		CM Real		CM Imag	
Kp	theory	panel	theory	panel	theory	panel	theory	panel
0.4	-0.0838	-0.0874	-0.0142	-0.0121	-0.0203	-0.0218	-0.0090	-0.0081
0.6	-0.0768	-0.0804	-0.0296	-0.0272	-0.0177	-0.0194	-0.0156	-0.0144
0.8	-0.0706	-0.0746	-0.0450	-0.0422	-0.0149	-0.0169	-0.0222	-0.0208
1.0	-0.0643	-0.0688	-0.0601	-0.0571	-0.0118	-0.0142	-0.0287	-0.0271
1.2	-0.0573	-0.0627	-0.0749	-0.0717	-0.0082	-0.0111	-0.0352	-0.0335
1.6	-0.0410	-0.0482	-0.1040	-0.1006	0.0007	-0.0034	-0.0479	-0.0460
2.4	0.0035	-0.0084	-0.1608	-0.1575	0.0256	0.0185	-0.0731	-0.0710
4.0	0.1441	0.1197	-0.2721	-0.2712	0.1046	0.0891	-0.1228	-0.1218
8.0	0.8020	0.7270	-0.5441	-0.5723	0.4747	0.4236	-0.2457	-0.2604

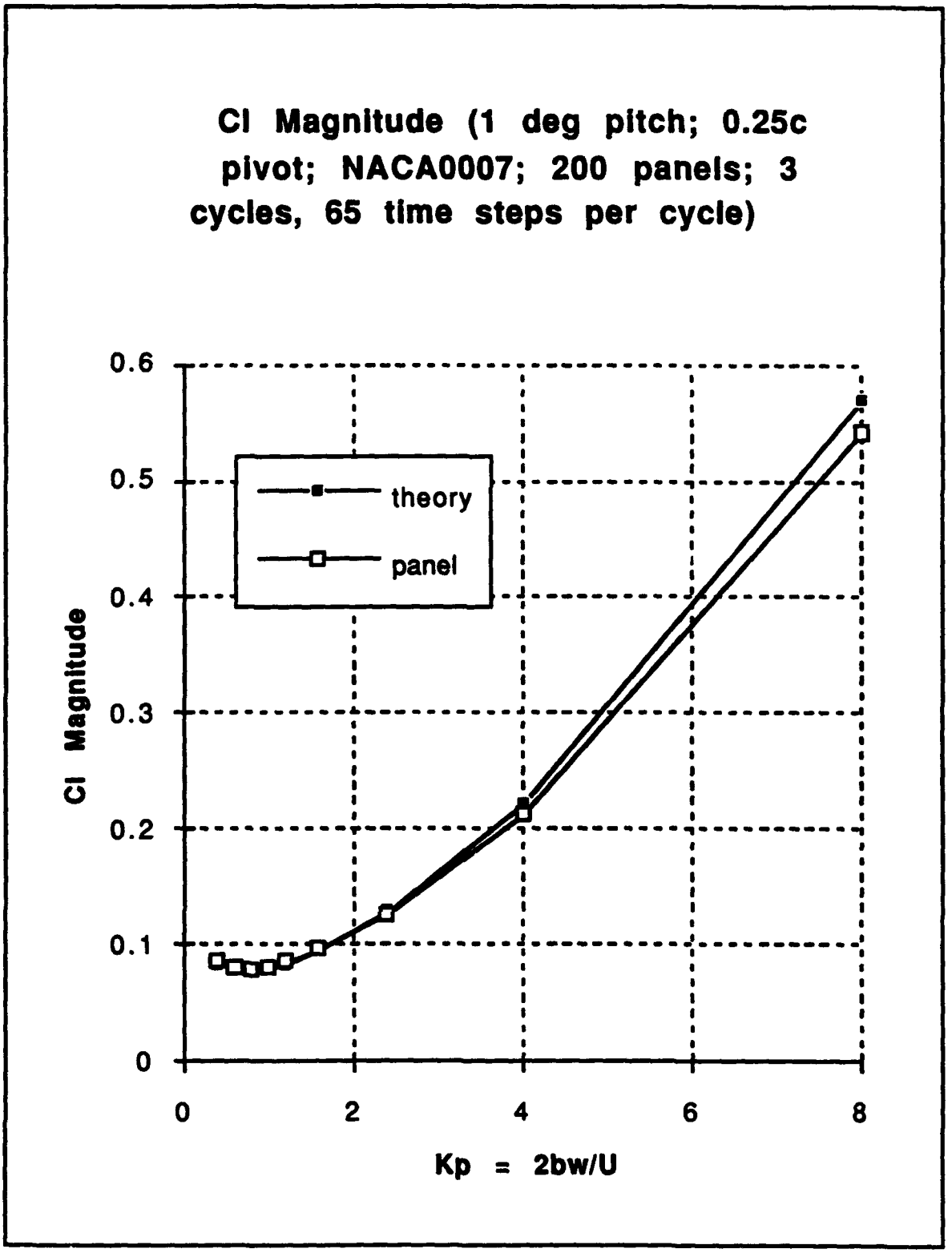

Figure 3.7 Cl Magnitude for Pitch about 1/4 Chord

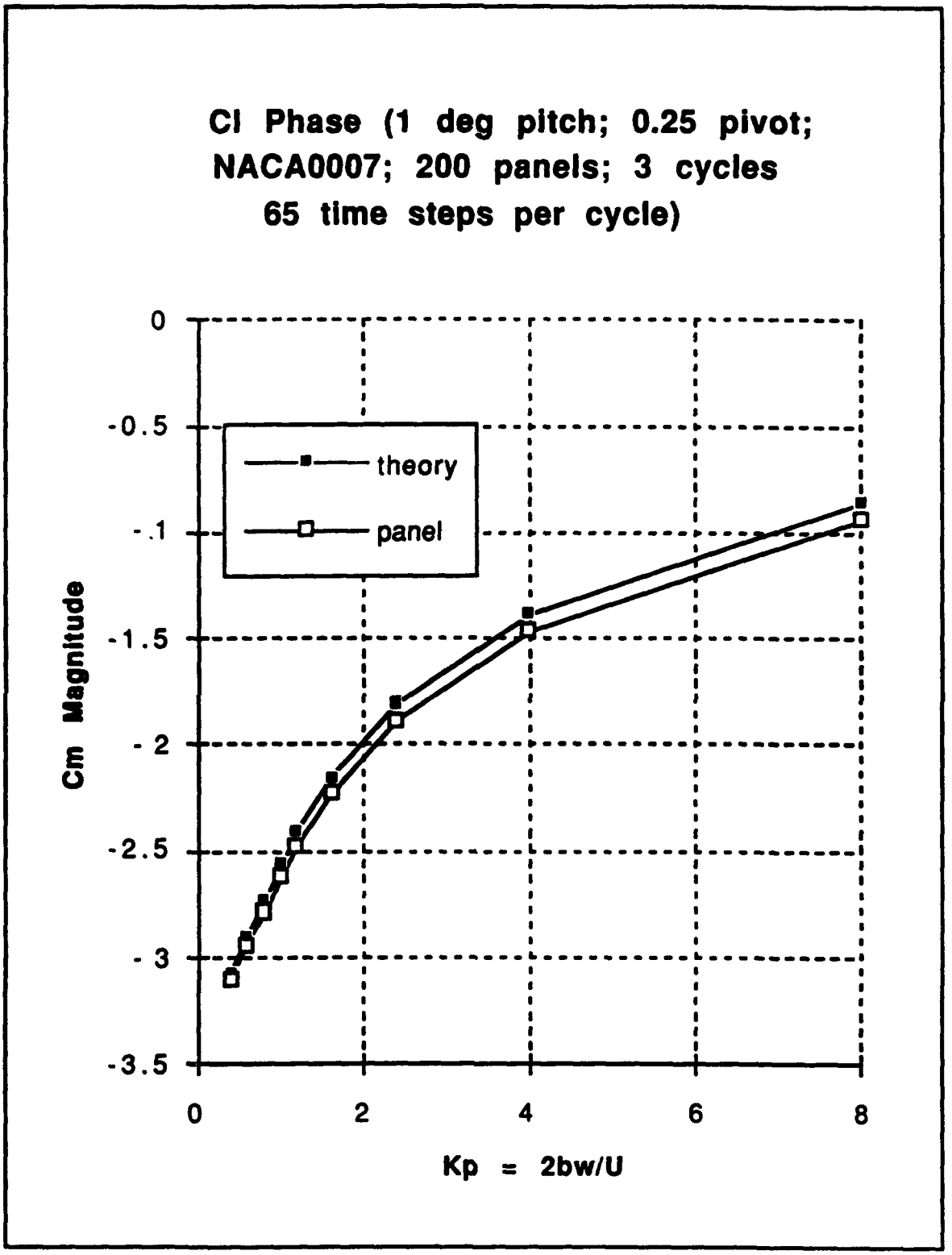

Figure 3.8 Cl Phase for Pitch about 1/4 Chord

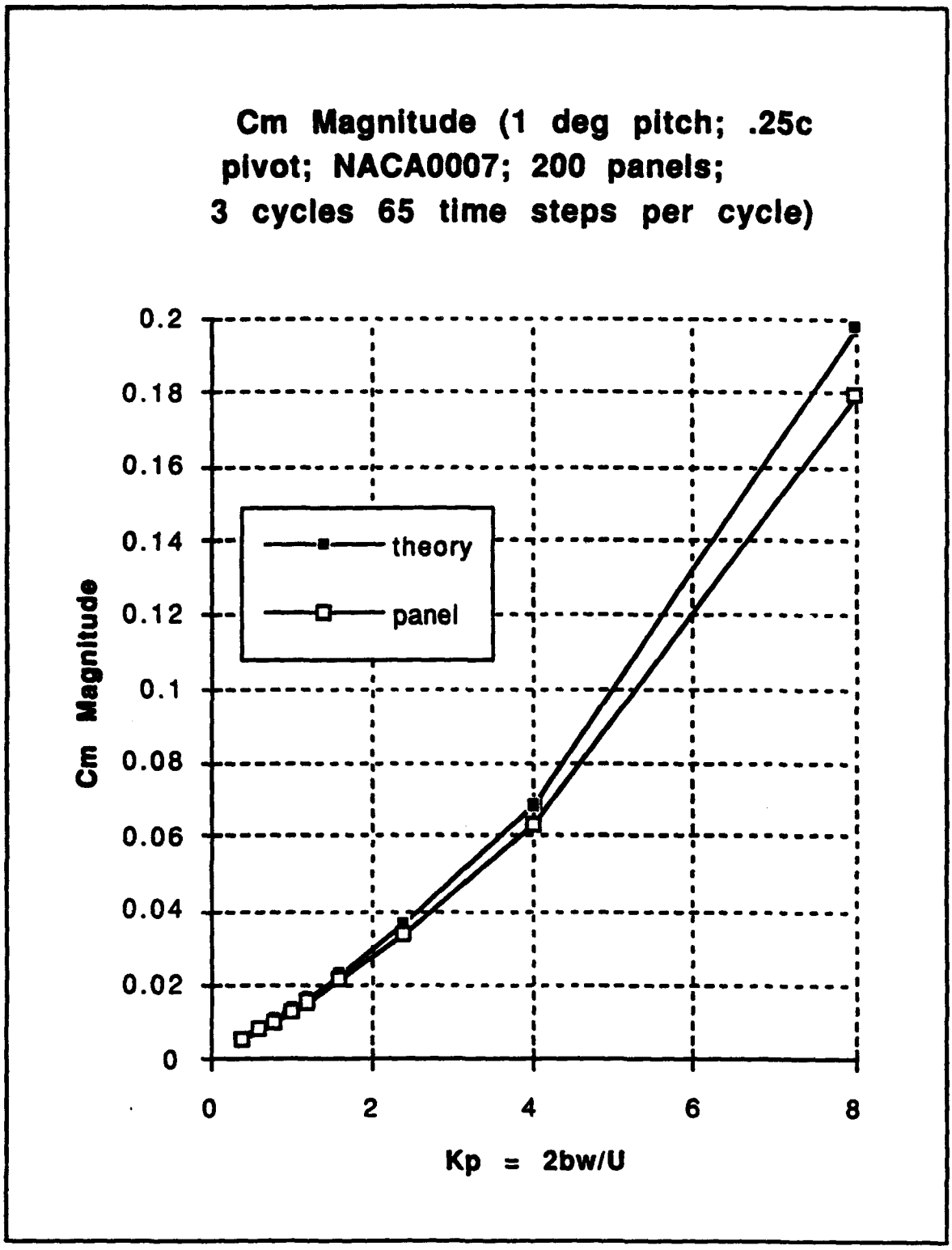

Figure 3.9 Cm Magnitude for Pitch about 1/4 Chord

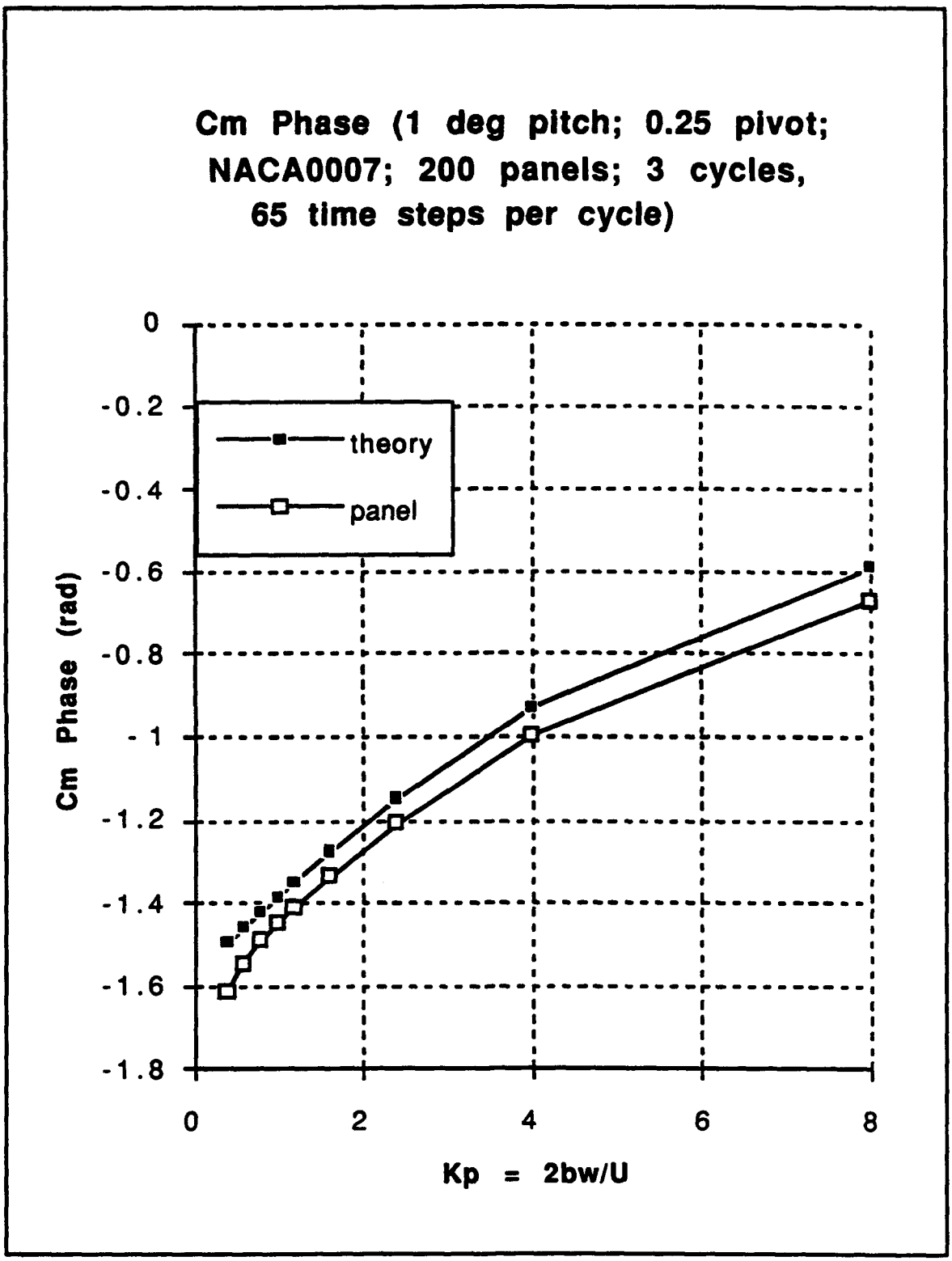

Figure 3.10 Cm Phase for Pitch about 1/4 Chord

TABLE 3.2 PITCH OSCILLATION PIVOT 1/4 CHORD

PITCH OSCILLATION PIVOT 0.25 (1/4 chord)
1 deg; 3 cycles; 65 time steps/cycle; 100 panels top and bottom

	CL Magnitude			CL Phase			CM Magnitude			CM Phase		
Kp	theory	panel		theory	panel		theory	panel		theory	panel	
0.4	0.0831	0.0863	3.81%	-3.0664	-3.1050	1.23%	0.0055	0.0050	9.22%	-1.4959	-1.6139	3.75%
0.6	0.0786	0.0811	3.13%	-2.9019	-2.9439	1.34%	0.0083	0.0076	8.93%	-1.4588	-1.5436	2.70%
0.8	0.0779	0.0798	2.42%	-2.7289	-2.7809	1.65%	0.0111	0.0102	8.36%	-1.4219	-1.4928	2.26%
1.0	0.0800	0.0813	1.64%	-2.5638	-2.6236	1.90%	0.0139	0.0128	7.63%	-1.3854	-1.4498	2.05%
1.2	0.0840	0.0848	0.98%	-2.4135	-2.4791	2.09%	0.0169	0.0156	7.95%	-1.3495	-1.4109	1.95%
1.6	0.0960	0.0959	0.15%	-2.1614	-2.2345	2.32%	0.0229	0.0212	7.52%	-1.2793	-1.3394	1.91%
2.4	0.1295	0.1273	1.70%	-1.8061	-1.8853	2.52%	0.0361	0.0334	7.56%	-1.1479	-1.2110	2.01%
4.0	0.2196	0.2120	3.48%	-1.3842	-1.4657	2.59%	0.0685	0.0630	8.01%	-0.9273	-0.9972	2.23%
8.0	0.5700	0.5408	5.12%	-0.8643	-0.9487	2.68%	0.1977	0.1794	9.26%	-0.5880	-0.6665	2.50%

	CL Real		CL Imag		CM Real		CM Imag	
Kp	theory	panel	theory	panel	theory	panel	theory	panel
0.4	-0.0828	-0.0862	-0.0062	-0.0032	0.0004	-0.0002	-0.0055	-0.0050
0.6	-0.0764	-0.0795	-0.0187	-0.0159	0.0009	0.0002	-0.0082	-0.0076
0.8	-0.0714	-0.0747	-0.0313	-0.0282	0.0016	0.0008	-0.0110	-0.0101
1.0	-0.0670	-0.0706	-0.0437	-0.0403	0.0026	0.0015	-0.0137	-0.0127
1.2	-0.0627	-0.0669	-0.0559	-0.0522	0.0037	0.0025	-0.0164	-0.0154
1.6	-0.0534	-0.0590	-0.0797	-0.0755	0.0066	0.0049	-0.0219	-0.0206
2.4	-0.0302	-0.0394	-0.1259	-0.1211	0.0148	0.0117	-0.0329	-0.0312
4.0	0.0408	0.0222	-0.2158	-0.2108	0.0411	0.0342	-0.0548	-0.0529
8.0	0.3700	0.3152	-0.4336	-0.4395	0.1645	0.1410	-0.1097	-0.1109

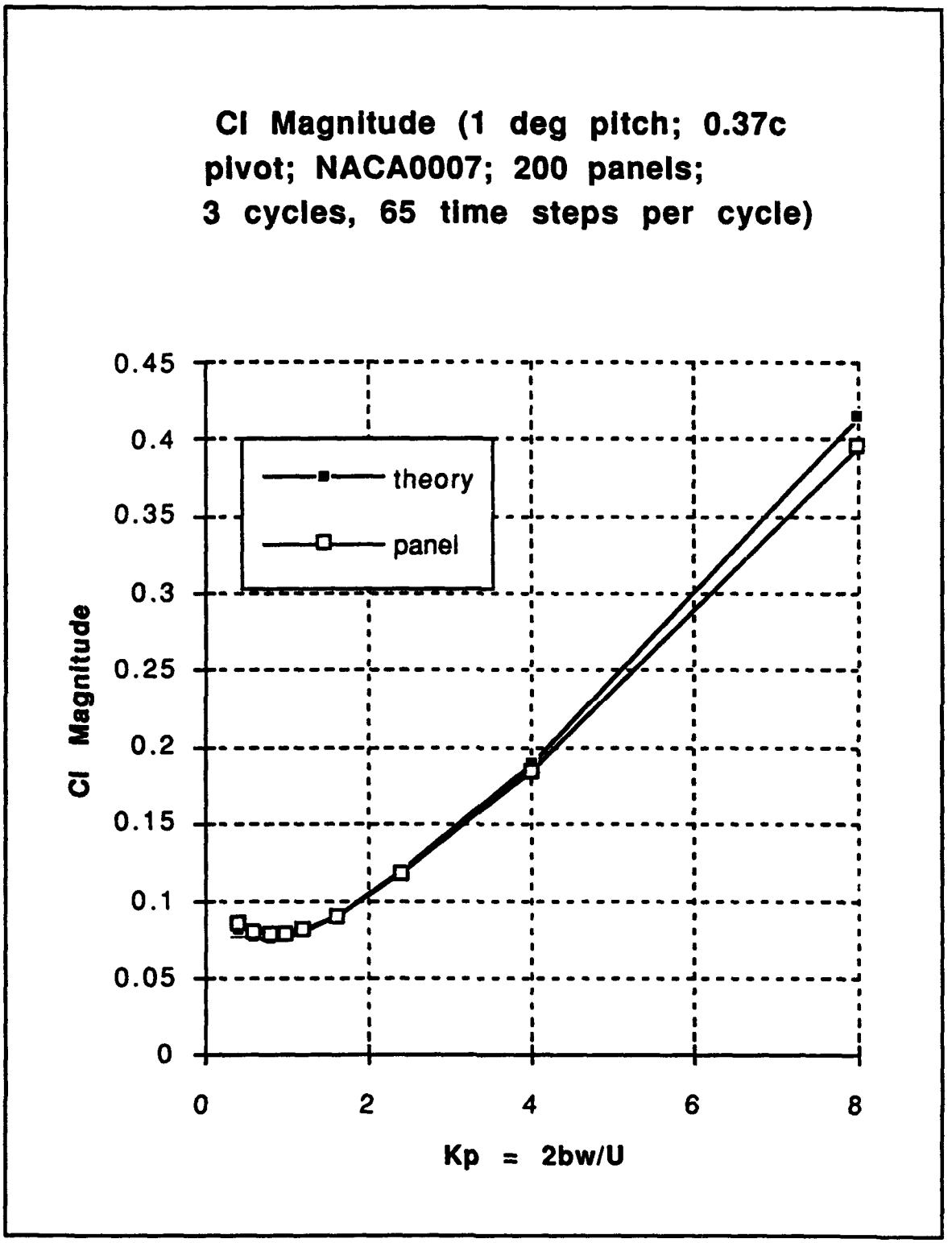

Figure 3.11 Cl Magnitude for Pitch about 0.37c

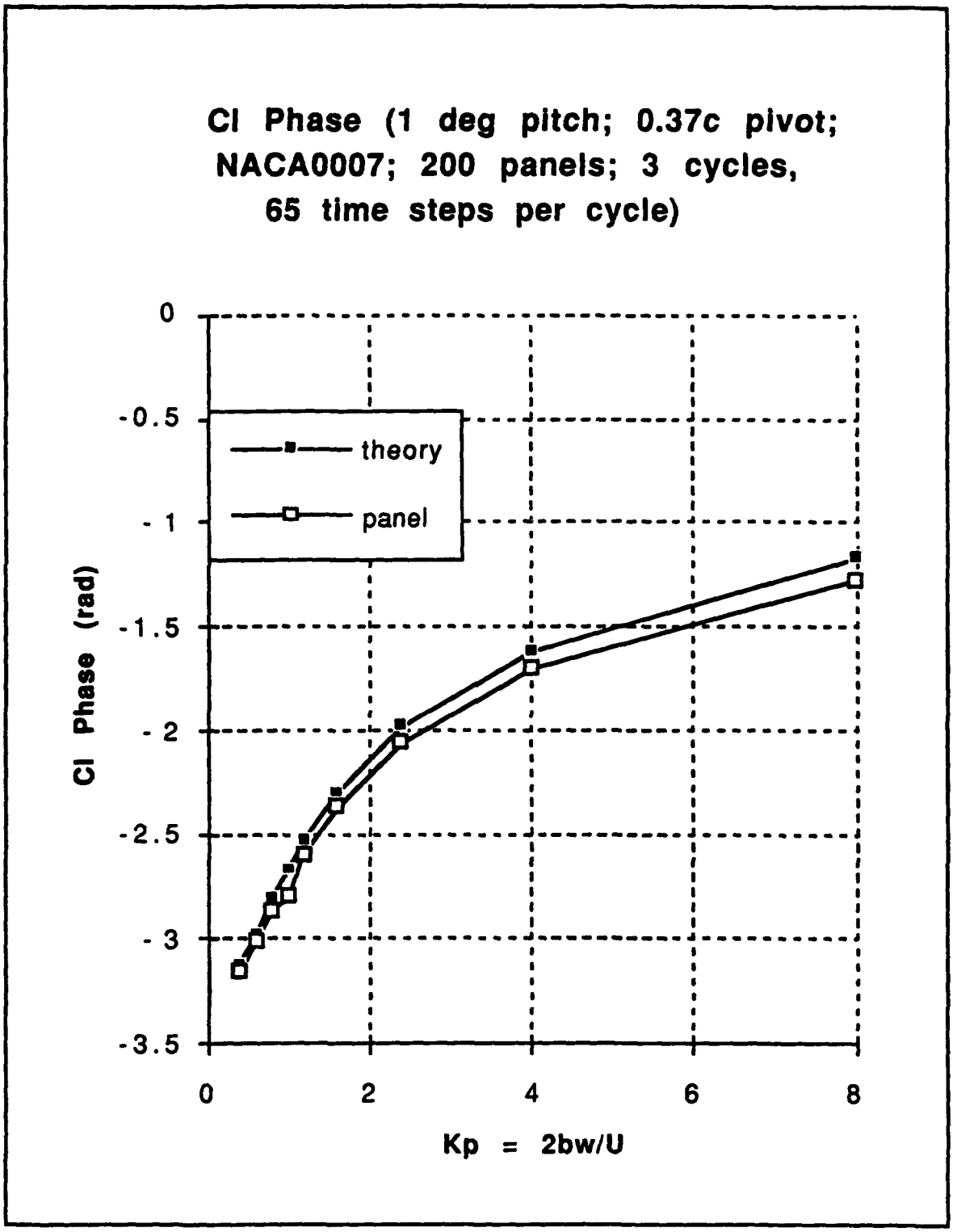

Figure 3.12 Cl Phase for Pitch about 0.37c

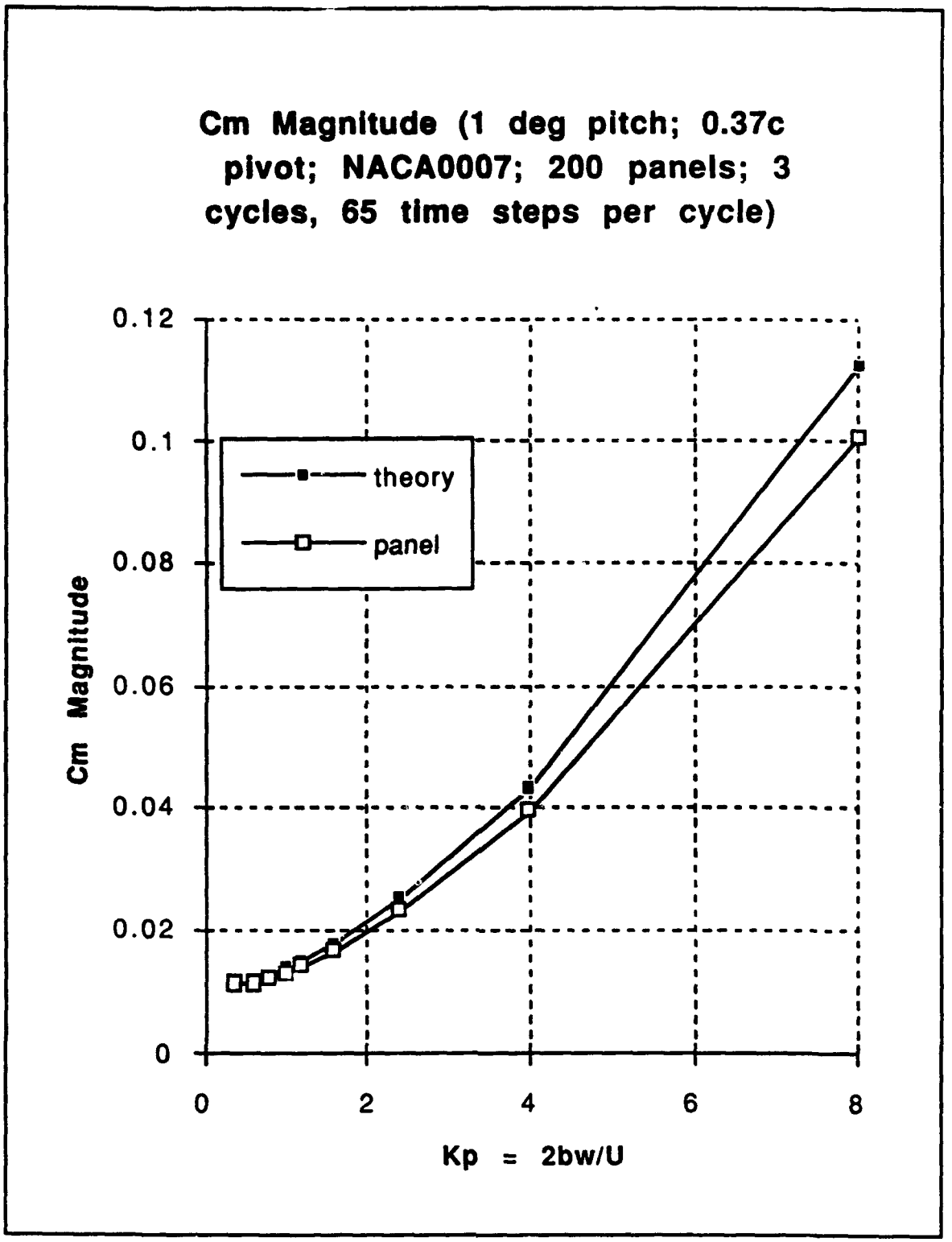

Figure 3.13 Cm Magnitude for Pitch about 0.37c

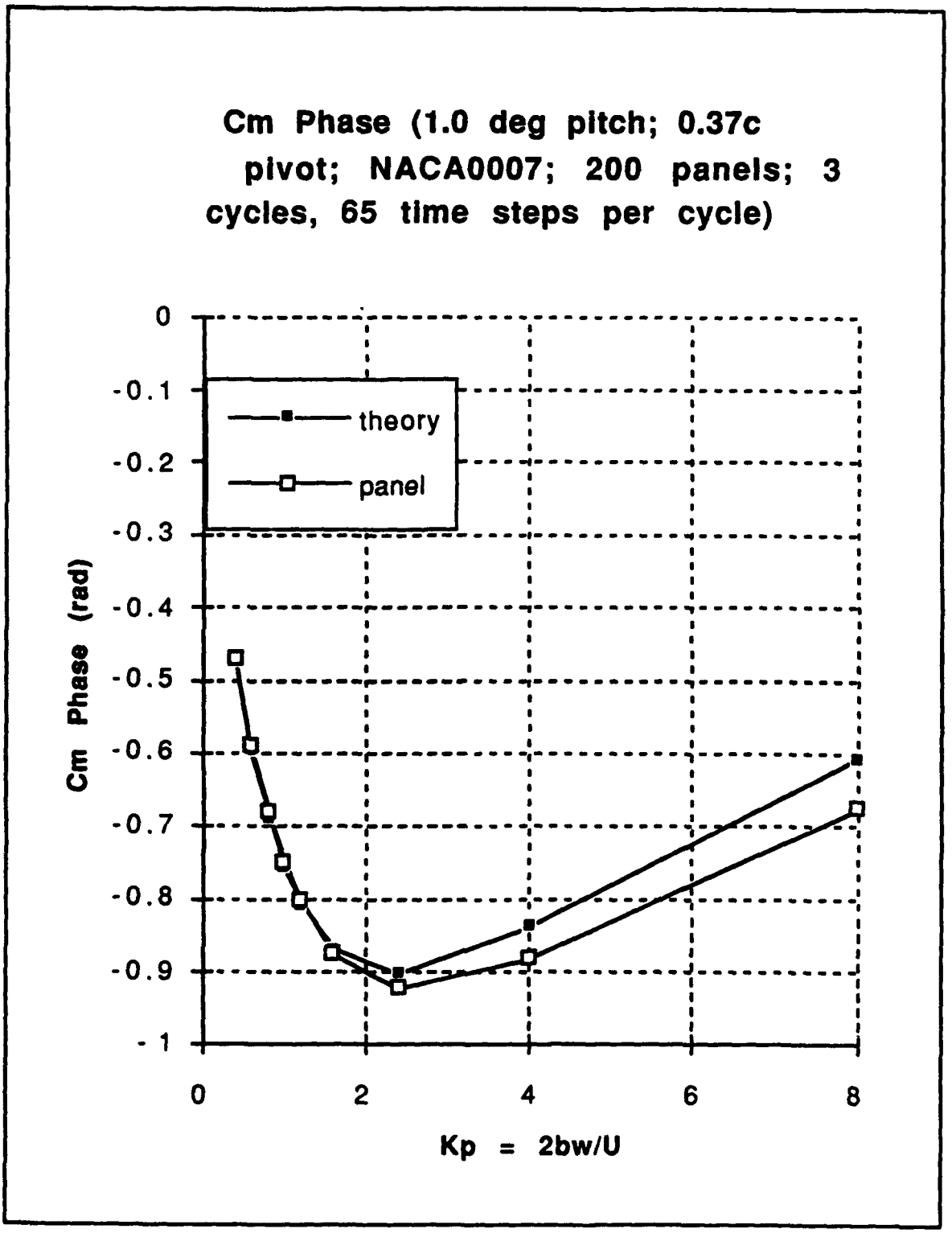

Figure 3.14 Cm Phase for Pitch about 0.37c

TABLE 3.3 PITCH OSCILLATION PIVOT 0.37C

PITCH OSCILLATION PIVOT 0.37

1 deg; 3 cycles; 65 time steps/cycle; 100 panels top and bottom

	CL Magnitude			CL Phase			CM Magnitude			CM Phase		
Kp	theory	panel		theory	panel		theory	panel		theory	panel	
0.4	0.0824	0.0856	3.87%	-3.1123	-3.1510	1.23%	0.0114	0.0111	2.29%	-0.4724	-0.4711	0.04%
0.6	0.0773	0.0797	3.13%	-2.9672	-3.0092	1.42%	0.0118	0.0113	3.84%	-0.5954	-0.5887	0.21%
0.8	0.0759	0.0777	2.40%	-2.8104	-2.8624	1.85%	0.0126	0.0120	4.88%	-0.6885	-0.6801	0.27%
1.0	0.0771	0.0784	1.73%	-2.6586	-2.7874	4.84%	0.0137	0.0129	5.77%	-0.7580	-0.7510	0.22%
1.2	0.0802	0.0811	1.11%	-2.5200	-2.5860	2.62%	0.0150	0.0140	6.38%	-0.8089	-0.8050	0.12%
1.6	0.0903	0.0903	0.00%	-2.2886	-2.3622	3.22%	0.0180	0.0167	7.01%	-0.8705	-0.8750	0.14%
2.4	0.1186	0.1169	1.46%	-1.9724	-2.0531	4.09%	0.0252	0.0233	7.70%	-0.9024	-0.9240	0.69%
4.0	0.1890	0.1834	2.99%	-1.6176	-1.7053	5.42%	0.0433	0.0396	8.55%	-0.8368	-0.8830	1.47%
8.0	0.4139	0.3946	4.65%	-1.1668	-1.2703	8.87%	0.1123	0.1006	10.39%	-0.6061	-0.6766	2.24%

	CL Real		CL Imag		CM Real		CM Imag	
Kp	theory	panel	theory	panel	theory	panel	theory	panel
0.4	-0.0824	-0.0856	-0.0024	0.0008	0.0102	0.0099	-0.0052	-0.0051
0.6	-0.0761	-0.0790	-0.0134	-0.0105	0.0098	0.0094	-0.0066	-0.0063
0.8	-0.0718	-0.0747	-0.0247	-0.0214	0.0097	0.0093	-0.0080	-0.0075
1.0	-0.0683	-0.0715	-0.0358	-0.0322	0.0099	0.0094	-0.0094	-0.0088
1.2	-0.0652	-0.0689	-0.0467	-0.0428	0.0103	0.0097	-0.0108	-0.0101
1.6	-0.0594	-0.0642	-0.0680	-0.0635	0.0116	0.0107	-0.0138	-0.0128
2.4	-0.0464	-0.0542	-0.1092	-0.1035	0.0156	0.0140	-0.0198	-0.0186
4.0	-0.0089	-0.0246	-0.1888	-0.1817	0.0290	0.0251	-0.0322	-0.0306
8.0	0.1627	0.1168	-0.3805	-0.3770	0.0923	0.0785	-0.0640	-0.0630

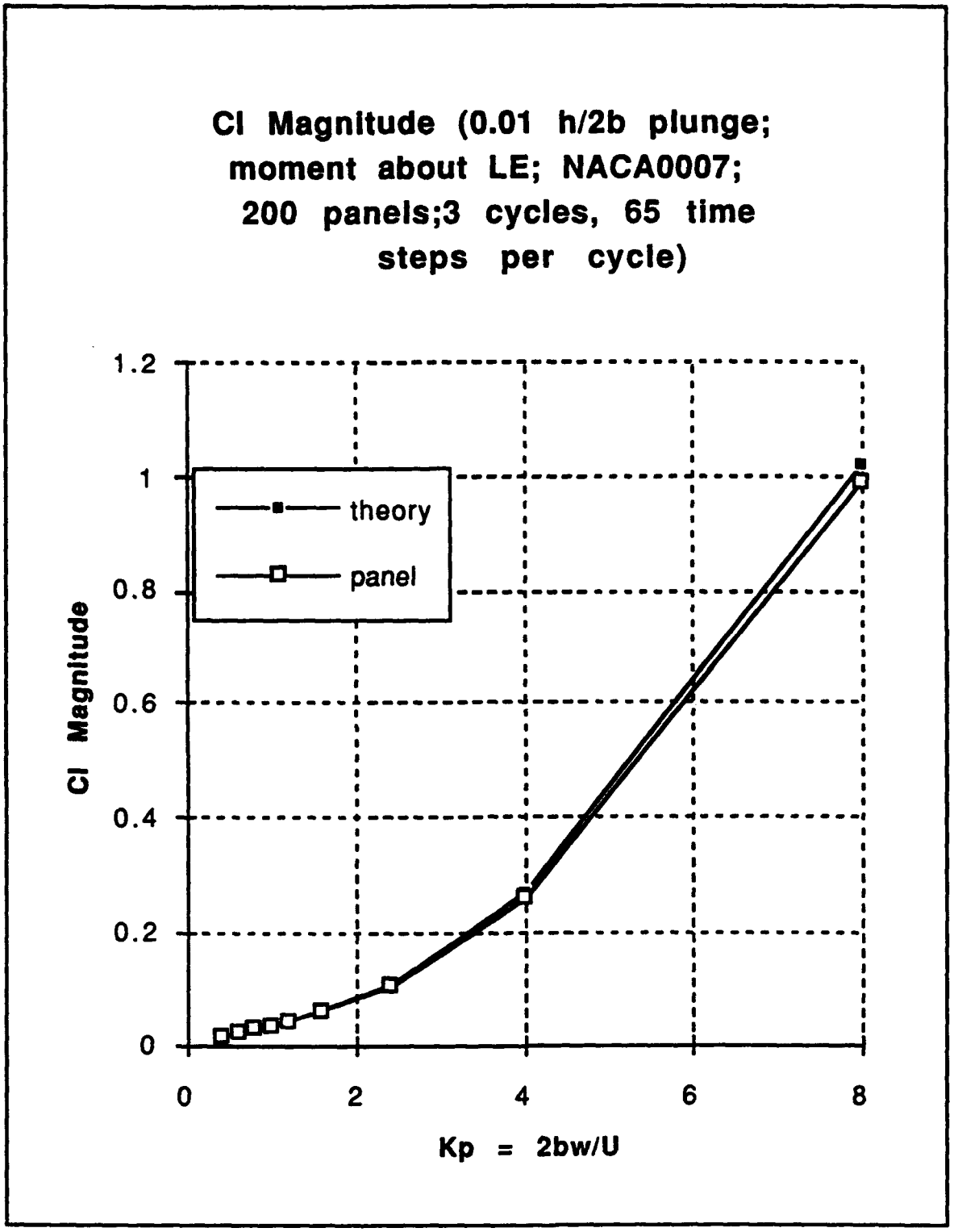

Figure 3.15 Cl Magnitude for Plunge

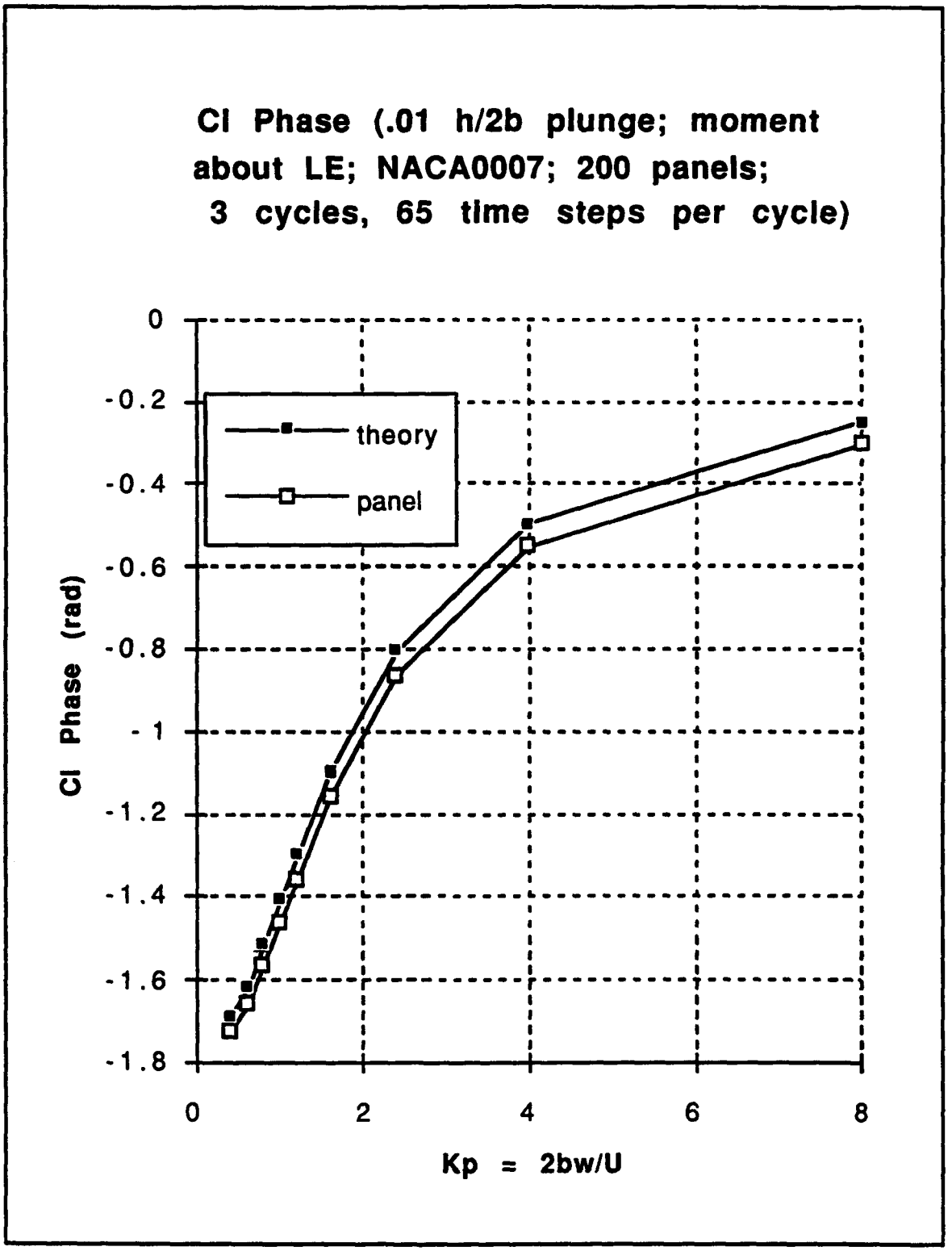

Figure 3.16 Cl Phase for Plunge

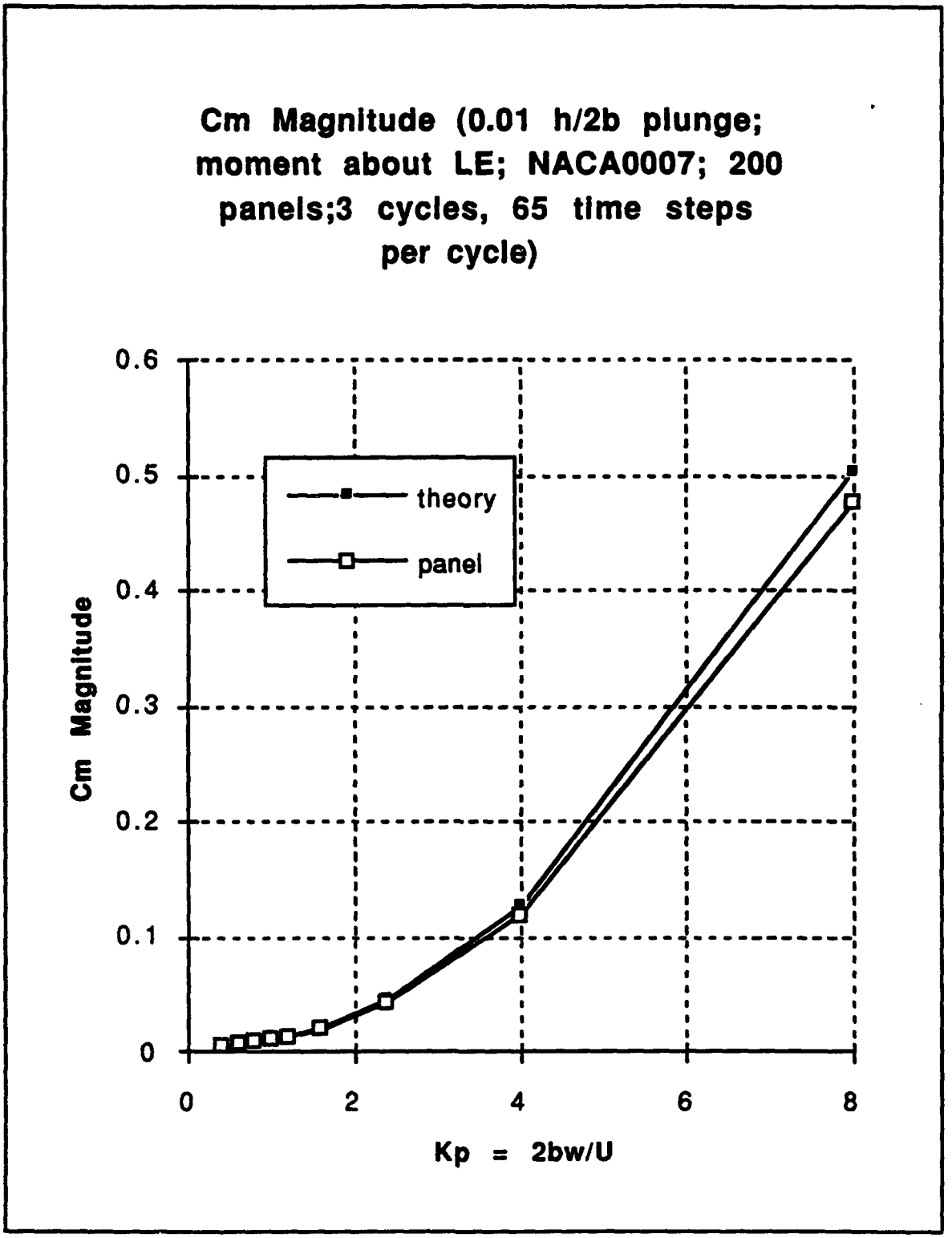

Figure 3.17 Cm Magnitude for Plunge

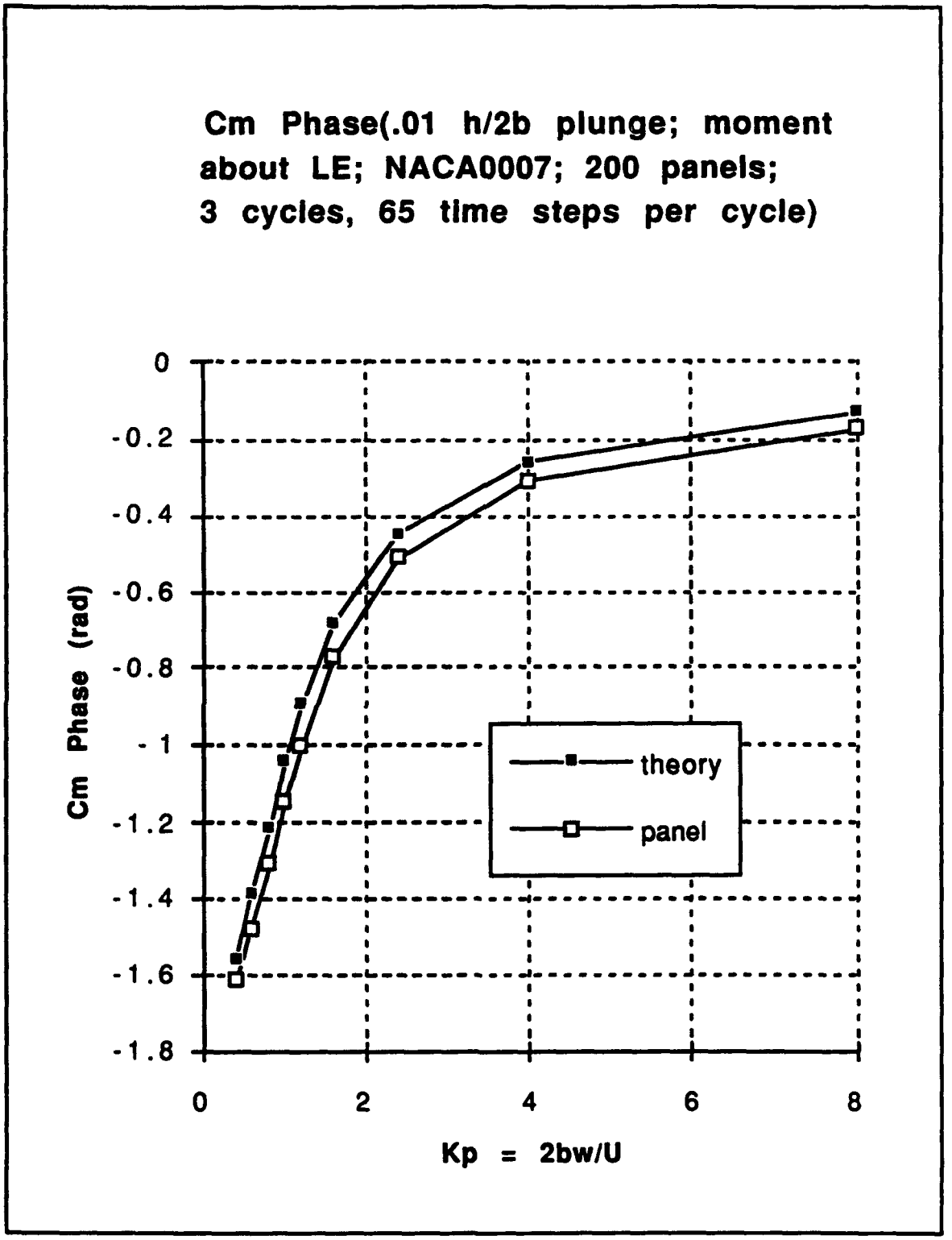

Figure 3.18 Cm Phase for Plunge

TABLE 3.4 PLUNGE TRANSLATION

PLUNGE TRANSLATION MOMENT ABOUT LEADING EDGE

0.01 h/2b; 3 cycles: 65 time steps/cycle; 100 panels top and bottom

	CL Magnitude			CL Phase			CM Magnitude			CM Phase		
Kp	theory	panel		theory	panel		theory	panel		theory	panel	
0.4	0.0184	0.0191	3.90%	-1.6920	-1.7253	1.06%	0.0046	0.0048	5.34%	-1.5551	-1.6177	1.99%
0.6	0.0251	0.0259	3.03%	-1.6148	-1.6569	1.34%	0.0064	0.0066	3.70%	-1.3912	-1.4777	2.75%
0.8	0.0315	0.0322	2.23%	-1.5148	-1.5637	1.55%	0.0084	0.0085	1.77%	-1.2111	-1.3130	3.24%
1.0	0.0381	0.0387	1.67%	-1.4062	-1.4602	1.72%	0.0109	0.0108	0.67%	-1.0421	-1.1496	3.42%
1.2	0.0453	0.0458	1.08%	-1.2975	-1.3553	1.84%	0.0140	0.0136	2.66%	-0.8969	-1.0024	3.36%
1.6	0.0626	0.0624	0.24%	-1.0979	-1.1588	1.94%	0.0221	0.0211	4.72%	-0.6812	-0.7737	2.94%
2.4	0.1112	0.1092	1.82%	-0.8024	-0.8609	1.86%	0.0464	0.0436	5.94%	-0.4447	-0.5140	2.21%
4.0	0.2696	0.2622	2.76%	-0.4985	-0.5503	1.65%	0.1262	0.1187	5.92%	-0.2582	-0.3113	1.69%
8.0	1.0219	0.9913	3.00%	-0.2504	-0.3007	1.60%	0.5028	0.4761	5.30%	-0.1262	-0.1778	1.64%

	CL Real		CL Imag		CM Real		CM Imag	
Kp	theory	panel	theory	panel	theory	panel	theory	panel
0.4	-0.0022	-0.0029	-0.0183	-0.0189	0.0001	-0.0002	-0.0046	-0.0048
0.6	-0.0011	-0.0022	-0.0251	-0.0258	0.0011	0.0006	-0.0063	-0.0066
0.8	0.0018	0.0002	-0.0314	-0.0322	0.0030	0.0022	-0.0079	-0.0083
1.0	0.0062	0.0043	-0.0376	-0.0385	0.0055	0.0044	-0.0094	-0.0099
1.2	0.0122	0.0098	-0.0436	-0.0447	0.0087	0.0073	-0.0109	-0.0115
1.6	0.0285	0.0250	-0.0557	-0.0572	0.0172	0.0151	-0.0139	-0.0147
2.4	0.0773	0.0712	-0.0799	-0.0828	0.0419	0.0380	-0.0200	-0.0215
4.0	0.2368	0.2235	-0.1289	-0.1371	0.1220	0.1130	-0.0322	-0.0364
8.0	0.9900	0.9468	-0.2532	-0.2936	0.4966	0.4686	-0.0633	-0.0842

IV. SINGLE DEGREE OF FREEDOM FLUTTER

When discussing flutter of a typical airfoil section, many text books begin the analysis of the flutter problem as a two-dimensional flexure-torsion problem. Smilg [Ref. 6] presents a theoretical study for one degree of freedom instability of pitching oscillations of an airfoil in incompressible flow. Theoretical results show that the single degree of freedom instability may occur if the airfoil's moment of inertia is sufficiently large and if the pitch axis is located forward of the quarter chord. The pitch axis should not be too far forward of the leading edge so that the wing becomes stable. It is important to distinguish between stall flutter due to flow separation and inviscid incompressible attached flow flutter as discussed here.

A. EQUATION OF MOTION FOR STEADY-STATE OSCILLATIONS IN ONE DEGREE OF FREEDOM.

The classical spring-mass damper equation of motion is:

$$m\ddot{x} + c\dot{x} + kx = F$$

The analogous equation for the pitch degree of freedom of a rigid airfoil in a two dimensional flow is:

$$I\ddot{\alpha} + g\dot{\alpha} + k\alpha = M_\alpha$$

Assuming no structural damping (g=0), $k = I\omega_\alpha^2$, $\ddot{\alpha} = -\omega^2\alpha_o e^{i\omega t}$, and $\alpha = \alpha_o e^{i\omega t}$:

$$I(\omega^2 - \omega_\alpha^2) = -M_\alpha$$

Defining the aerodynamic pitching moment as $M_\alpha = C_{m\alpha}\frac{1}{2}\rho U^2 4b^2$ and substituting into the above equation gives:

$$\alpha_o I\omega^2\left(1-\left(\frac{\omega_\alpha}{\omega}\right)^2\right)=-C_{m\alpha}\frac{1}{2}\rho U^2 4b^2$$

$$\frac{I}{\pi\rho b^4}\left(1-\left(\frac{\omega_\alpha}{\omega}\right)^2\right)=-\frac{8C_{m\alpha}U^2}{4\pi\alpha\omega^2 b^2}$$

$$\frac{I}{\pi\rho b^4}\left(1-\left(\frac{\omega_\alpha}{\omega}\right)^2\right)=-\frac{8C_{m\alpha}}{\pi\alpha K_p^2}$$

For undamped oscillations of the airfoil to exist, the non-dimensional inertia parameter $I_\alpha/\pi\rho b^4$ must exceed approximately 550. As the elastic stiffness increases, the inertia parameter must also increase for instability to occur. For a full scale aircraft at sea level, the inertia parameter typically will not exceed 30 for control surfaces, wings or stabilizers [Ref. 6].

For the oscillations to damp out, Imaginary($C_{M\alpha}$) must be negative and the net work done on the airfoil per cycle must be negative. Negative work implies that the airfoil is performing work on the air, dissipating energy from the wing. When the aerodynamic moment and pitch displacement are in the same direction throughout the entire cycle positive work is performed on the airfoil. This transfer of energy is the origin of negative damping which leads to instability of pitch oscillations. The neutral stability boundary corresponds to 180 degrees phase lag between airfoil motion and lift and moment time history. This phase lag is defined by the necessary condition:

$$\text{Imag}(C_{M\alpha})=0$$

The real part of the lift and moment coefficients represents the in-phase aerodynamic loading while the imaginary part of the coefficients is the out-of-phase portion.

B. SINGLE AIRFOIL FLUTTER VERIFICATION

Pitch damping (Imag($C_{M\alpha}$)) is plotted for several amplitudes in Figure 4.2. The critical reduced frequency representing the flutter boundary is approximately 0.115 compared to a theoretical value of 0.078. The accuracy of the critical reduced frequency increases as the pitch amplitude is decreased.

C. AIRFOIL IN-GROUND EFFECT SIMULATION

To perform a ground effect simulation, the additional boundary condition of flow tangency at ground level requires a second airfoil's reflection about ground level. Distance from the ground is non-dimensionalized by chord length. First, the steady state effects were examined by placing the two airfoils at zero degrees angle of attack and varying the vertical distance between them. At less than 3 chord lengths of separation, the venturi effect or accelerated flow between the airfoils causes a decrease in lift corresponding to a positive pitching moment [Figure 4.3].

The critical reduced frequency of a pitching airfoil in ground effect initially increases slightly then decreases rapidly as the airfoil separation is reduced [Figure 4.4]. For an airfoil with a one foot chord, a natural frequency of one cycle per second and inertia parameter $I/\pi\rho b^4$ equal to 550, the panel code calculates the flutter boundary to occur at a reduced frequency of Kp equal to 0.115 and $C_{M\alpha}$ equals -0.026613 out-of-ground effect. The out-of-ground effect flutter speed is 80 ft/sec and flutter frequency ω/ω_α equals 1.464. At 4.5 chord lengths separation or 2.25 chord lengths above ground level the critical reduced frequency Kp equals 0.101 and $C_{M\alpha}$ equals -0.028942, which corresponds to an in-ground effect flutter speed of 125 ft/sec and flutter frequency ω/ω_α of 2.011. Clearly, the flutter speed and flutter frequency increase in-ground effect.

The same type of simulation was conducted for two airfoils pitching in-phase. The flutter speed decreased and the critical reduced frequency of the flutter boundary increased [Figure 4.5].

A physical understanding of these results requires visualization of the wake. The in ground effect simulation tends to cancel the wake's effect because the reflected wake has the same strength and opposite direction [Figure 4.6]. In-phase oscillations will enhance the wake's effect upon the aerodynamics of the airfoil [Figure 4.7]. The two wakes maintain the same separation as the airfoils have and the vortices have the same direction.

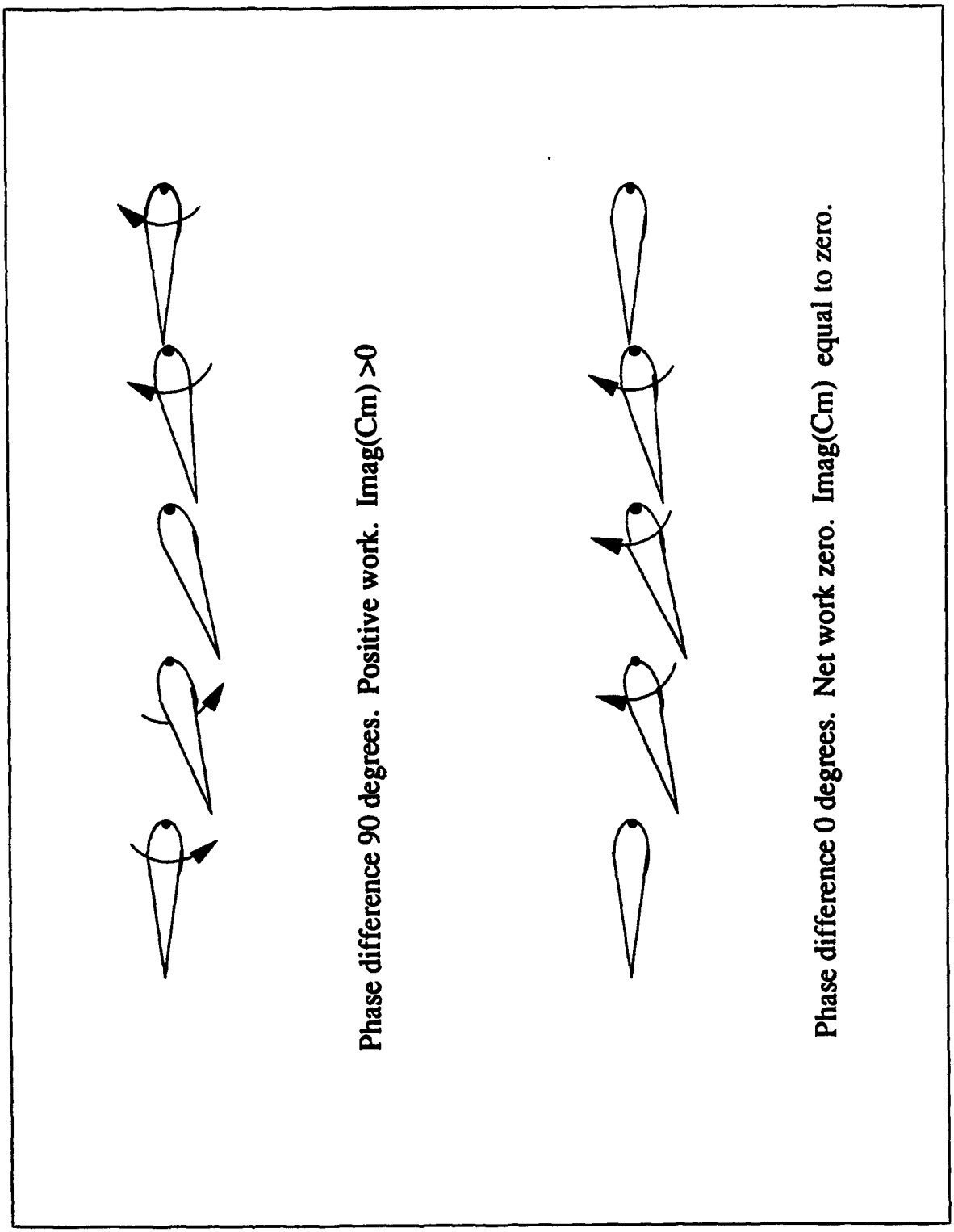

Figure 4.1 Phase Diagram for Airfoil Stability

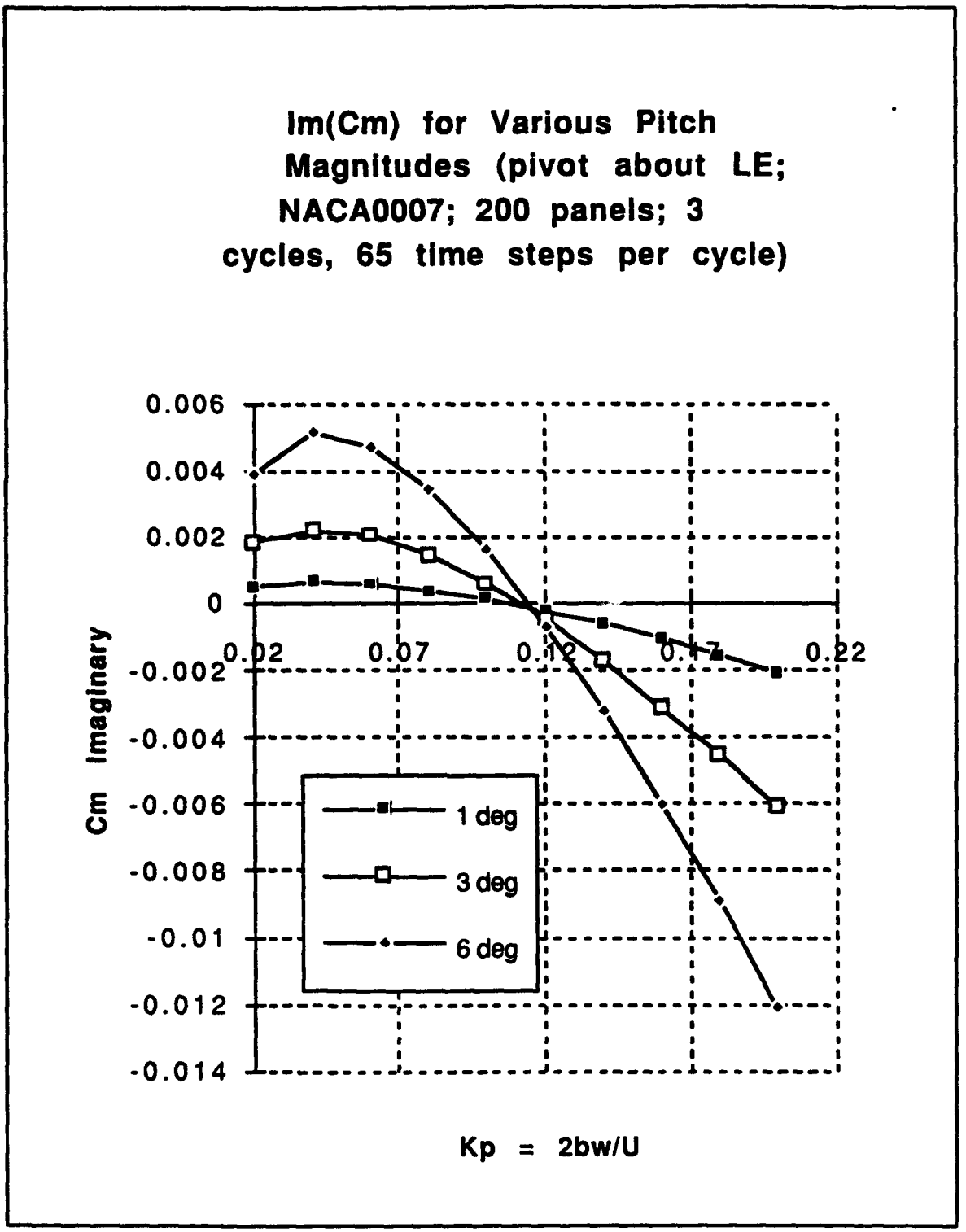

Figure 4.2 Single Airfoil Flutter Verification

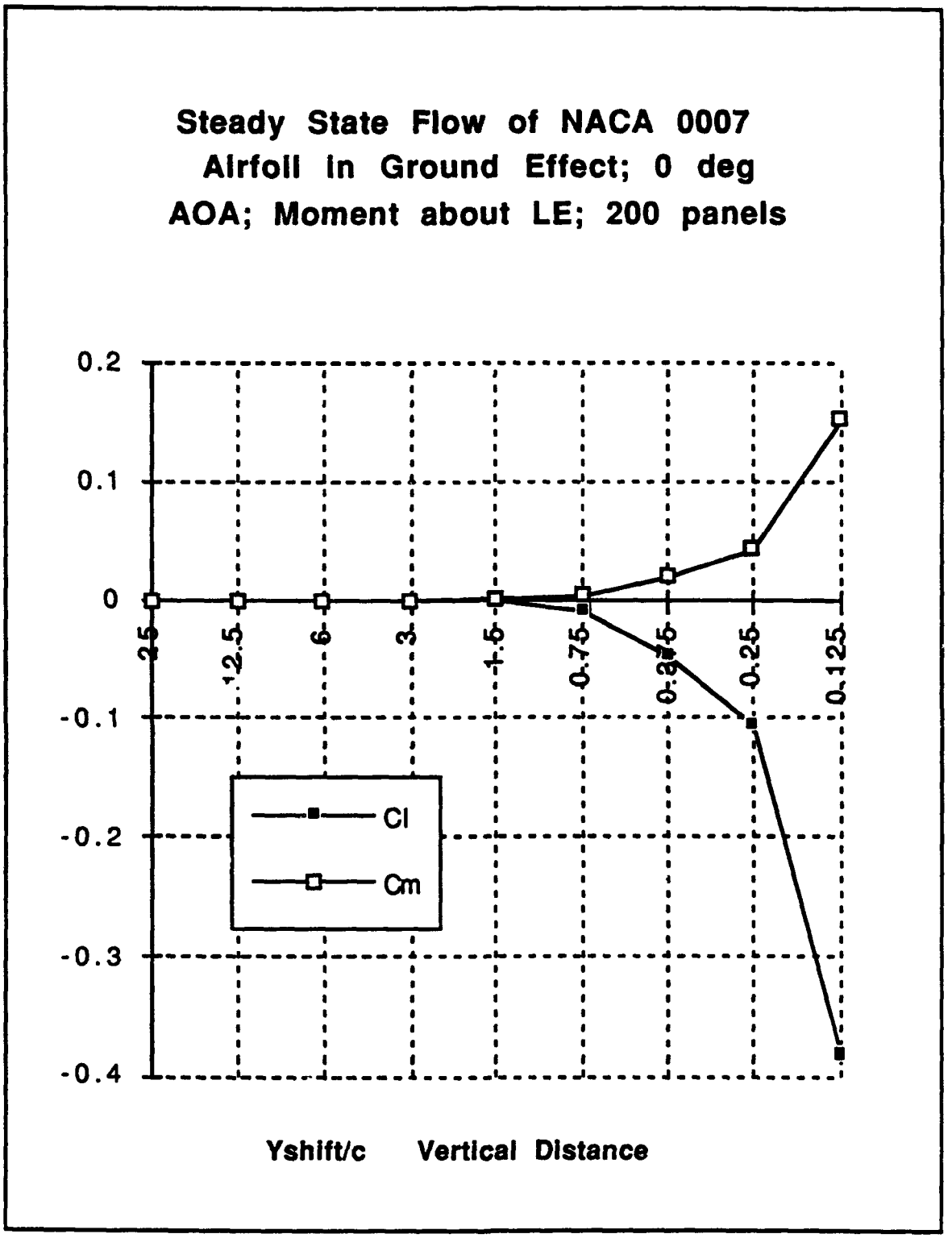

Figure 4.3 Steady State Aerodynamics, Moment Referenced to Leading Edge

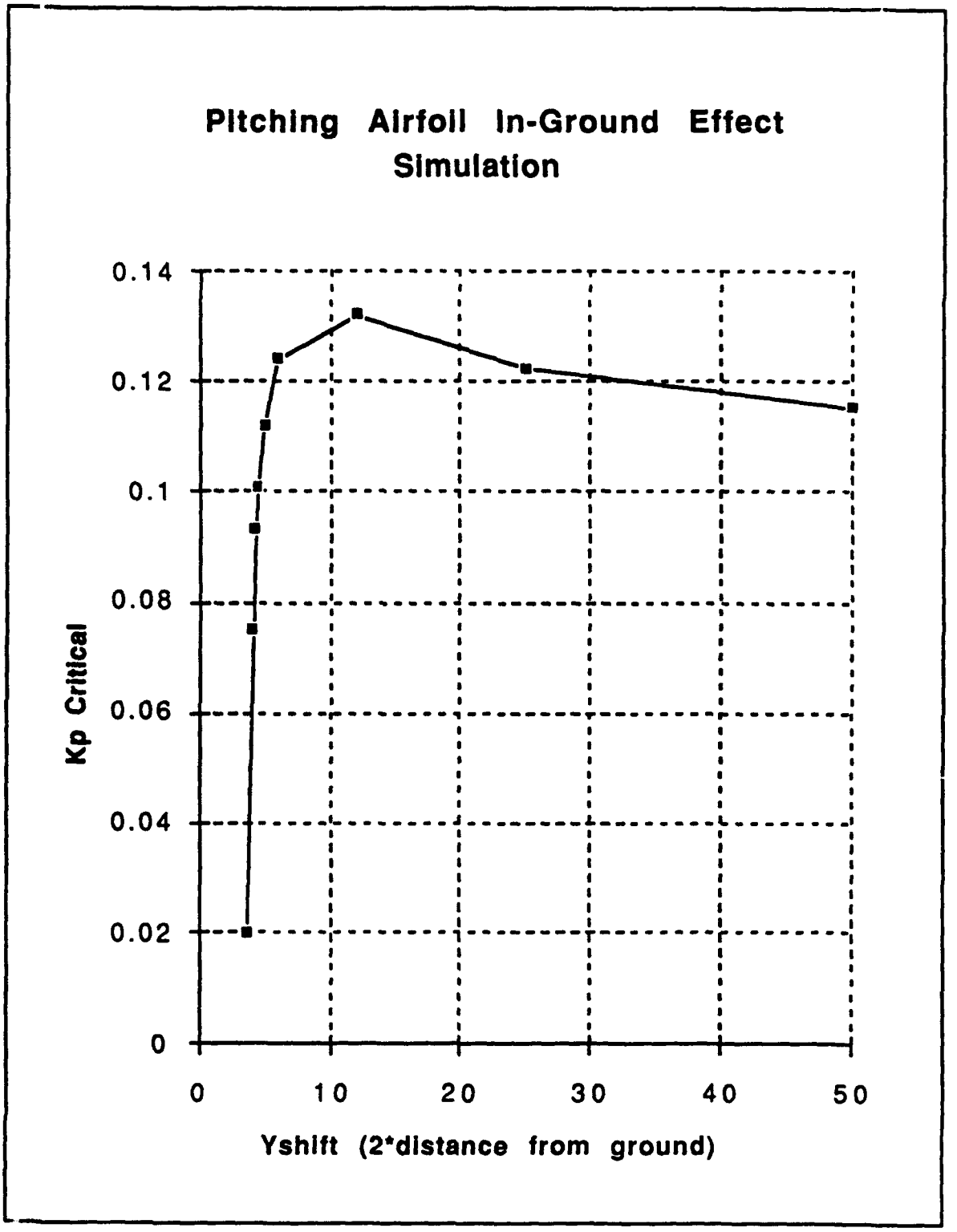

Figure 4.4 Flutter Boundary In Ground Effect

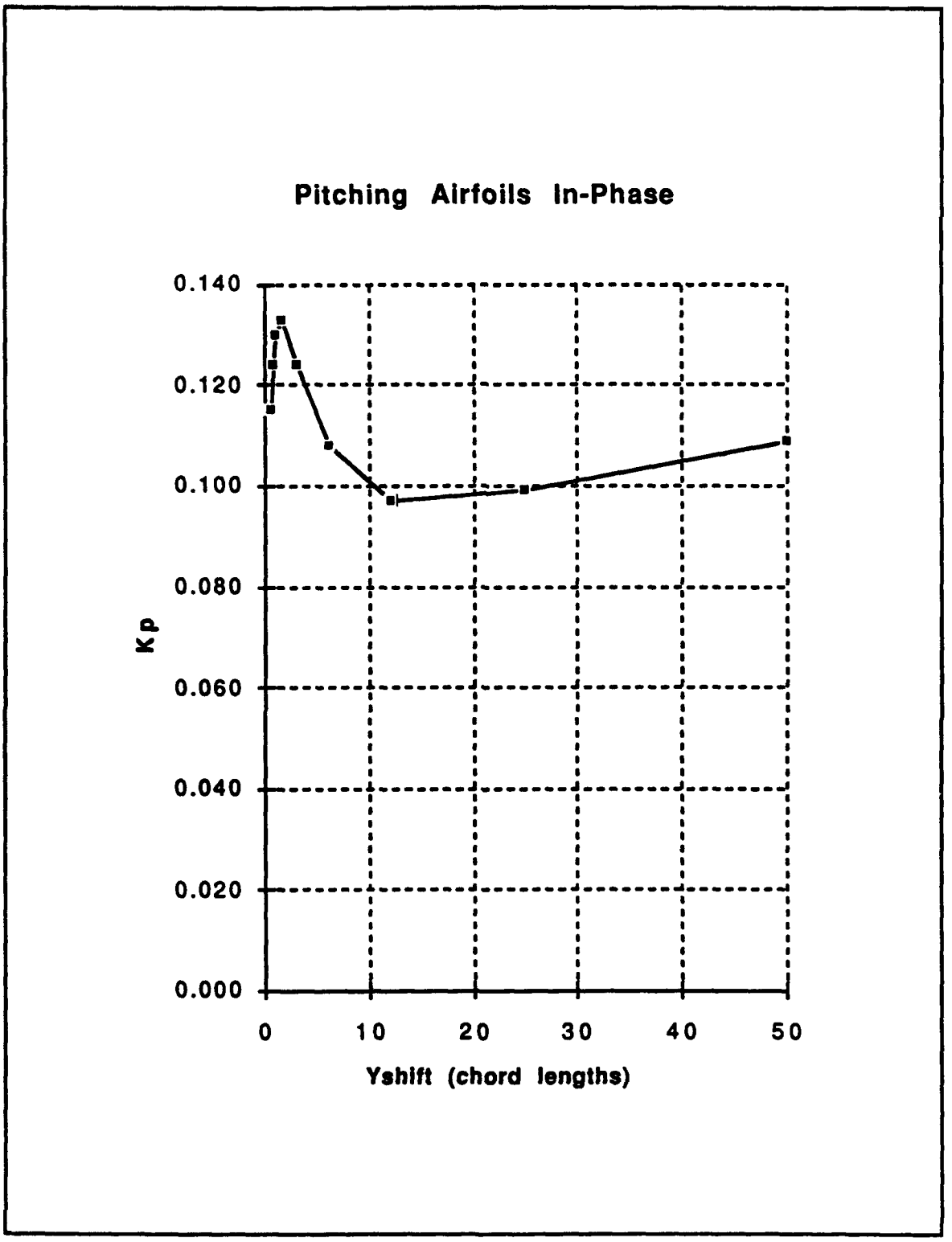

Figure 4.5 Flutter Boundary for In-Phase Oscillations

TABLE 4.1 REFERENCES FIGURE 4.2

Cm Imaginary due to pitch			
NACA0007; 200 panels; 3 cycles 65 steps per cycle			
Kp	1 deg	3 deg	6 deg
0.02	0.000537	0.001857	0.003895
0.04	0.000639	0.002247	0.005146
0.06	0.000570	0.002043	0.004750
0.08	0.000393	0.001456	0.003459
0.10	0.000126	0.000594	0.001610
0.12	-0.000217	-0.000480	-0.000638
0.14	-0.000618	-0.001718	-0.003193
0.16	-0.001065	-0.003084	-0.005978
0.18	-0.001545	-0.004544	-0.008884
0.20	-0.002060	-0.006101	-0.012034

TABLE 4.2 REFERENCES FIGURE 4.3

Steady Airfoil Analysis for NACA0007 in Ground Effect			
Moment about LE; 0 deg AOA; 200 panels			
x/c	Cl	Cm	
25	0.000004	0.000001	
12.5	0.000014	-0.000001	
6	0.000019	0.000001	
3	-0.000076	0.00005	
1.5	-0.001135	0.000513	
0.75	-0.008657	0.003706	
0.375	-0.046132	0.019223	
0.25	-0.105136	0.043154	
0.125	-0.380161	0.151543	

TABLE 4.3 REFERENCES FIGURE 4.4

Pitching airfoil in ground effect simulation.				
Pivot about LE; NACA0007; 200 panels; 3 cycles 65 steps per cycle.				
Yshift is airfoil separation in chord lengths.				
Kp critical represents the flutter boundary.				
Yshift	Kp critical			
50	0.115			
25	0.123			
12	0.132			
6	0.124			
5	0.112			
4.5	0.101			
4.25	0.093			
4	0.075			
3.75	0.020			

TABLE 4.4 REFERENCES FIGURE 4.5

Pitching Airfoils in Phase				
Pivot about LE; NACA0007; 200 panels; 3 cycles 65 steps per cycle.				
Yshift is airfoil separation in chord lengths.				
Kp is the reduced frequency at the flutter boundary.				
Yshift	Kp			
50	0.109			
25	0.099			
12	0.097			
6	0.108			
3	0.124			
1.5	0.133			
1	0.130			
0.75	0.124			
0.5	0.115			

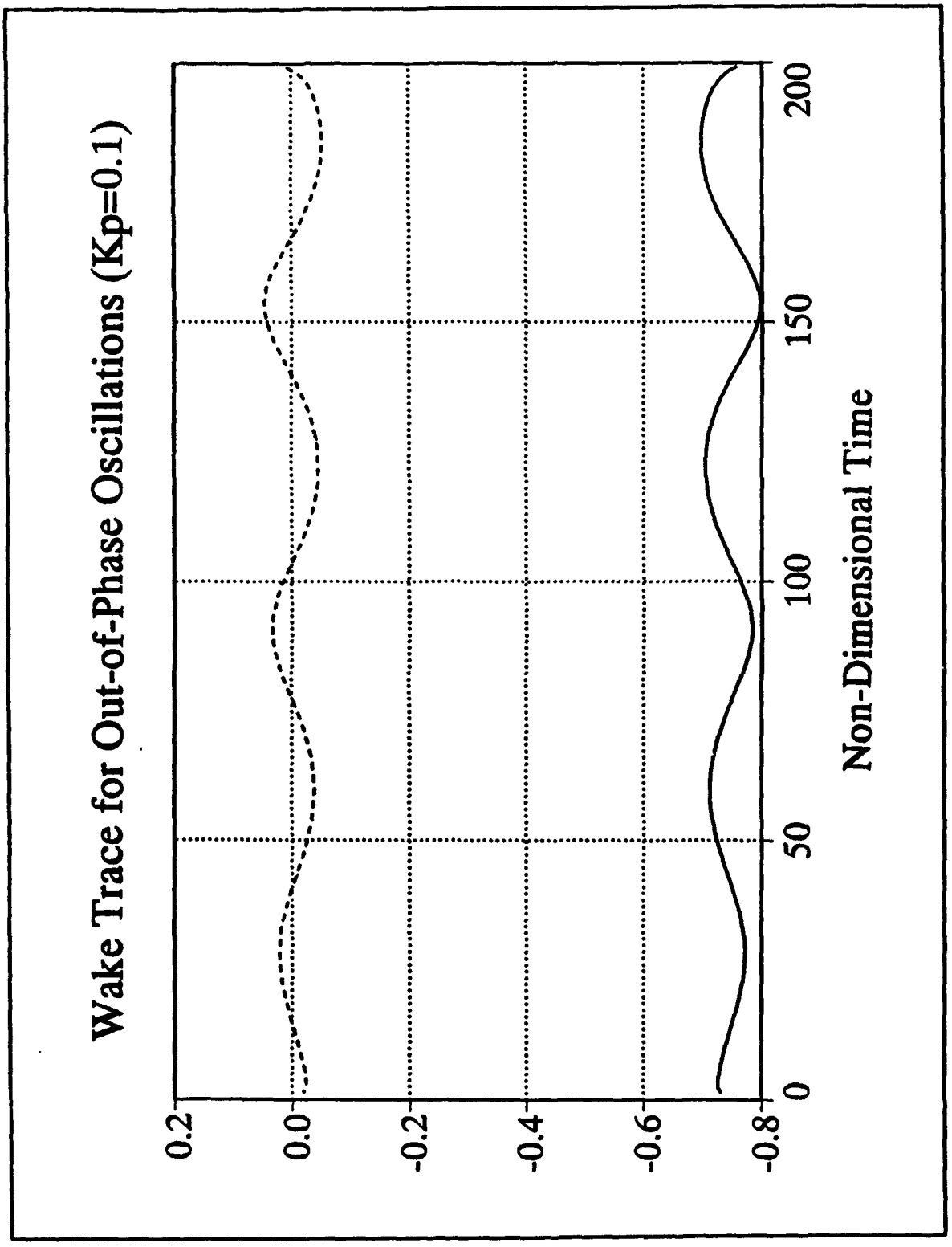

Figure 4.6 Out-of-Phase Oscillations, Wake Cancellation

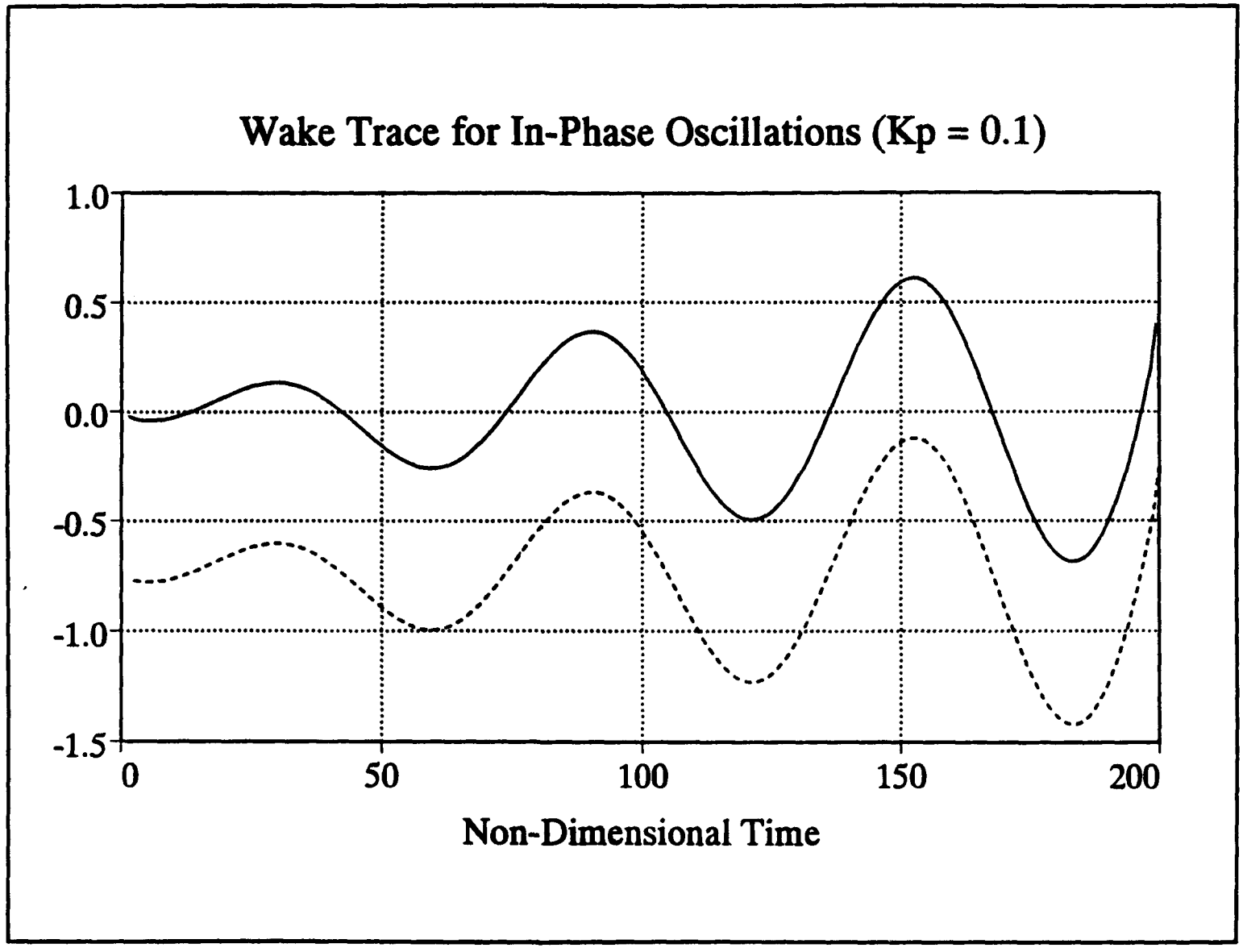

Figure 4.7 In-Phase Oscillations, Wake Enhancement

V. ACTIVE FLUTTER CONTROL

The traditionally accepted methods of moving an airfoil's flutter boundary is shifting the center of gravity or stiffening the structure. These two methods affect the inertial and elastic forces. In the past, aerodynamic forces were accepted as an uncontrollable quantity dependent upon reduced frequency. Through active flutter control, these forces can be controlled.

An investigation of how the one-dimensional flutter boundary may be shifted by positioning an oscillating control airfoil upstream of a neutrally stable reference airfoil is presented in this chapter. The aerodynamic forces may be modified to stabilize an airfoil.

A. INVESTIGATION OF AIRFOIL POSITIONING AND SIZE FOR ACTIVE FLUTTER CONTROL.

The USPOTF2F code can accommodate and scale a second control airfoil while the reference airfoil remains fixed at the origin of the global coordinate system. The variables manipulated are horizontal spacing, vertical spacing and scaling of the control airfoil. The physical pitching frequencies of the two airfoils are equal for all cases presented in this chapter. The pitch axis is located at the leading edge.

Pitch damping results are dependent upon the wavelength of the wake, defined as:

$$K_p = \frac{2\pi c}{\lambda}$$

where K_p is reduced frequency based on full chord, c is chord length and λ is the wavelength of the wake. Pitch damping refers to the imaginary part of the

moment coefficient. Positive Imag(Cm) corresponds to negative pitch damping or instability.

Figure 5.1 displays the pitch damping-frequency dependence for identically sized airfoils staggered by two chord lengths ahead and below the reference airfoil. Figure 5.1 is very similar to Figure 4.2 constructed for single airfoil flutter verification. The staggered airfoil curve [Fig. 5.1] shifts down and slightly to the left when compared to Figure 4.2.

Figure 5.2 shows the airfoil interaction at positive and negative Xshift values. For positive Xshift, the pitch damping asymptotically approaches the single airfoil value of 0.000126 [Table 4.1]. Between Xshift values of -5 to +10 the airfoil influence supersedes wake effects. The periodicity of pitch damping-Xshift is the wake wavelength. The mean of the sine curves in Figure 5.3 through Figure 5.5 follows the single airfoil pitch damping curve [Fig. 4.2]. As the reduced frequency increases, the amplitude of Imag(Cm) decreases and the airfoil becomes more stable. In summary, the frequency dependence of pitch damping is inversely proportional to Cm imaginary period, mean and amplitude.

The effect of scaling or sizing the control airfoil is displayed in Figures 5.6 and 5.7. The ability of the control airfoil to affect the flutter boundary decreases proportionally with control airfoil size. As the size of an airfoil decreases, the strength of the wake core vortex shed from the trailing edge also decreases due reduced circulation around the control airfoil.

B. APPLICATION TO UNSTEADY AERODYNAMICS OF ROTARY WINGS.

The USPOTF2F code is well suited for unsteady aerodynamic simulation of a hovering helicopter. A two dimensional approximation considers the influence of

shed vortices that have translated below the rotor disc and passed under the next blade. Wake-excited flutter has been documented in laboratory tests and during initial whirl tower testing of the AH-56 Cheyenne. Wake-excited flutter will only occur at low inflow rates when wake spacing is minimal. The low inflow configuration occurs during ground operations when blade pitch angles are small. In an actual helicopter rotor flow field, the shed vorticity sheets will superimpose upon each other becoming stronger with the passage of each successive blade. A drawback to the USPOTF2F code is that it only accounts for the wake of one previous blade.

C. COMPARISON TO TWO DIMENSIONAL APPROXIMATION TO WAKE FLUTTER OF ROTARY WINGS BY ROBERT LOEWY.

1. Parameters

In Reference 7, page 90, Figure 15 Loewy presents a graph of pitch damping coefficient versus frequency ratio as a function of inflow parameter [Fig. 5.8]. The inflow parameter is the vertical spacing of the wakes of previous blades corresponding to Yshift in USPOTF2F code. The frequency ratio $m = \omega/\Omega$ is divided into two portions, the integer and non-integer part.

The non-integer portion of m represents wake phasing. When m equals 0.5, this corresponds to the wakes being out of phase as shown in Figure 4.6. The vortex from the control airfoil or preceding blade is directly below a core vortex from the reference airfoil in the opposite direction. The wakes are counter phase or 180 degrees out of phase. When m equals zero or one, the phase shift is 0 and 360 degrees respectively [Fig. 4.7]. The vortex wake sheet has equal spacing vertically with equal vortex strength and direction for identical airfoils. Couch in Reference 10, page 39 treats m exclusively as a phasing parameter in his finite wake theory.

The integer portion of m represents the reduced frequency of the airfoil.

$$m=\frac{\omega}{\Omega}$$

Multiplying by the inverse of aspect ratio for a rectangular wing yields reduced frequency.

$$\frac{\omega}{\Omega}\frac{c}{r}=\frac{\omega c}{U}=\frac{c}{U/\omega}=\frac{c}{\lambda}$$

Reduced frequency is physically defined as the ratio of chord length to wake wavelength as shown above.

2. Comparison to Loewy Results

Figure 5.8 shows areas of negative pitch damping between m=0.5 to 1.0 and m=1.5 to 2.0. The m=0.5 to 1.0 region corresponding to a phase shift of 180 to 360 degrees is illustrated in Figure 5.3 when Xshift ranges from -31.4 to -62.8, which is a region of instability. Figure 5.3 through Figure 5.5 confirms that as the reduced frequency increases (Kp=0.1 to 1.0), the amplitude of the pitch damping curve will decrease. The difference in shape of Loewy's pitch damping curve [Fig. 5.8] and sinusoidal shape of Figure 5.3 is due to Loewy's use of an infinite number of wakes in his classical closed form solution while USPOTF2F code only accounts for one wake.

D. USPOTF2F CODE LIMITATIONS

Theodorsen's flutter theory for simple harmonic motion assumes sinusoidally varying lift and moment coefficients, which are represented mathematically by $e^{i\omega t}$. The primary limitation is that the unequal physical frequencies of control and reference airfoil yield higher harmonic time histories of sine and cosine. The phase subroutine attempts to curve fit a sine wave to a higher harmonic time history resulting in rapid inconsistent phase shifts.

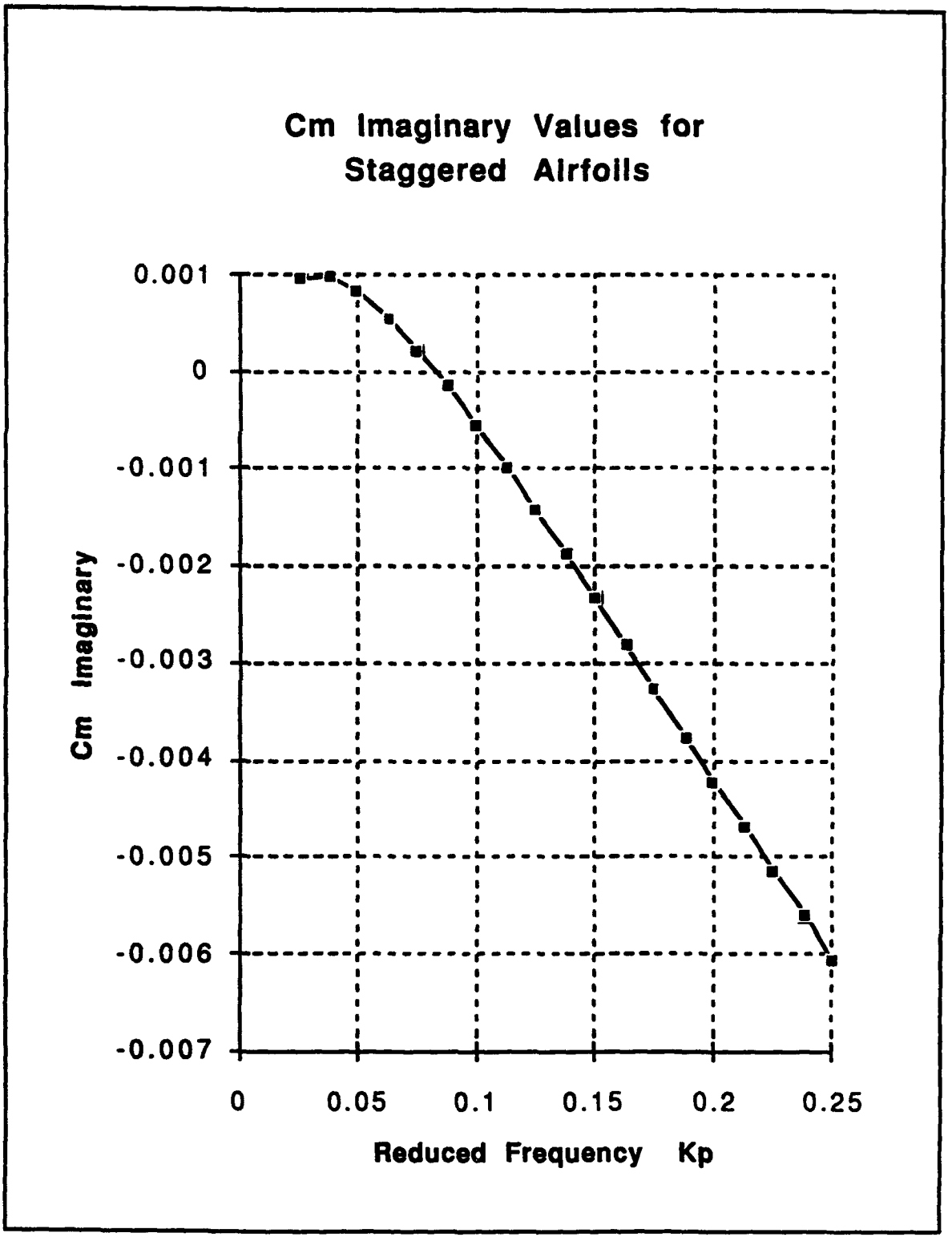

Figure 5.1 Frequency Dependence of Pitch Damping Xshift=-2, Yshift=-2

TABLE 5.1 DATA REFERENCES FIGURE 5.1

Pitching Airfoils in Phase at Various Frequencies				
Pivot about LE; NACA0007; 200 panels; 3 cycles 65 steps per cycle;				
Xshift -2.0; Yshift -2.0; Dalp1 = 1.0; Dalp2 = 1.0;				
Airfoils 1 and 2 frequency sweep from .025 to .250;				
Freq1	Freq2	Cm Imaginary		
0.025	0.025	0.000959		
0.038	0.038	0.000972		
0.050	0.050	0.000822		
0.063	0.063	0.000545		
0.075	0.075	0.000222		
0.088	0.088	-0.000141		
0.100	0.100	-0.000549		
0.113	0.113	-0.000982		
0.125	0.125	-0.001432		
0.138	0.138	-0.001887		
0.150	0.150	-0.002345		
0.163	0.163	-0.00282		
0.175	0.175	-0.003297		
0.188	0.188	-0.003774		
0.200	0.200	-0.004234		
0.213	0.213	-0.004698		
0.225	0.225	-0.005149		
0.238	0.238	-0.005603		
0.250	0.250	-0.00607		

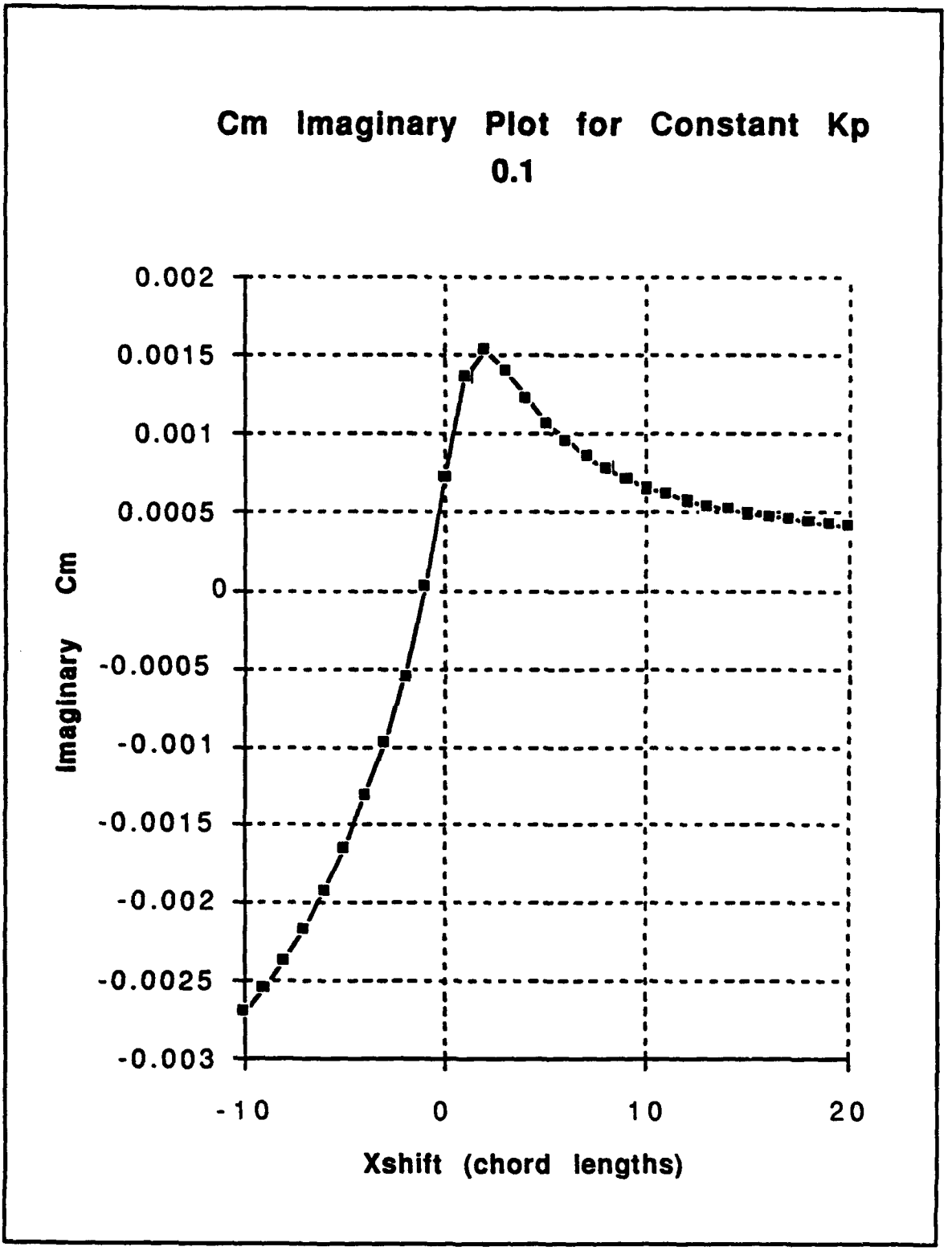

Figure 5.2 Pitch Damping at Small Xshift Values Compared to Wake Wavelength

TABLE 5.2 DATA REFERENCES FIGURE 5.2

Pitching Airfoils Kp = 0.1				
Pivot about LE; NACA0007; 200 panels; 3 cycles 65 steps per cycle;				
Yshift -2.0; Dalp1 1.0; Dalp2 1.0;				
Xshift varied from -10 to +20				
Xshift	Cm Imaginary			
-10	-0.002689			
-9	-0.002543			
-8	-0.002368			
-7	-0.002164			
-6	-0.001926			
-5	-0.001646			
-4	-0.001314			
-3	-0.000970			
-2	-0.000549			
-1	0.000029			
0	0.000737			
1	0.001365			
2	0.001533			
3	0.001410			
4	0.001229			
5	0.001076			
6	0.000955			
7	0.000855			
8	0.000776			
9	0.000709			
10	0.000656			
11	0.000612			
12	0.000576			
13	0.000546			
14	0.000519			
15	0.000495			
16	0.000475			
17	0.000457			
18	0.000440			
19	0.000426			
20	0.000412			

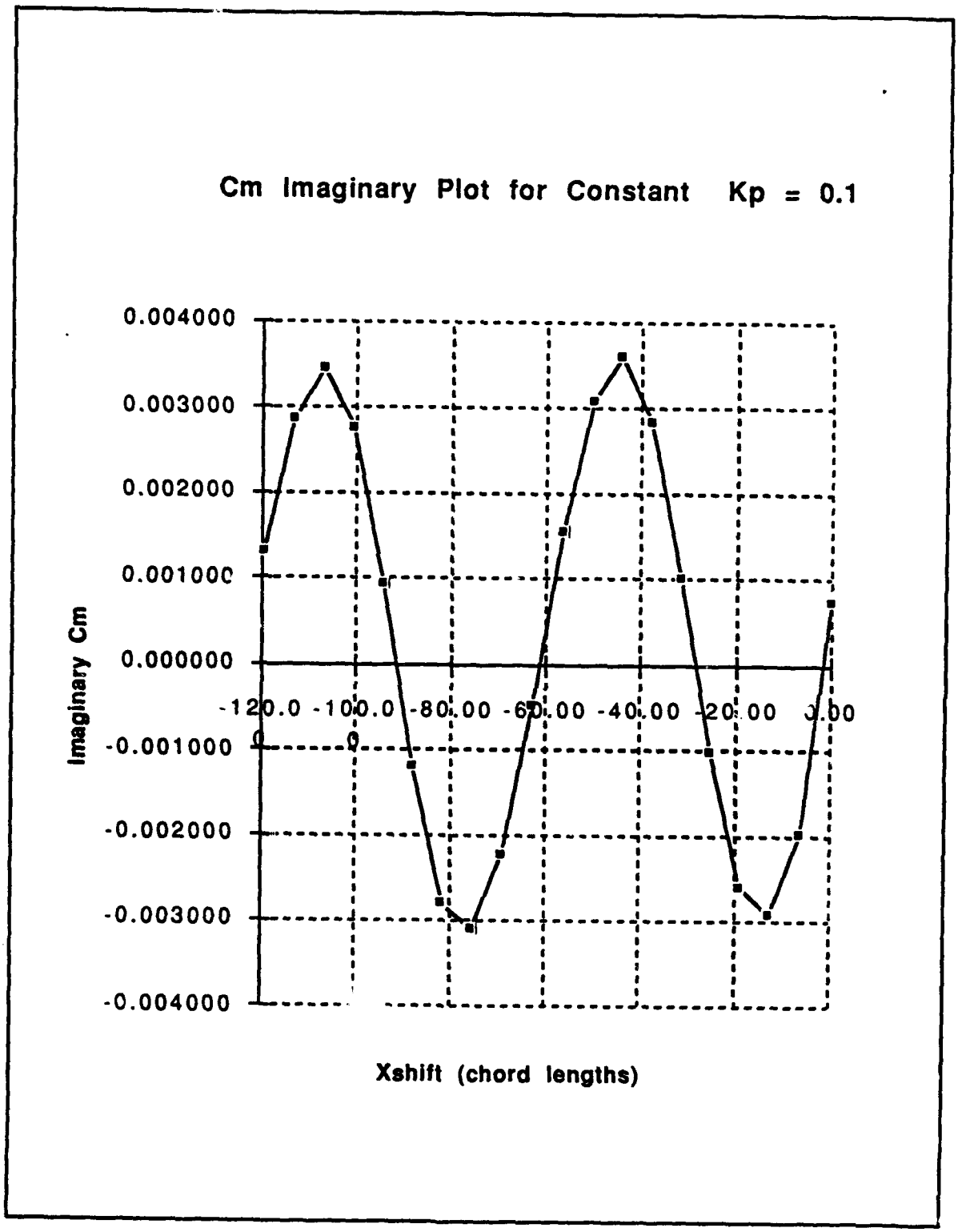

Figure 5.3 Pitch Damping-Xshift Dependence

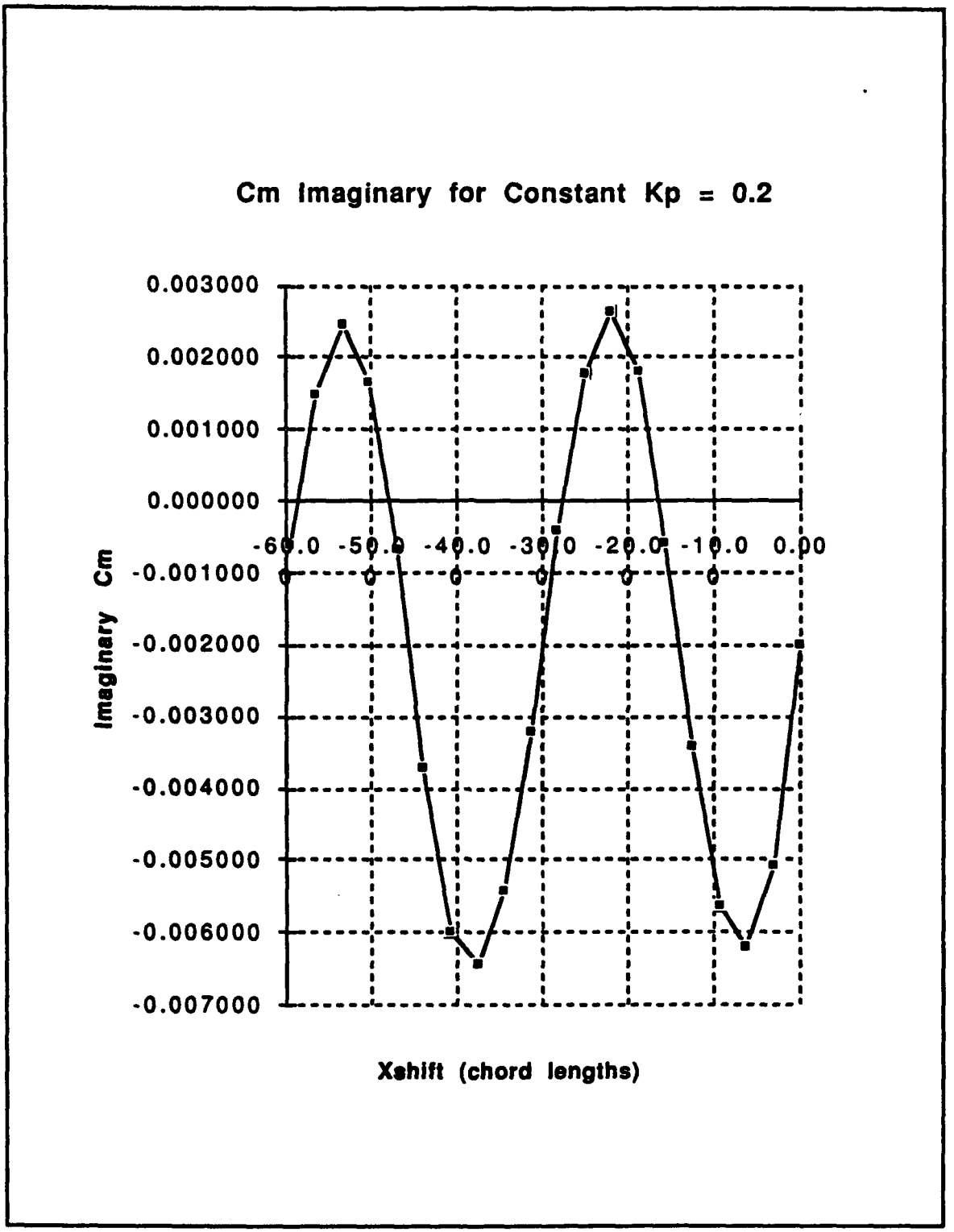

Figure 5.4 Pitch Damping-Xshift Dependence

TABLE 5.3 DATA REFERENCES FIGURE 5.3 AND FIGURE 5.4

Pitching Airfoils				
Pivot about LE; NACA0007; 200 panels; 3 cycles 65 steps per cycle;				
Yshift -2.0; Dalp1 1.0; Dalp2 1.0				
Xshift varied from 0.0 to -120 chord lengths				
Kp = 0.1			Kp = 0.2	
Xshift	Cm Imaginary		Xshift	Cm Imaginary
0.00	0.000737		0.00	-0.001999
-6.28	-0.001992		-3.14	-0.005072
-12.57	-0.002929		-6.28	-0.006196
-18.85	-0.002595		-9.42	-0.005637
-25.13	-0.001021		-12.57	-0.003424
-31.42	0.001010		-15.71	-0.000595
-37.70	0.002836		-18.85	0.001795
-43.98	0.003599		-21.99	0.002647
-50.26	0.003089		-25.13	0.001769
-56.55	0.001560		-28.27	-0.000400
-62.83	-0.000474		-31.42	-0.003206
-69.11	-0.002236		-34.56	-0.005419
-75.40	-0.003109		-37.70	-0.006422
-81.68	-0.002814		-40.84	-0.005997
-87.96	-0.001184		-43.98	-0.003724
-94.25	0.000944		-47.12	-0.000667
-100.53	0.002751		-50.27	0.001671
-106.81	0.003464		-53.41	0.002466
-113.10	0.002851		-56.55	0.001482
-119.38	0.001307		-59.69	-0.000611

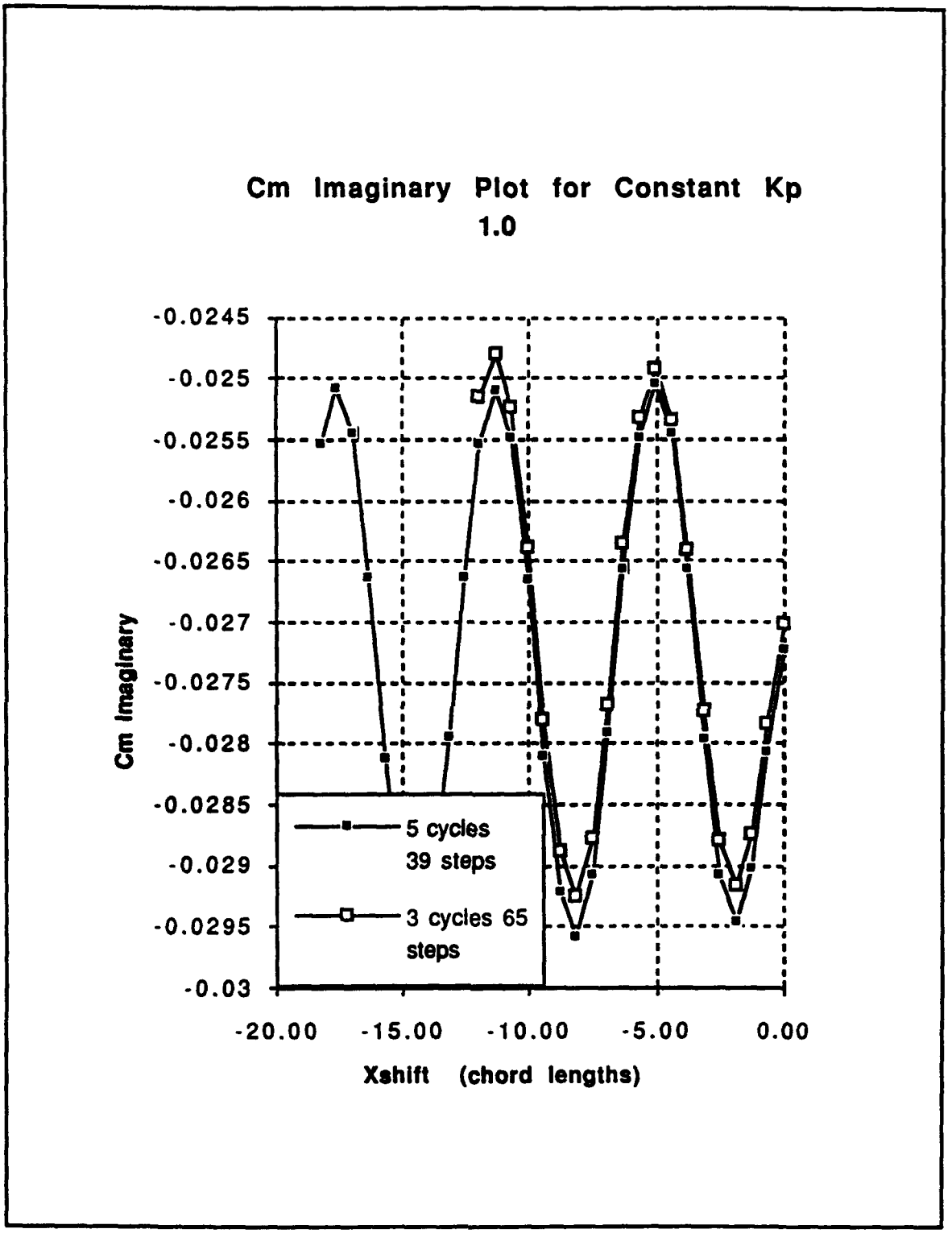

Figure 5.5 Pitch Damping for Different Time Step Cycle Combinations

TABLE 5.4 DATA REFERENCES FIGURE 5.5

Pitching Airfoils Kp = 1.0		
Pivot about LE; NACA0007; 200 panels;		
Yshift -2.0; Dalp1 1.0; Dalp2 1.0		
Xshift varied from 0.0 to -18.22 chord lengths		
Xshift	5 cycles 39 steps	3 cycles 65 steps
0.00	-0.027219	-0.027008
-0.63	-0.028060	-0.027836
-1.26	-0.029022	-0.028742
-1.88	-0.029452	-0.029159
-2.51	-0.029082	-0.028802
-3.14	-0.027958	-0.027730
-3.77	-0.026568	-0.026411
-4.40	-0.025448	-0.025333
-5.03	-0.025049	-0.024928
-5.65	-0.025478	-0.025330
-6.28	-0.026566	-0.026357
-6.91	-0.027912	-0.027685
-7.54	-0.029073	-0.028777
-8.17	-0.029587	-0.029245
-8.80	-0.029219	-0.028880
-9.42	-0.028093	-0.027792
-10.05	-0.026656	-0.026394
-10.68	-0.025488	-0.025244
-11.31	-0.025106	-0.024793
-11.94	-0.025538	-0.025154
-12.57	-0.026627	
-13.19	-0.027934	
-13.82	-0.029100	
-14.45	-0.029640	
-15.08	-0.029299	
-15.71	-0.028121	
-16.34	-0.026633	
-16.96	-0.025452	
-17.59	-0.025088	
-18.22	-0.025537	

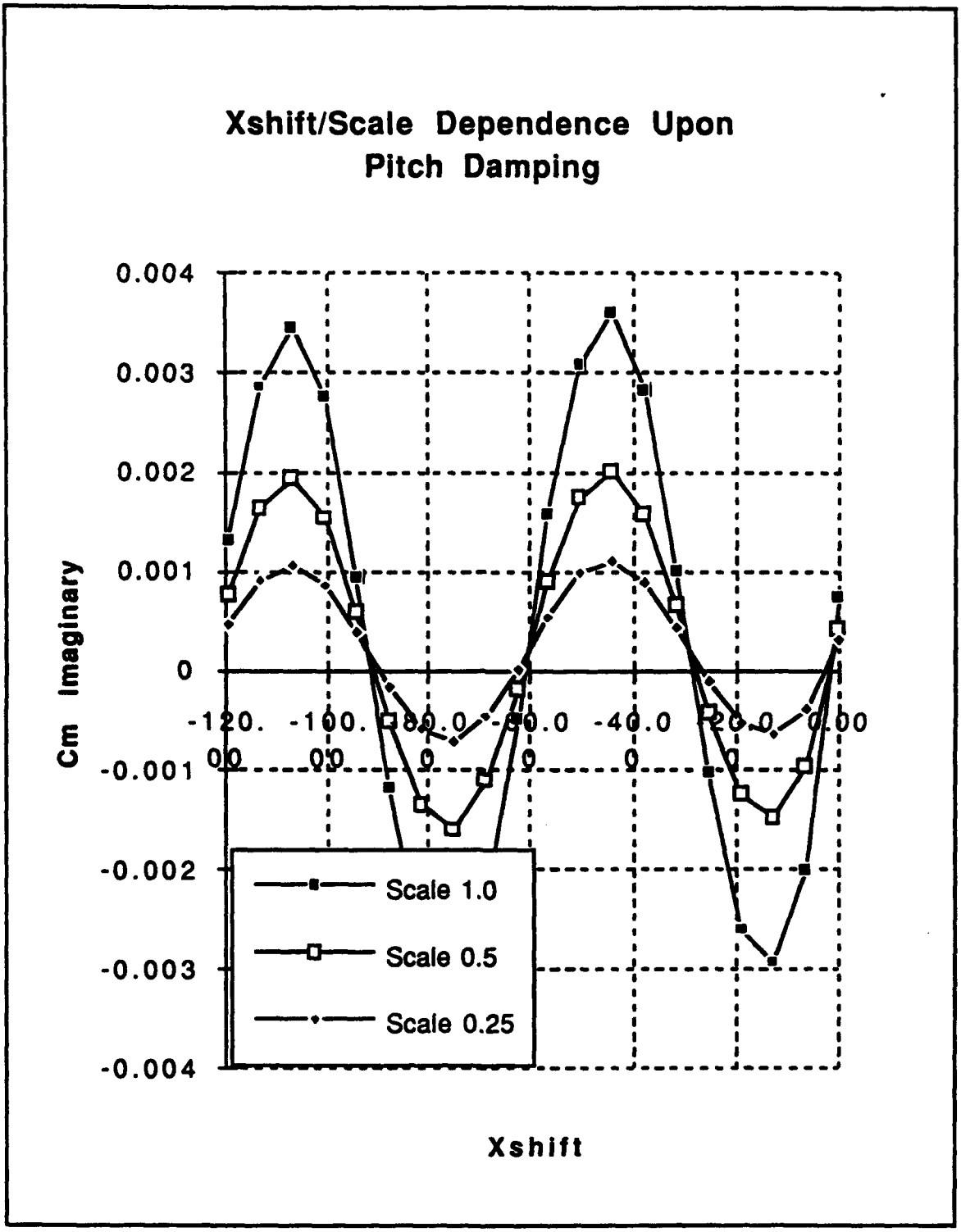

Figure 5.6 Xshift/Scale Dependence Upon Pitch Damping

TABLE 5.5 DATA REFERENCES FIGURE 5.6

Pitching Airfoils Kp = 0.1				
Pivot about LE; NACA0007; 200 panels; 3 cycles 65 steps per cycle;				
Yshift -2.0; Dalp1 = 1.0; Dalp2 = 1.0;				
Xshift varied from 0 to 120 chord lengths for scales of 0.25, 0.50 and 1.00				
Xshift	Scale 1.0	Scale 0.5	Scale 0.25	
0.00	0.000737	0.000429	0.000317	
-6.28	-0.001992	-0.000939	-0.000383	
-12.57	-0.002929	-0.001471	-0.000638	
-18.85	-0.002595	-0.00125	-0.000532	
-25.13	-0.001021	-0.000415	-0.000114	
-31.42	0.001010	0.000659	0.000437	
-37.70	0.002836	0.001579	0.000903	
-43.98	0.003599	0.002005	0.001116	
-50.26	0.003089	0.001742	0.000988	
-56.55	0.001560	0.000901	0.000557	
-62.83	-0.000474	-0.000172	0.000013	
-69.11	-0.002236	-0.001098	-0.000455	
-75.40	-0.003123	-0.001599	-0.000697	
-81.68	-0.002814	-0.001355	-0.000581	
-87.96	-0.001184	-0.000495	-0.000154	
-94.25	0.000944	0.000597	0.000402	
-100.53	0.002751	0.001536	0.000869	
-106.81	0.003464	0.001932	0.001076	
-113.10	0.002851	0.001641	0.000929	
-119.38	0.001307	0.000765	0.000477	

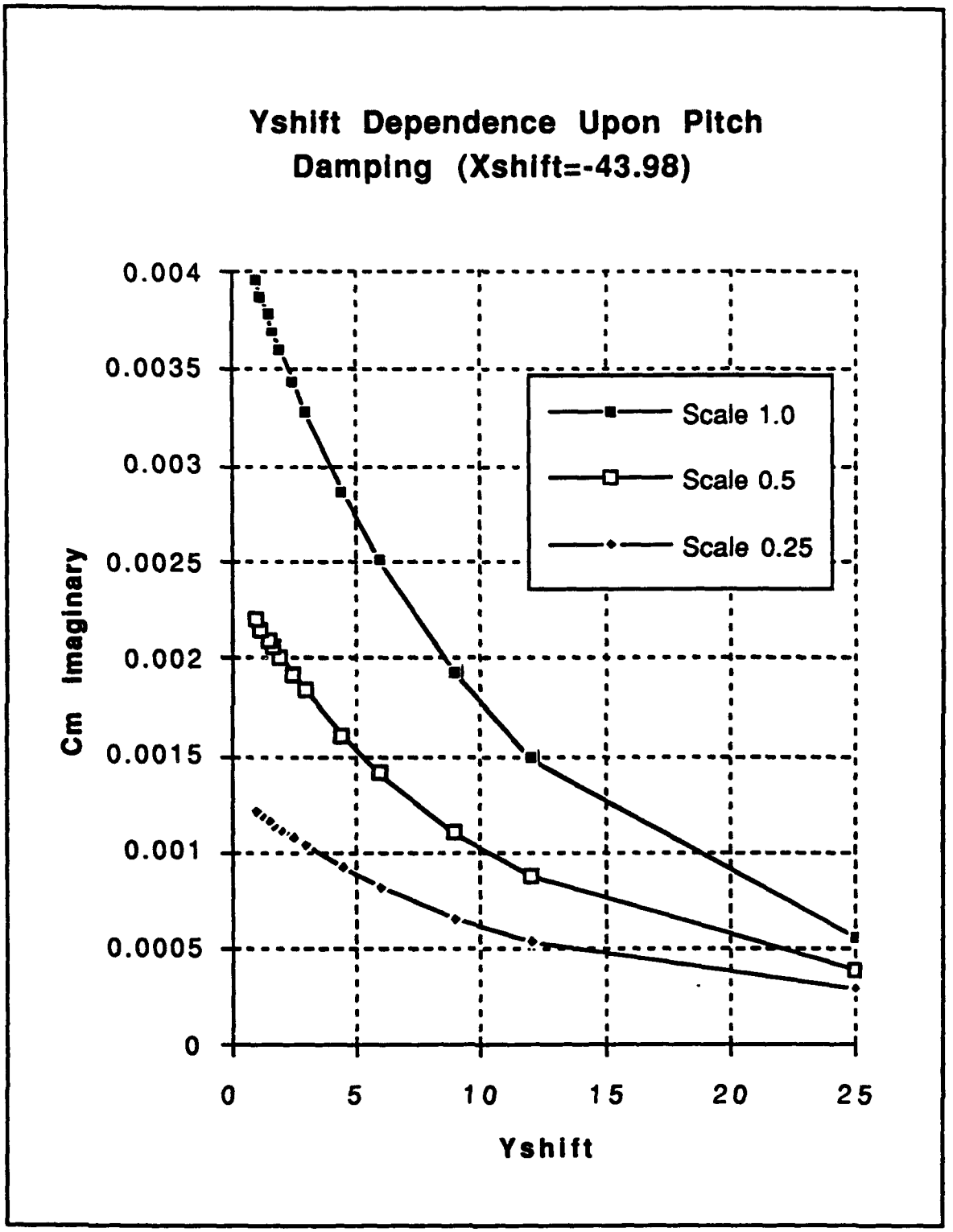

Figure 5.7 Yshift Dependence

TABLE 5.6 DATA REFERENCES FIGURE 5.7

Pitching Airfoils Kp = 0.1				
Pivot about LE; NACA0007; 200 panels; 3 cycles 65 steps per cycle;				
Xshift -43.98; Dalp1 = 1.0; Dalp2 = 1.0;				
Yshift varied from 1 to 25 chord lengths for scales of 0.25, 0.50 and 1.00				
Yshift	Scale 1.0	Scale 0.5	Scale 0.25	
25	0.000557	0.000387	0.000298	
12	0.001478	0.000872	0.000540	
9	0.001923	0.001098	0.000657	
6	0.002499	0.001403	0.000820	
4.5	0.002858	0.001601	0.000918	
3	0.003278	0.001832	0.001030	
2.5	0.003432	0.001916	0.001073	
2	0.003599	0.002005	0.001116	
1.75	0.003685	0.002050	0.001139	
1.5	0.003774	0.002096	0.001163	
1.25	0.003864	0.002141	0.001188	
1	0.003957	0.002189	0.001213	

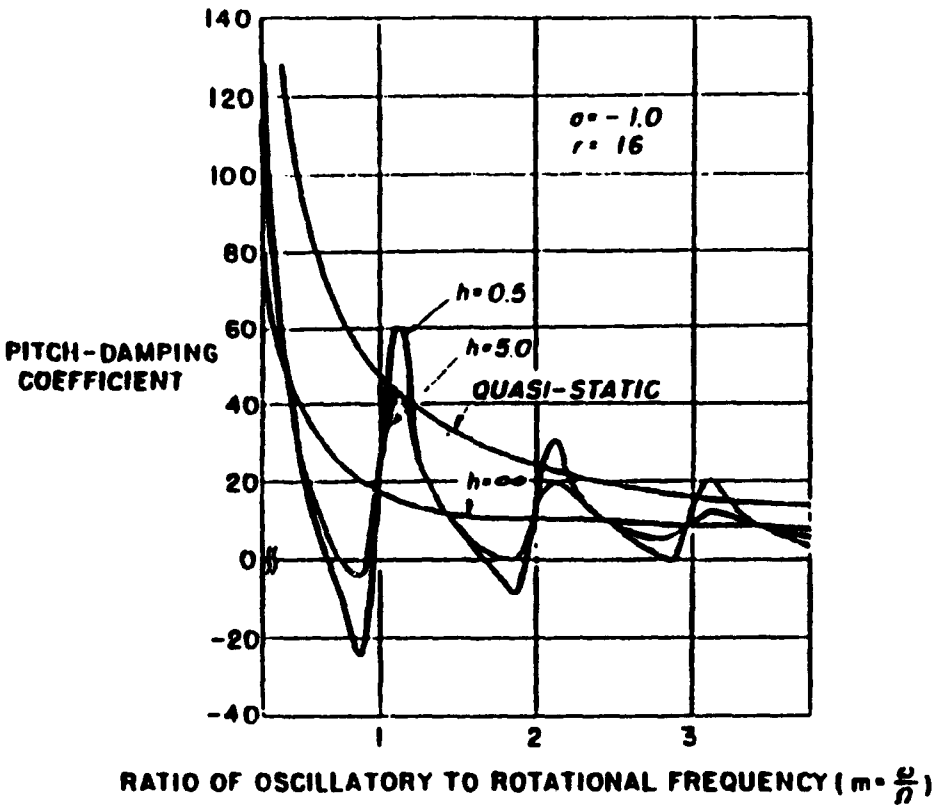

Figure 5.8 Loewy Pitch Damping Curves [Ref. 7]

VI. CONCLUSIONS AND RECOMMENDATIONS

A. SINGLE AIRFOIL ANALYSIS

Aerodynamic verification of UPOTFLUT code is consistent with results by Riester [Ref. 1]. Incompressible bending-torsion flutter computations compare favorably with Theodorsen theory when the natural frequency ratios are less than 1.2. It was shown that the critical reduced frequency may differ by up to a factor of three from Theodorsen's result for high critical frequencies and high natural frequency ratios.

B. TWO AIRFOIL ANALYSIS

The nonlinear theory for simple harmonic motion, magnitude and phase relationships that exist between airfoil motion and aerodynamic forces have been verified by comparison to the classical Theodorsen analysis. Agreement with theory consistent with previous panel codes was obtained. Aerodynamic coefficient magnitude errors were less than five percent and phase errors typically ranged from one to three degrees.

A single degree of freedom flutter analysis of an airfoil in-ground effect simulation showed that the flutter speed increases as ground distance decreases due to wake cancellation. The one dimensional flutter boundary may be shifted by positioning and oscillating a control airfoil upstream of a neutrally stable reference airfoil. An investigation of positioning and size of a control airfoil for active flutter control showed the pitch damping was periodic with wake phasing. Pitch damping period, mean and amplitude are inversely proportional to reduced

frequency. A trend comparison with the wake flutter theory by Loewy illustrated consistent code results.

Theodorsen flutter theory for simple harmonic motion assumed sinusoidally varying lift and moment coefficients, which were represented mathematically by $e^{i\omega t}$. The physical frequency differences between the control and reference airfoil yielded higher harmonics in the time history, causing Theodorsen theory to be invalid.

C. RECOMMENDATIONS

A drawback to this code was the lengthy computer run times which were approximately 60 hours per figure on a 100 Mhz SGI Workstation. Run times could be reduced by running the code in parallel. Dividing the simulation into separate directories or cases and running up to ten workstations simultaneously make time requirements manageable. This requires the availability of batch queues and access to a network. Streamlining of the code by an experienced programmer is recommended.

The frequency dependence of the control airfoil upon a reference airfoil was not resolved. The non-sinusoidal lift and moment time histo. . will require computations to be completed in the time domain. The concept of active flutter control is feasible and certainly worthy of further theoretical study.

APPENDIX

This appendix contains theoretical Theodorsen flutter analysis as described by Fung [Ref. 8]. The MATLAB program was written for the Macintosh. Next, time histories of lift, moment and pitch angle for various cases are illustrated. Finally, three sample wake position plots show the core vortex position at the final time step.

```
% This program performs theoretical theodorsen analysis as
% described by Fung.
clear
clg
%
% Aerodynamic Coefficients
K(1) = 100;
Lh(1) = 1;
Malpha(1) = 0.375;
Lalpha(1) = 0.5;
K(2) = 4;
Lh(2) = 0.9848-0.2519*i;
Malpha(2) = 0.375-0.250*i;
Lalpha(2) = 0.42179-0.49423*i;
K(3) = 2;
Lh(3) = 0.9423-0.5129*i;
Malpha(3) = 0.375-0.5*i;
Lalpha(3) = 0.18580-0.98405*i;
K(4) = 1.2;
Lh(4) = 0.8538-0.8833*i;
Malpha(4) = 0.375-0.83333*i;
Lalpha(4) = -0.38230-1.59487*i;
K(5) = 0.8;
Lh(5) = 0.7088-1.3853*i;
Malpha(5) = 0.375-1.25*i;
Lalpha(5) = -1.5228-2.27119*i;
K(6) = 0.6;
Lh(6) = 0.5407-1.9293*i;
Malpha(6) = 0.375-1.66667*i;
Lalpha(6) = -3.17490-2.83045*i;
K(7) = 0.5;
Lh(7) = 0.3972-2.3916*i;
Malpha(7) = 0.375-2.0*i;
Lalpha(7) = -4.8860-3.1860*i;
K(8) = 0.4;
Lh(8) = 0.1752-3.1250*i;
Malpha(8) = 0.375-2.5*i;
Lalpha(8) = -8.1375-3.5625*i;
K(9) = 0.34;
Lh(9) = -0.022-3.8053*i;
Malpha(9) = 0.375-2.94118*i;
Lalpha(9) = -11.714-3.7396*i;
K(10) = 0.3;
Lh(10) = -0.1950-4.4333*i;
Malpha(10) = 0.375-3.333333*i;
```

```
Lalpha(10) = -15.473-3.7822*i;
K(11) = 0.266666667;
Lh(11) = -0.3798-5.1084*i;
Malpha(11) = 0.375-3.75*i;
Lalpha(11) = -20.0337-3.6847*i;
K(12) = 0.24;
Lh(12) = -0.552-5.8242*i;
Malpha(12) = 0.375-4.16667*i;
Lalpha(12) = -25.319-3.5256*i;
K(13) = 0.2;
Lh(13) = -0.886-7.2760*i;
Malpha(13) = 0.375-5.0*i;
Lalpha(13) = -37.766-2.8460*i;
Mh = 0.5;

% Non-dimensional coefficients

g = 0;
whwa = 1.6;
mu = 4;
a = -0.3;
xalpha = 0.2;
ralpha2 = 0.25;

% Flutter Determinant

% Search for real root using bisection method

% Outside for loop conducts the frequency sweep

for m = 1:13

X(1) = 0.2;
X(3) = 2;
X(2) = (X(3)-X(1))/2;

for its = 1:50

A = mu*(1-X*(whwa^2)*(1+i*g))+Lh(m);
B = mu*xalpha+Lalpha(m)-Lh(m)*(0.5+a);
D = mu*xalpha+Mh-Lh(m)*(0.5+a);
E=mu*ralpha2*(1-X*(1+i*g))-0.5*(0.5+a)+Malpha(m)-Lalpha(m)*(0.5+a)+Lh(m)*(0.5+a
^2;
DET = A.*E - B*D;
R = real(DET);
```

```
  if R(1)*R(2) < 0
     X(3) = X(2);
  else
     X(1) = X(2);
  end
X(2) = (X(3)+X(1))/2;
end

Rroot(m) = X(2);
Rerror(m) = X(3) - X(1);

% Search for imaginary root

X(1) = 0.2;
X(3) = 2;
X(2) = (X(3)-X(1))/2;

for its = 1:50

A = mu*(1-X*(whwa^2)*(1+i*g))+Lh(m);
B = mu*xalpha+Lalpha(m)-Lh(m)*(0.5+a);
D = mu*xalpha+Mh-Lh(m)*(0.5+a);
E=mu*ralpha2*(1-X*(1+i*g))-0.5*(0.5+a)+Malpha(m)-Lalpha(m)*(0.5+a)+Lh(m)*(0.5+a
^2;
DET = A.*E - B*D;
I = imag(DET);
  if I(1)*I(2) < 0
     X(3) = X(2);
  else
     X(1) = X(2);
  end
X(2) = (X(3)+X(1))/2;
end
Iroot(m) = X(2);
Ierror(m) = X(3) - X(1);
end
Rroot
Iroot
diff = Rroot - Iroot;

%  Plot of real and imaginary roots

%plot(1 ./ K, Rroot,1 ./ K, Iroot)
%grid
%xlabel('1/k')
```

```
%ylabel('(X)')
%pause

% Search of roots for critical frequency

n = length(Rroot);
for m=1:n
   if diff(m) > 0
       krf=K(m);
       break
   end
end

%  Calculation of the flutter coefficent that lies between
%  m and m-1 reduced frequency.

IovK(1) = 1/K(m-1);
Xreal(1) = sqrt(Rroot(m-1));
Ximag(1) = sqrt(Iroot(m-1));

IovK(2) = 1/K(m);
Xreal(2) = sqrt(Rroot(m));
Ximag(2) = sqrt(Iroot(m));

x1 = IovK(1):0.0001:IovK(2);
n = length(x1);
y1 = 1/(IovK(2) - IovK(1))*((IovK(2) - x1)*Xreal(1) + (x1 - IovK(1))*Xreal(2));
y2 = 1/(IovK(2) - IovK(1))*((IovK(2) - x1)*Ximag(1) + (x1 - IovK(1))*Ximag(2));

plot (x1,y1,x1,y2)
grid
xlabel('1/k')
ylabel('sqrt(X)')

for m = 1:n
    if y2(m)-y1(m) < 0,
          Iok = x1(m)
          Xroot = y2(m)
          break
    end
end

kcrit = 1/Iok
coef = Iok / Xroot
```

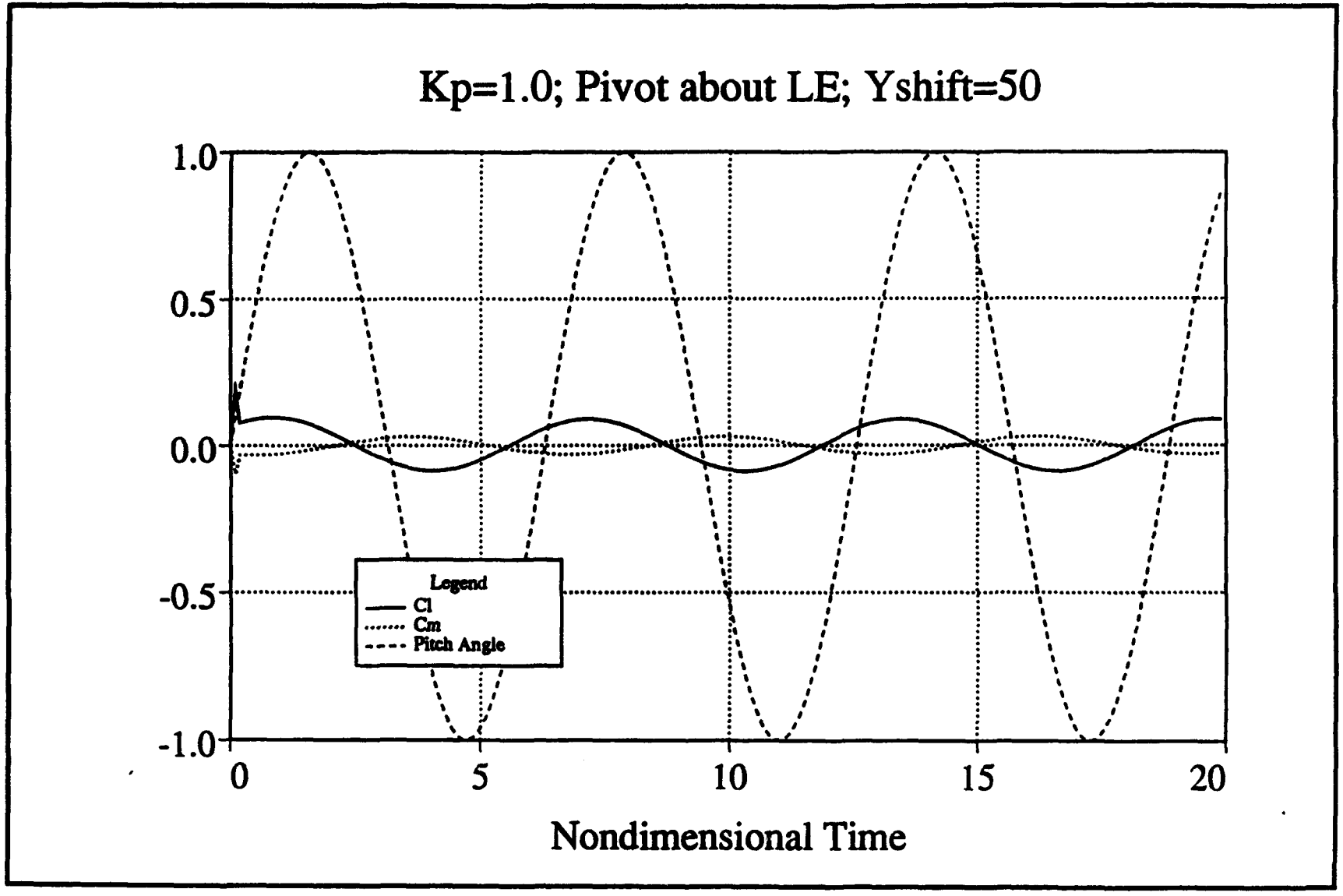
Kp=1.0; Pivot about LE; Yshift=50
1.0
0.5
0.0
-0.5
-1.0
0
5
10
15
20
Nondimensional Time
Legend
Cl
Cm
Pitch Angle

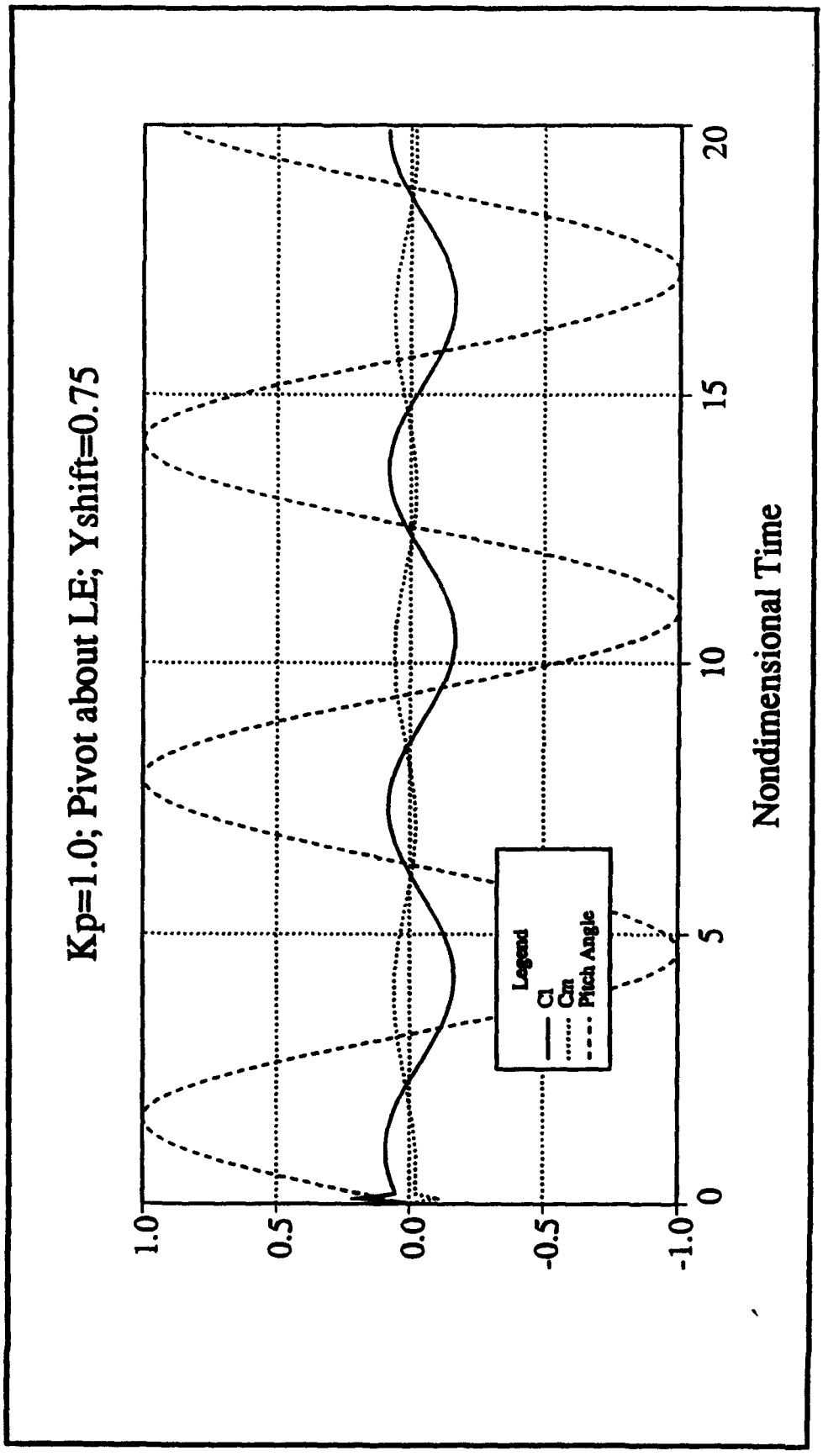
Kp=1.0; Pivot about LE; Yshift=0.75
1.0
0.5
0.0
-0.5
-1.0
0
5
10
15
20
Nondimensional Time
Legend
Cl
Cm
Pitch Angle

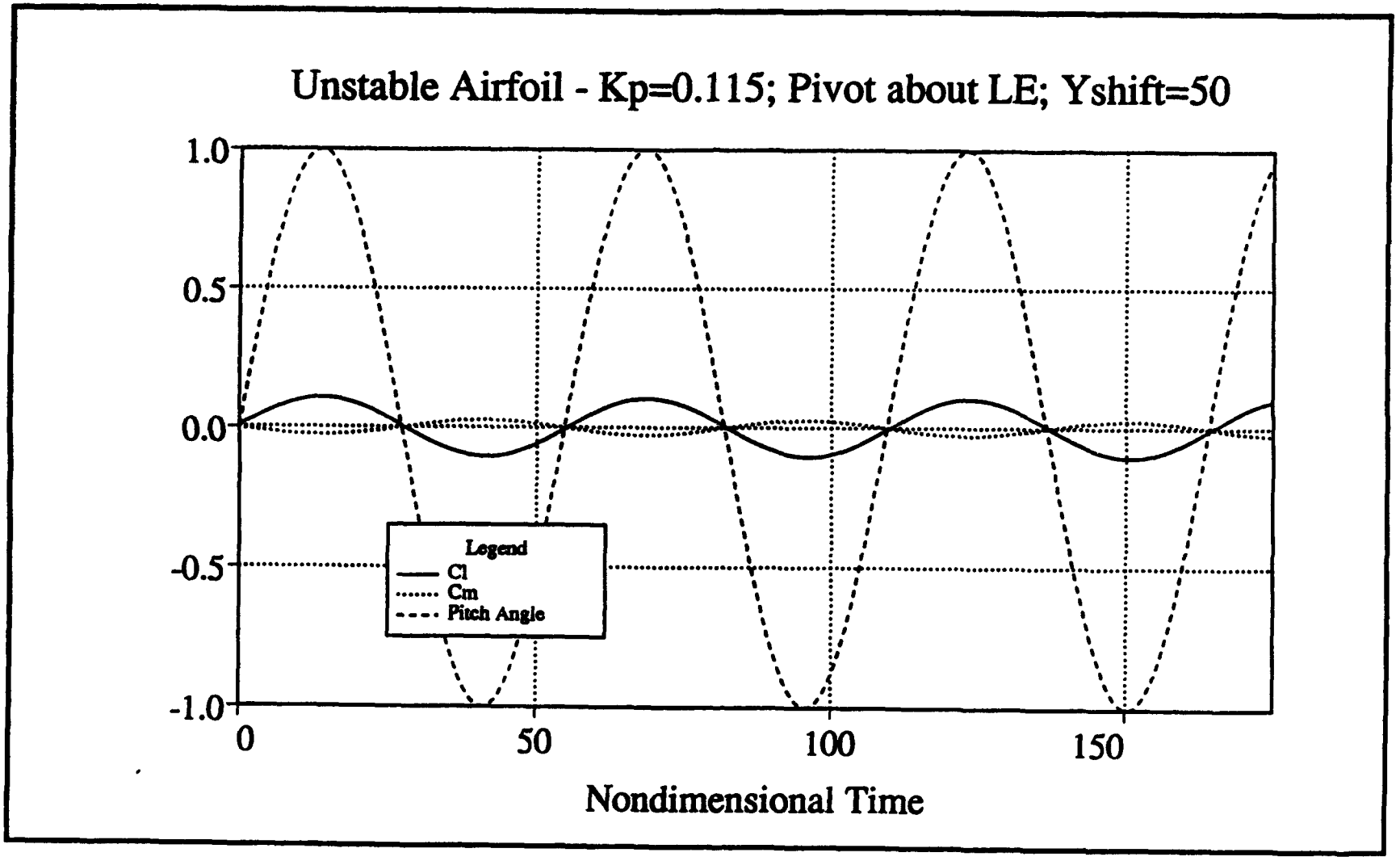
Unstable Airfoil - Kp=0.115; Pivot about LE; Yshift=50
1.0
0.5
0.0
-0.5
-1.0
0
50
100
150
Nondimensional Time
Legend
Cl
Cm
Pitch Angle

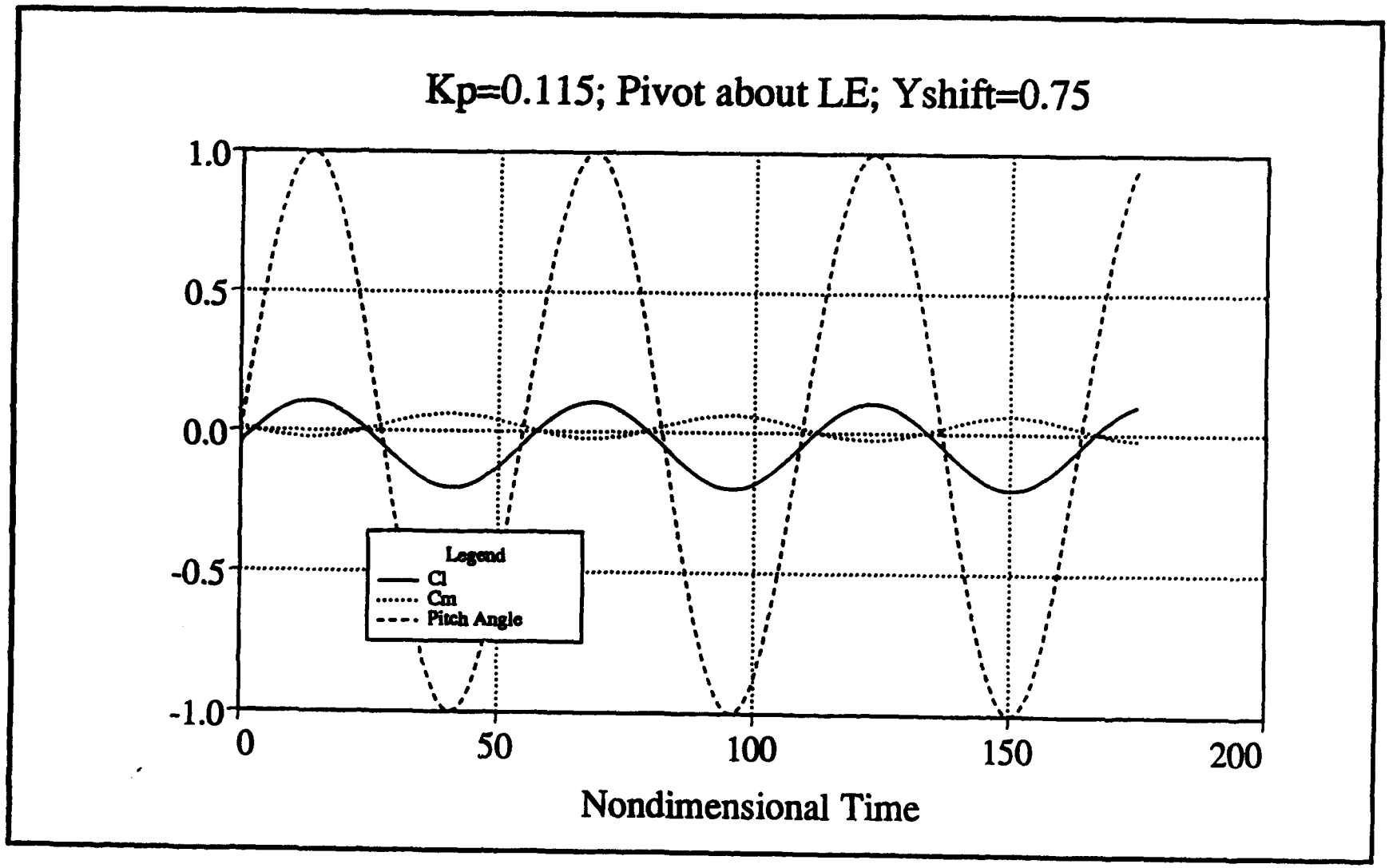
Kp=0.115; Pivot about LE; Yshift=0.75
1.0
0.5
0.0
-0.5
-1.0
0
50
100
150
200
Nondimensional Time
Legend
Cl
Cm
Pitch Angle

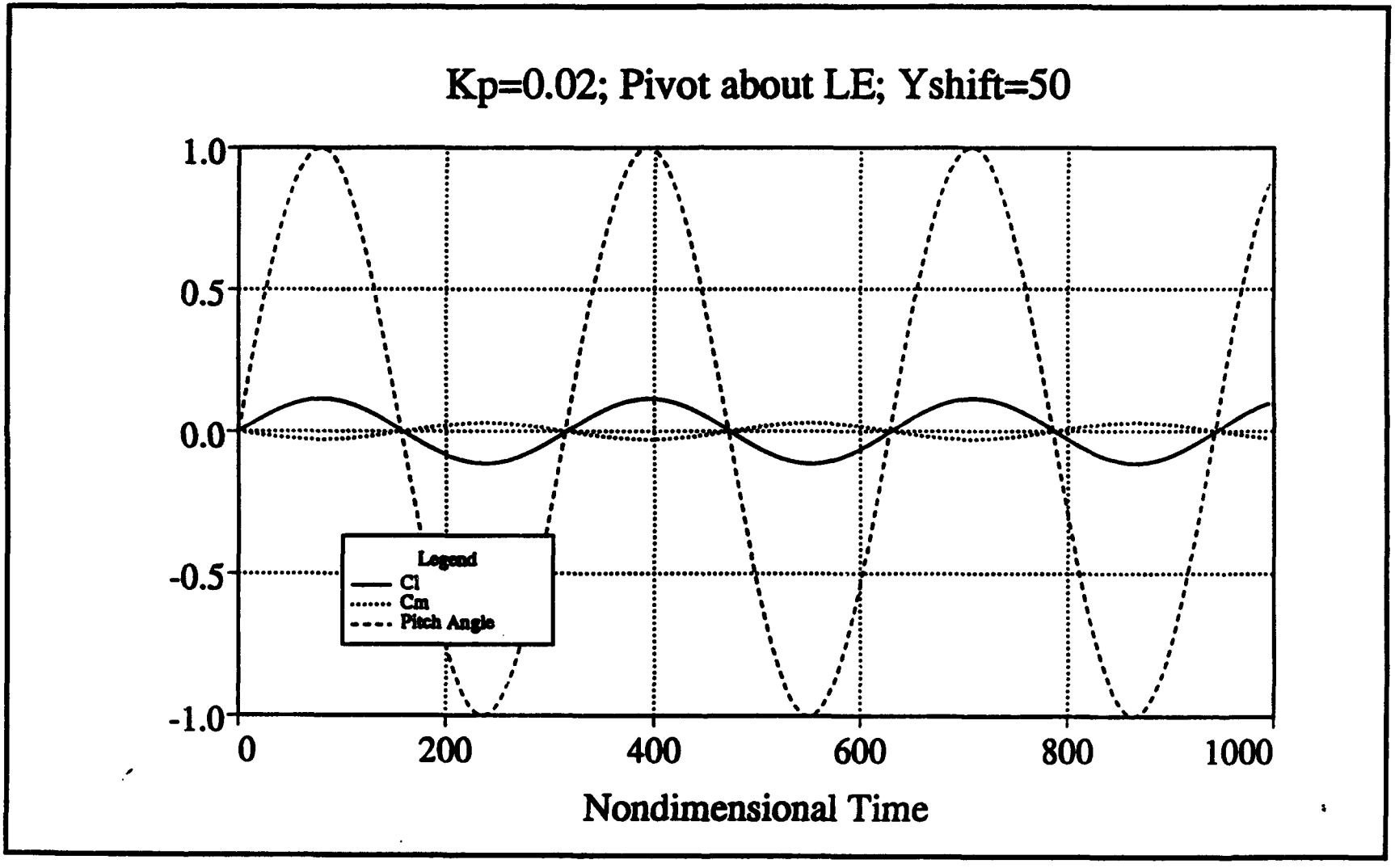
Kp=0.02; Pivot about LE; Yshift=50
1.0
0.5
0.0
-0.5
-1.0
0
200
400
600
800
1000
Nondimensional Time
Legend
Cl
Cm
Pitch Angle

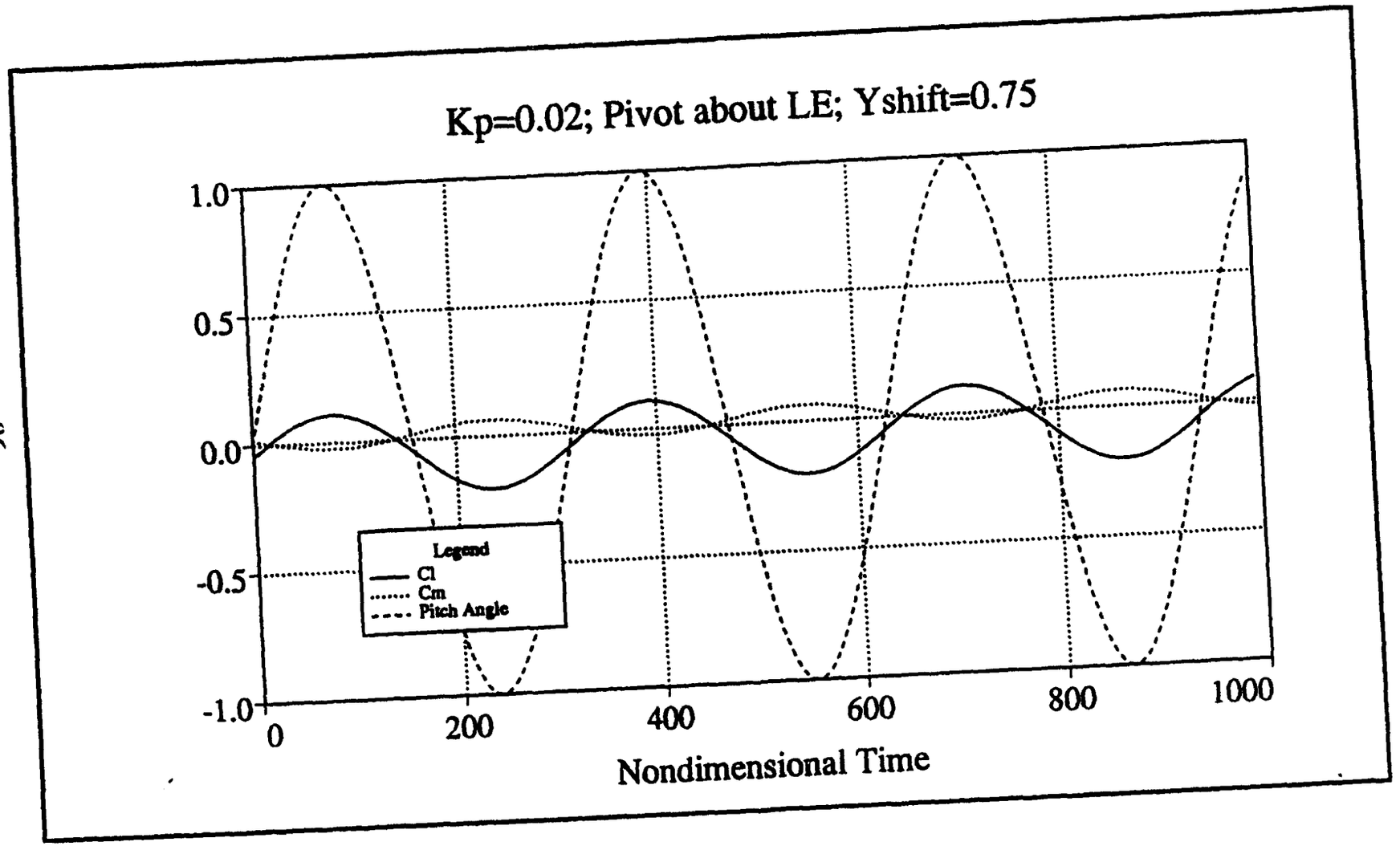
Kp=0.02; Pivot about LE; Yshift=0.75
1.0
0.5
0.0
-0.5
-1.0
0
200
400
600
800
1000
Nondimensional Time
Legend
Cl
Cm
Pitch Angle

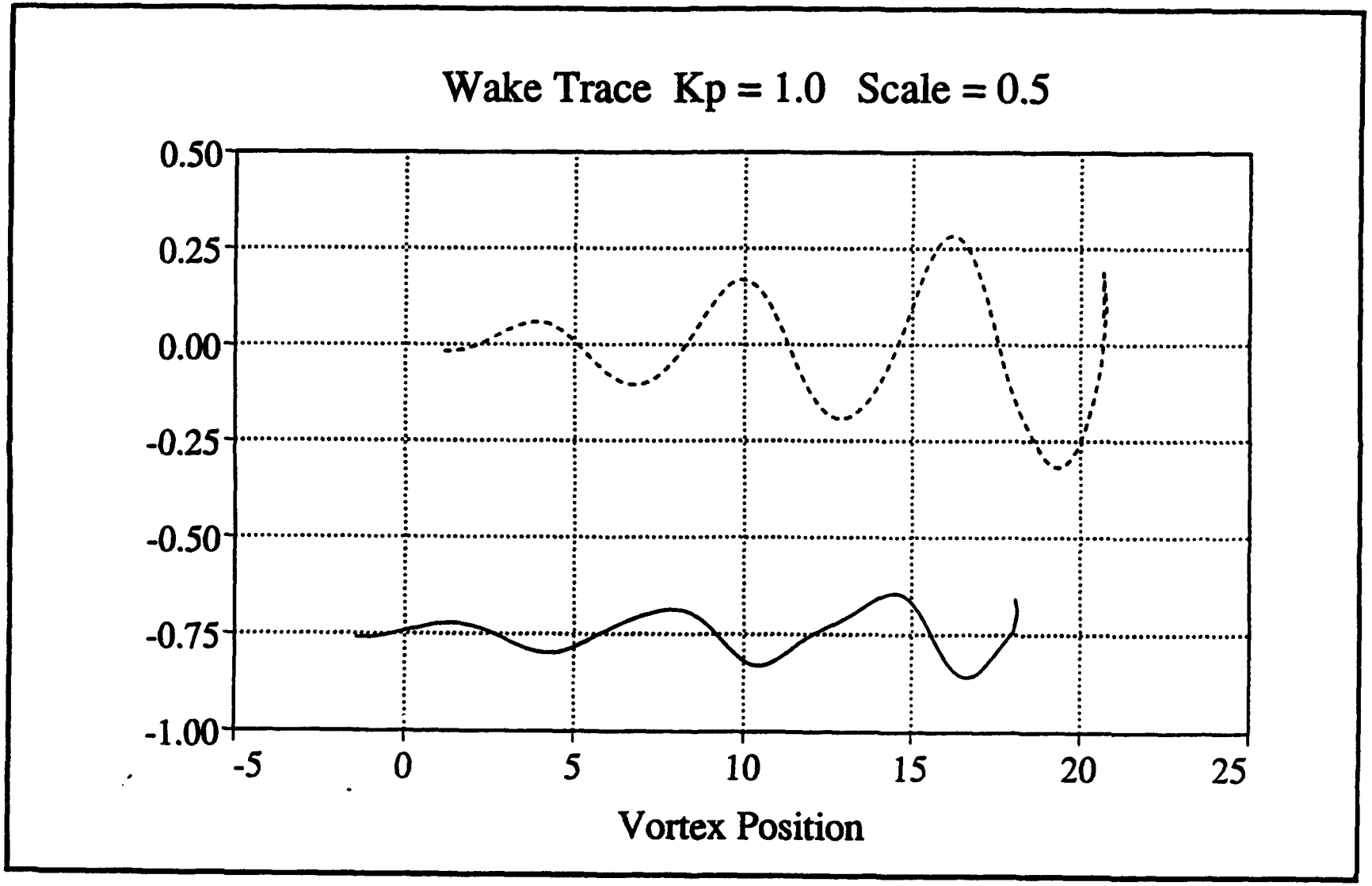
Wake Trace Kp = 1.0 Scale = 0.5
0.50
0.25
0.00
-0.25
-0.50
-0.75
-1.00
-5
0
5
10
15
20
25
Vortex Position

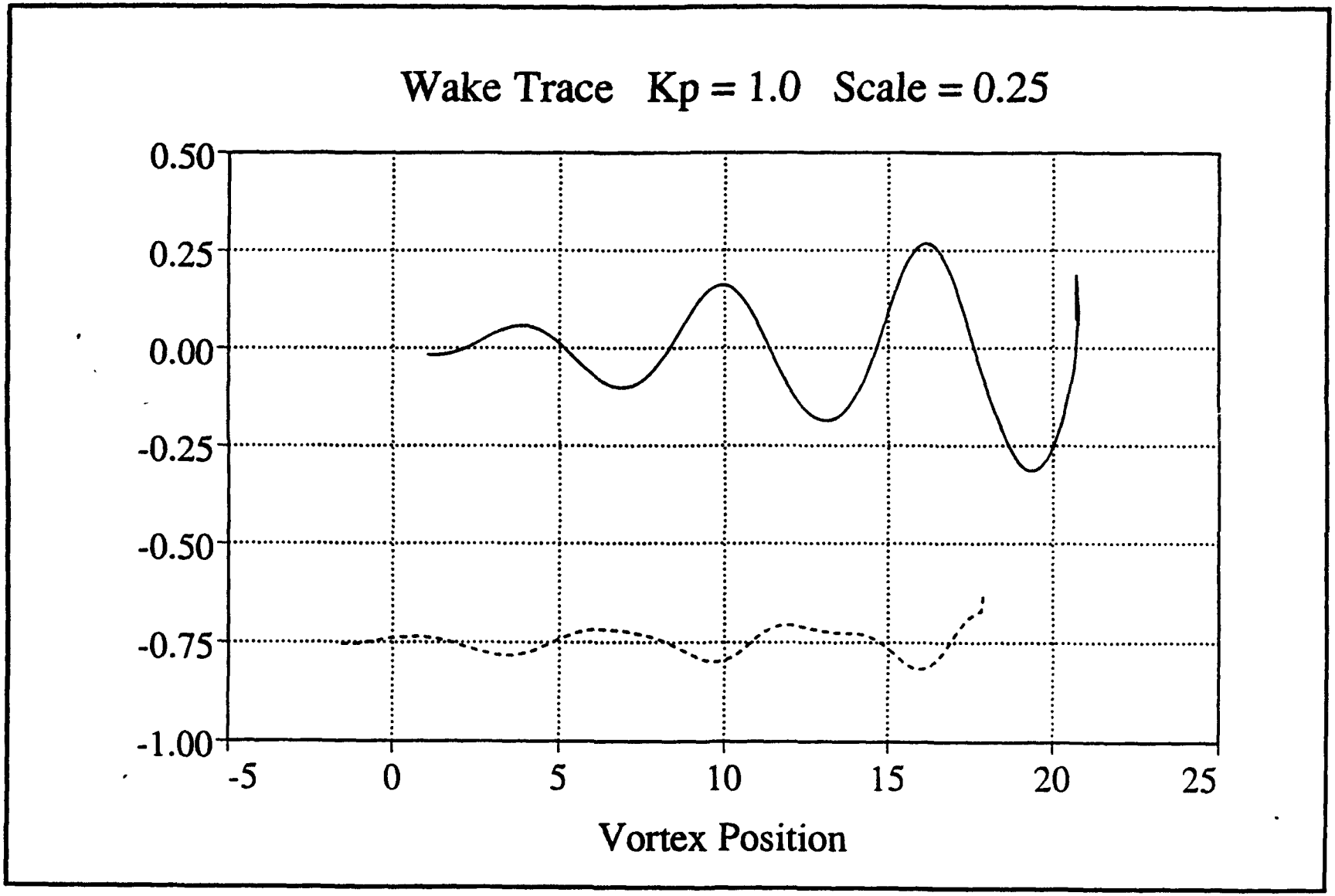
Wake Trace Kp = 1.0 Scale = 0.25
0.50
0.25
0.00
-0.25
-0.50
-0.75
-1.00
-5
0
5
10
15
20
25
Vortex Position

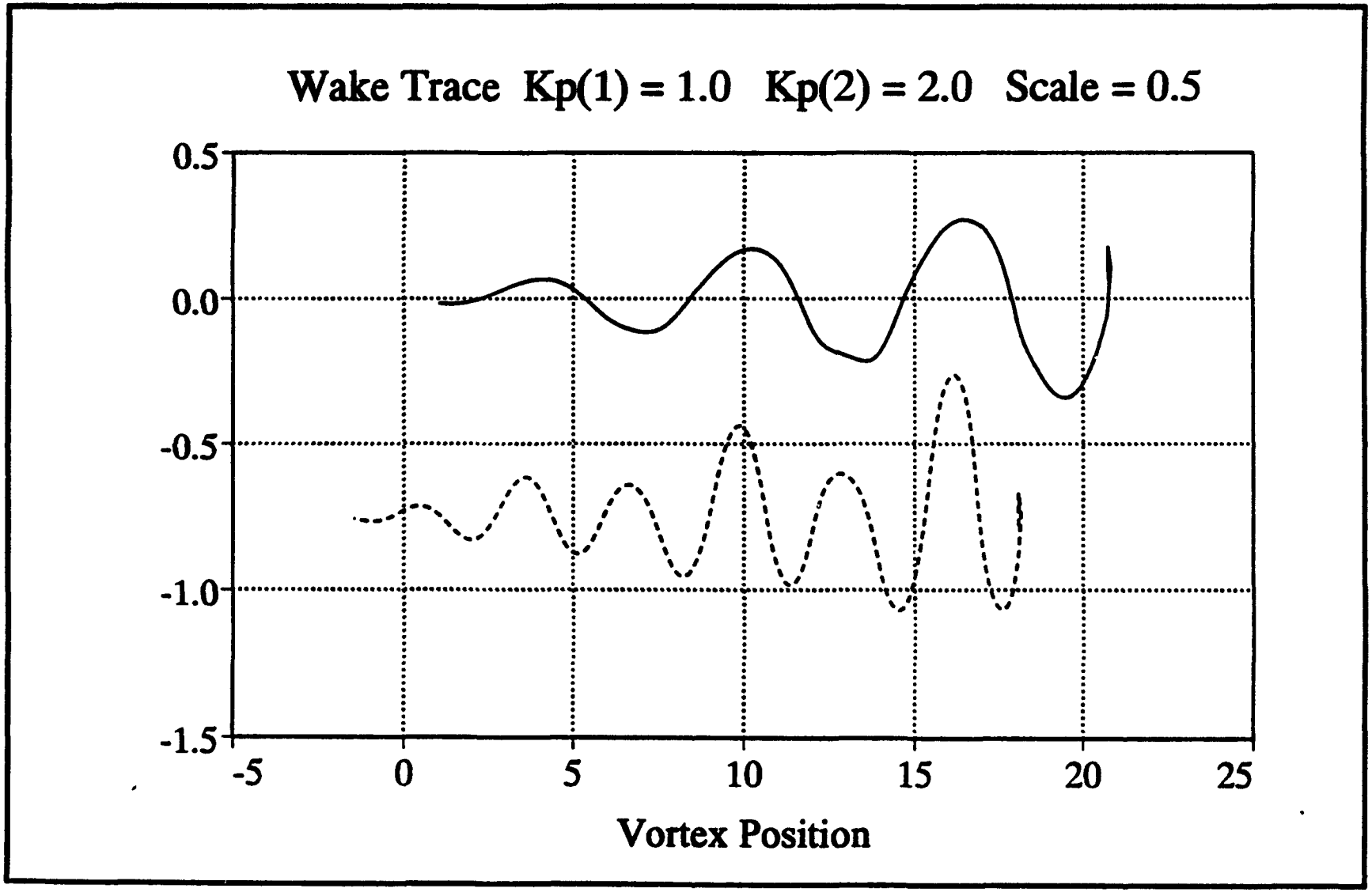
Wake Trace Kp(1) = 1.0 Kp(2) = 2.0 Scale = 0.5
0.5
0.0
-0.5
-1.0
-1.5
-5
0
5
10
15
20
25
Vortex Position

LIST OF REFERENCES

1. Riester, P.J., *A Computational and Experimental Investigation of Incompressible Oscillatory Airfoil Flow and Flutter Problems*, Master's Thesis, Naval Postgraduate School, Monterey, California, June 1993.

2. Pang, K.C., *A Computer Code (USPOTF2) for Unsteady Incompressible Flow Past Two Airfoils*, Master's Thesis, Naval Postgraduate School, Monterey, California, September 1988.

3. Teng, N.H., *The Development of a Computer Code (U2DIIF) for the Numerical Solution of Unsteady, Inviscid and Incompressible Flow over an Airfoil*, Master's Thesis, Naval Postgraduate School, Monterey, California, June 1987.

4. Hess, J.L. and Smith A.M.O., *Calculation of Potential Flow about Arbitrary Bodies*, Progress in Aeronautical Sciences, Vol. 8, Pergamon Press, Oxford, 1966, pp. 1-138.

5. Theodorsen, T., Garrick, T.E., *Mechanism of Flutter A Theoretical and Experimental Investigation of the Flutter Problem*, NACA TR-685, 1940.

6. Smilg, B., *The Instability of Pitching Oscillations of and Airfoil in Subsonic Incompressible Potential Flow*, Journal of the Aeronautical Sciences, November 1949.

7. Loewy, R.G., *A Two-Dimensional Approximation to the Unsteady Aerodynamics of Rotary Wings*, Journal of the Aeronautical Sciences, Volume 24 Number 24, February 1957.

8. Fung, Y.C., *The Theory of Aeroelasticity*, Dover Publications, Inc. New York, 1969.

9. Scanlan, R.H., Rosenbaum, R., *Introduction to the Study of Aircraft Vibration and Flutter*, The Macmillian Company, 1960

10. Couch, M.A., *A Finite Wake Theory For Two-Dimensional Rotary Wing Unsteady Aerodynamics*, Master's Thesis, Naval Postgraduate School, Monterey, California, September 1993.

11. Platzer, M.F., *Class Lecture Notes*, Naval Postgraduate School, Monterey, California, Oct. 1993.

12. Bisplinghoff, R.L. and Holt, A., *Principles of Aeroelasticity*, Dover Publications, Inc. New York, 1962.

INITIAL DISTRIBUTION LIST

		No. Copies
1.	Defense Technical Information Center Cameron Station Alexandria, Virginia 22304-6145	2
2.	Library, Code 052 Naval Postgraduate School Monterey, California 93943-5100	2
3.	Chairman, Code AA/CO Dept. of Aeronautics and Astronautics Naval Postgraduate School Monterey, California 93943-5100	1
4.	Dr. M.F. Platzer Dept. of Aeronautics and Astronautics, Code AA/PL Naval Postgraduate School Monterey, California 93943-5100	6
5.	Dr. I. Tuncer Dept. of Aeronautics and Astronautics, Code AA/TU Naval Postgraduate School Monterey, California 93943-5100	2
6.	LT Mark A. Turner 6435 Scarff Rd. New Carlisle, Ohio 45344	2